

# **QCD and Monte Carlo**

H. Jung

DESY (Hamburg, FRG)  
University of Antwerp (Antwerp, Belgium)



# Contents

<b>1</b>	<b>Introduction</b>	<b>5</b>
<b>2</b>	<b>Monte Carlo methods</b>	<b>7</b>
2.1	Random Numbers . . . . .	7
2.2	Statistics and Probabilities . . . . .	10
2.3	Random Numbers from arbitrary distributions . . . . .	14
2.4	Law of Large Numbers and Central Limit Theorem . . . . .	17
2.5	Monte Carlo Integration . . . . .	18
<b>3</b>	<b>Probing the Structure of Matter</b>	<b>23</b>
3.1	Kinematics and Cross Section definition . . . . .	23
3.1.1	Four-Vector Kinematics . . . . .	23
3.1.2	Light Cone Variables . . . . .	24
3.1.3	Cross Section definition . . . . .	26
3.2	The Quark Parton Model . . . . .	27
3.3	Cross Section in DIS . . . . .	32
3.4	The photon-proton cross section . . . . .	37
3.5	$\mathcal{O}(\alpha_s)$ contribution to DIS . . . . .	38
3.5.1	QCDC process . . . . .	39
3.5.2	BGF process . . . . .	41
<b>4</b>	<b>Parton evolution equation</b>	<b>45</b>
4.1	Conservation and Sum Rules . . . . .	48
4.1.1	Flavor Conservation . . . . .	48
4.1.2	Conservation Rules of Splitting Functions . . . . .	51
4.2	Collinear factorization . . . . .	52
4.2.1	Factorization Schemes . . . . .	52
4.3	Solution of DGLAP equations . . . . .	53
4.3.1	Double Leading Log approximation for small $x$ . . . . .	54
4.3.2	From evolution equation to parton branching . . . . .	55
4.4	Solution of evolution equation with Monte Carlo method . . . . .	61

<b>5</b>	<b>BFKL and CCFM evolution equations</b>	<b>65</b>
5.1	Why are transverse momenta important for the evolution ? . . . . .	65
5.2	$k_t$ -dependent Evolution Equation: BFKL Equation . . . . .	67
5.3	$k_t$ -dependent Evolution Equation: CCFM Equation . . . . .	70
5.3.1	Angular Ordering . . . . .	70
5.3.2	CCFM Equation . . . . .	73
5.4	High energy or $k_t$ -factorization . . . . .	74
5.5	Comparison with measurements in $ep$ . . . . .	76
<b>6</b>	<b>Hadron-Hadron scattering</b>	<b>79</b>
6.1	Drell-Yan production in $pp$ . . . . .	79
6.1.1	Factorization of production and decay in Drell Yan processes . . . . .	82
6.1.2	Factorization in Drell Yan processes . . . . .	83
6.1.3	$\mathcal{O}(\alpha_s)$ contributions to Drell Yan production . . . . .	85
6.1.4	The $p_t$ spectrum of Drell Yan production . . . . .	87
6.1.5	Measurement of the $W$ mass . . . . .	89
<b>7</b>	<b>High Parton Densities and small <math>x</math> effects</b>	<b>93</b>
7.1	The high energy behavior of the $\gamma^*p$ cross section . . . . .	93
7.2	The $p_t$ spectrum of Drell Yan production at high energies . . . . .	93
7.2.1	Multiparton interactions . . . . .	94
<b>8</b>	<b>Appendix</b>	<b>99</b>
8.1	Kinematics . . . . .	99
8.1.1	$ep$ - case . . . . .	99
8.1.2	$pp$ - case . . . . .	100
8.2	Calculation of transverse momentum of Drell Yan pair . . . . .	101

# Chapter 1

## Introduction

This lecture is based on a series of lectures on *QCD and Collider physics* and *QCD and MC* given in the years 2005 – 2014 at University Hamburg/DESY and at University of Antwerp.

The aim is to introduce the basic concepts of QCD and how this can be used for comparison with measurements at the past and present high energy particle colliders, HERA and the LHC. Since events produced at high energy collisions contain many particles, most of the calculations cannot be performed analytically. Even for the calculation of integrals, numerical methods have to be applied and for complicated multidimensional integrals the Monte Carlo method is best suited. The basics of the MC method will be discussed in chapter 2. The basics of QCD and the naive quark parton model will be discussed in Chapter 2, with its extension to include QCD effects, where the parton evolution equations will be discussed.

While the basic concepts and methods did not change in the last few years, the experimental results and the interest to understand the measurements has changed: LHC has started and the experiments have published already within one year a large number of measurements, many of them confirming the predictions coming from QCD or more generally from the Standard Model of Particle Physics, but also some which came as a big surprise. During the lecture, some of those results in the area of QCD, which were not expected, will be discussed, of course without aiming to give here a complete interpretation, since those results are still subject to hot discussions and further investigations.

A warning is needed here: although the lecture will cover Monte Carlo methods, it will not be a description how to run a given Monte Carlo event generator, nor it will describe the detailed implementation of QCD processes in Monte Carlo generators. The lectures will provide the basics to understand the principles of Monte Carlo event simulation and basic QCD calculations.



## Chapter 2

# Monte Carlo methods

The general case of a process  $A + B \rightarrow$  anything to be calculated is given in fig. 2.1. A more

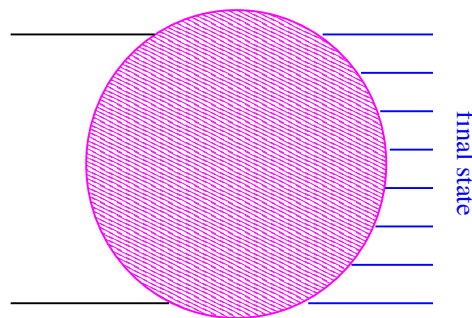


Figure 2.1: General case of scattering  $A + B \rightarrow$  anything

detailed figure of the process to be studied is shown in fig 2.2, where on the left side is shown the lowest order process for jet production in hadron hadron collisions and on the right side the process is shown including multiparton radiation, which is the subject of this lecture. It becomes clear, that with many partons<sup>1</sup> involved in the calculation this cannot be done analytically, and numerical methods are needed, one of them is the Monte Carlo method.

### 2.1 Random Numbers

Monte Carlo method refers to any procedure, which makes use of random numbers and uses probability statistics to solve the problem<sup>2</sup>. The Monte Carlo method was invented and developed in the 1930's for the calculation of nuclear decays, but nowadays is widely used in any calculation of complicated processes for the simulation of natural phenomena, simulation of the experimental apparatus, simulation of the underlying physics process but also in economy for risk analysis etc.

<sup>1</sup>Partons are used as a generic name for quarks and gluons

<sup>2</sup>The name comes from a saga, that the first true random numbers were obtained by recording the results of the roulette game in the casino of Monte Carlo.

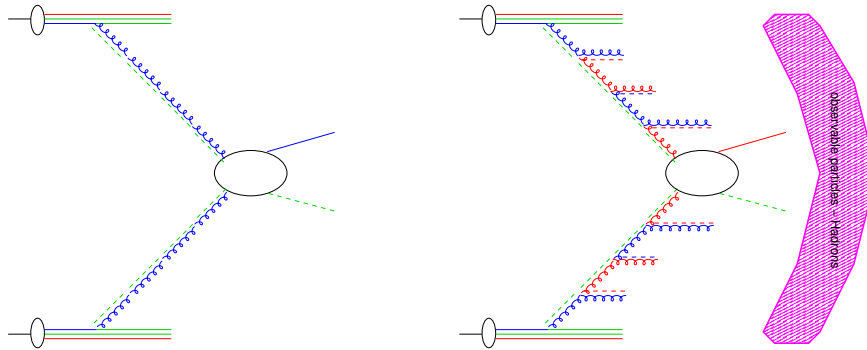


Figure 2.2: Left: lowest order process for jet production in hadron hadron collisions. Right: Process for jet production including multiparton radiation and hadronization

Monte Carlo methods make use of random numbers. An example of a random number is 3 or 4. There is nothing like *a random number*. Any number can appear to be random. Only if we have a sequence of numbers, where each number has nothing to do with the other numbers in the series, we can say the numbers appear to be random.

In the following we consider random numbers always only in the interval  $[0, 1]$ . In a uniform distribution of random numbers in this interval  $[0, 1]$  all numbers have the same chance to appear, note that 0.00000034 has the same chance to appear as 0.5.

Random numbers can be obtained by several methods:

- using a truly chaotic system like roulette, lotto or 6-49
- using a process which is inherently random
- generating "random numbers" on a computer

Examples for random numbers obtained from chaotic processes are using atmospheric noise [1] or using quantum physics which is intrinsically random [2].

Random numbers generated on a computer are never really random, since they always are determined according to some algorithm [3]. They may appear random to someone, who does not know the algorithm. The randomness of random numbers can be checked by several test, which will be discussed later. Random numbers, which are generated on a computer are called *pseudo-random numbers*. Sometime *quasi-random numbers* are discussed. Such random numbers are by intention not random but are designed to be as uniform as possible in order to minimize the uncertainties in integration procedures.

A simple random number generator (so called *multiplicative congruential linear random number generator*) can be build as follows [4][p 40ff] and [5][Vol II,p 9]. From an initial number  $I_0$  we generate a series of random numbers  $R_j$  according to:

$$\begin{aligned} I_j &= \text{mod}(aI_{j-1} + c, m) \\ R_j &= \frac{I_j}{m} \end{aligned} \quad (2.1)$$



with  $a$  being an multiplicative and  $c$  a additive constant and  $m$  the modulus<sup>3</sup>. With this procedure one obtains a series of number  $R_j$  in the interval  $(0, 1)$  (note that the values 0 and 1 are excluded). This random number generator will be tested in the exercise. In fig 2.3 the correlation of 2 random numbers is shown on the left side. The right side shows the same correlation for another random number generator RANLUX [6–8], which will be used later in the calculations. It is obvious, that the *multiplicative congruential linear random number generator* produces random numbers, which show correlations and does therefore not satisfy quality criteria for a good random number generator; the RANLUX generator seems to be better.

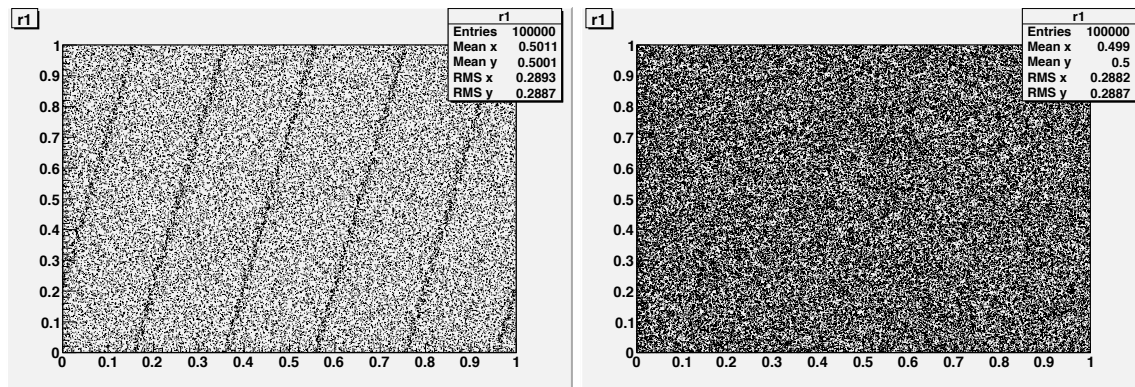


Figure 2.3: Left: correlation of two successive random numbers obtained according to 2.1. Right: correlation of two random numbers obtained with RANLUX [8]

Several criteria on the randomness of a series of *pseudo random numbers* can be applied to test the quality of the random number generator [5][Vol II,p 59]:

- **statistical test** (test uniformity of distribution, frequency test, equi-distribution test)  
Divide the interval  $(0, 1)$  into  $k$ -subintervals with length  $1/k$ . Count how many random numbers fall into the  $k$ 's interval [9]. Calculate:

$$\chi^2 = \sum_{i=1}^k \frac{(N_i - N/k)^2}{N/k} \quad (2.2)$$

with  $N$  random numbers  $R_i$ . If the random numbers are uniformly distributed, then Eq. 2.2 is a  $\chi^2$  distribution with  $k - 1$  degrees of freedom and should give  $\chi^2/(ndf) \sim 1$ , with  $ndf$  being the number of degrees of freedom.

- **serial test** (pairs of successive random numbers should be distributed in an independent way (see fig. 2.3)). *The sun comes up just about as often as it goes down, in the long run, but this does not make its motion random* [5][Vol II,p 60].  
Count pairs of random numbers  $(Y_{2j}, Y_{2j+1}) = (q, r)$  for any  $0 \leq j \leq n$  and apply a  $\chi^2$  test as above.

<sup>3</sup>the modulus function is defined as  $mod(i_1, i_2) = i_1 - INT(i_1/i_2) \cdot i_2$

- **sequence up-down test**

Count the number of runs, where the random numbers are increasing  $Y_{j+1} > Y_j$ . Example: take the sequence 1298536704 and insert vertical lines for  $Y_{j+1} > Y_j$ , resulting in |129|8|5|367|0|4|. Count the number of runs-up with length  $k$ . The number of runs-up and the number of runs-down should be similar, but they should not be adjacent: often a long run will be followed by a short one.

- **gap test**

Choose two numbers  $\alpha, \beta$  with  $0 \leq \alpha < \beta \leq 1$ . Generate  $r + 1$  random numbers. The probability that the first  $r$  random numbers are outside  $(\alpha, \beta)$  is  $P_r = p(1-p)^r$  with  $p = \beta - \alpha$  being the probability for the  $r + 1$  event to be inside  $(\alpha, \beta)$ .

- **Random walk test**

Choose  $0 \leq \alpha \leq 1$  and generate a large number of random variables. Count how often  $Y_i < \alpha$  and call it  $r$ . We expect a binominal distribution for  $r$  with  $p = \alpha$ . The same test can be performed for  $Y_i > (1 - \alpha)$ .

Practical criteria for random numbers can be formulated as follows [3]:

- **Long period**

- **Repeatability**

for testing and development one needs to repeat calculations. Repeatability also allows to repeat only part of the job, without re-doing the whole.

- **Long disjoint sequences**

for long procedures one needs to be able to perform independent sub-calculations which can be added later.

- **Portability**

not only the code should be portable but also the results should be the same, independent on which platform the calculations are done.

- **Efficiency**

generation of random numbers should be fast.

To test a random number generator, a series of tests have to be performed. Even if a Random Number generator passes all  $n$ -tests, one cannot assume that it also passes the  $n + 1$ -test.

## 2.2 Statistics and Probabilities

A very good overview on statistics and probabilities is given in [4, 10], which was used for the discussion in this chapter. In an experiment where the outcome depends on a single variable  $x$  one can ask what is the probability to find values of  $x$  in the interval  $[x, x + dx]$ . This is given by  $f(x)dx$  with  $f(x)$  being the probability density function *p.d.f* (not to be confused with the pdf

which is used for the parton density function to be discussed later). Since we assume, there is an experiment with some outcome, the probability to find  $x$  anywhere must be unity, that is:

$$\int_{-\infty}^{\infty} f(x)dx = 1 \quad (2.3)$$

The *p.d.f* has to satisfy in addition:

$$f(\infty) = f(-\infty) = 0 \quad (2.4)$$

The expectation value (mean values or average value) of a function  $h(x)$  is defined as:

$$E[h] = \int_{-\infty}^{+\infty} h(x)f(x)dx = \int h(x)dG(x) = \frac{1}{b-a} \int h(x)dx \quad (2.5)$$

with  $f(x)$  being the probability density function. In the right part of the equation we used the special case  $dG(x) = dx/(b-a)$  for a uniform distribution. In case of discrete distributions we have:

$$E[h] = \sum_i^{\infty} h(x_i)f(x_i) \quad (2.6)$$

A special case is the expectation value of  $x$  (or the mean on the distribution)

$$E[x] = \int_{-\infty}^{+\infty} f(x)x dx \stackrel{def}{=} \langle x \rangle \quad (2.7)$$

From the definition of the expectation value we see that  $E[h]$  is a **linear operator**:

$$\begin{aligned} E[cg(x) + h(x)] &= \int (cg(x) + h(x)) f(x)dx \\ &= c \int g(x)dx + \int h(x)f(x)dx \\ &= cE[g] + E[h] \end{aligned} \quad (2.8)$$

with  $c$  being a constant. Similarly we can see that the expectation value of the expectation value  $E[E[g]]$  is simply  $E[g]$ :

$$\begin{aligned} E[E[g(x)]] &= \int \left( \int g(x)f(x)dx \right) f(x')dx' \\ &= E[g(x)] \int f(x')dx' \\ &= E[g(x)] \end{aligned} \quad (2.9)$$

because  $\int f(x')dx' = 1$  by definition of the *p.d.f*

The variance  $\sigma^2$  measures the spread of a distribution and can be defined as the mean quadratic deviation from the mean value. The square-root of  $\sigma^2$  is also called the *standard deviation*. The variance  $V[h]$  is defined as:

$$V[h] = \sigma^2 = E [(h(x) - E[h(x)])^2] = \int (h(x) - E[h(x)])^2 f(x) dx \quad (2.10)$$

From the definition, the variance  $V[cg(x) + h(x)]$  can be calculated:

$$\begin{aligned} V[cg(x) + h(x)] &= \int (cg(x) + h(x) - E[cg(x) + h(x)])^2 f(x) dx \\ &= \int (cg(x) + h(x) - cE[g(x)] - E[h(x)])^2 f(x) dx \\ &= \int ((c(g - E[g]) + (h - E[h]))^2 f(x) dx \\ &= \int (c^2(g - E[g])^2 + 2c(g - E[g])(h - E[h]) + (h - E[h])^2) f(x) dx \\ &= c^2V[g] + 2cE[(g - E[g])(h - E[h])] + V[h] \\ &= c^2V[g] + V[h] + 2cE[g \cdot h - gE[h] - hE[g] + E[g]E[h]] \\ &= c^2V[g] + V[h] + 2c(E[g \cdot h] - E[g]E[h] - E[h]E[g] + E[g]E[h]) \\ V[cg(x) + h(x)] &= c^2V[g] + V[h] + 2c(E[g \cdot h] - E[g]E[h]) \end{aligned} \quad (2.11)$$

In the case that  $g(x)$  and  $h(x)$  are uncorrelated, we have  $E[g \cdot h] = E[g]E[h]$  and the expression simplifies to:

$$V[cg(x) + h(x)] = c^2V[g] + V[h] \quad (2.12)$$

A special case is the variance of  $x$ :

$$\begin{aligned} V[x] &= E((x - \langle x \rangle)^2) = \int (x - E[x])^2 f(x) dx \\ &= E[x^2 - 2x\langle x \rangle + \langle x \rangle^2] \\ &= E[x^2] - 2E[x]\langle x \rangle + \langle x \rangle^2 \\ V[x] &= E[x^2] - \langle x \rangle^2 \\ V[x] &= E[x^2] - E[x]^2 \end{aligned} \quad (2.13)$$

where the relation  $E[x] = \langle x \rangle$  has been applied.

Consider independent random numbers  $x_1$  and  $x_2$  with variances  $V[x_1] = \sigma_1^2$  and  $V[x_2] = \sigma_2^2$  and mean values  $\mu_1$  and  $\mu_2$ . The expectation value of the sum of  $x_1$  and  $x_2$  is:

$$\begin{aligned} E[x_1 + x_2] &= E[x_1] + E[x_2] \\ &= \mu_1 + \mu_2 \end{aligned} \quad (2.14)$$

The variance of the sum is (using  $x = x_1 + x_2$ ):

$$\begin{aligned}
 \sigma^2 &= \langle x - \langle x \rangle \rangle \\
 &= E[(x - \langle x \rangle)^2] \\
 &= E[(x - \mu_1 - \mu_2)^2] \\
 &= E[(x - \mu_1 + x_2 - \mu_2)^2] \\
 &= \underbrace{E[(x_1 - \mu_1)^2]}_{\sigma_1^2} + \underbrace{2(x_1 - \mu_1)(x_2 - \mu_2)}_0 + \underbrace{E[(x_2 - \mu_2)^2]}_{\sigma_2^2} \\
 \sigma^2 &= \sigma_1^2 + \sigma_2^2
 \end{aligned} \tag{2.15}$$

because  $E[x_1] = \mu_1$ , since  $x_1$  and  $x_2$  are independent. The general form is then:

$$\sigma^2 = \sum_{i=1}^N \sigma_i^2 \tag{2.16}$$

Consider now a sample of  $x_i$  where all  $x_i$  follow the same probability density function  $f(x)$ , having the same variance  $\sigma^2$  and the same  $\mu$ . The mean of the sample is defined as:

$$\bar{x} = \frac{1}{N} \sum_{i=1}^N x_i \tag{2.17}$$

The expectation value  $E[\bar{x}]$  is given by:

$$\begin{aligned}
 E[\bar{x}] &= E \left[ \frac{1}{N} \sum_{i=1}^N x_i \right] \\
 &= \frac{1}{N} E \left[ \sum_{i=1}^N x_i \right] \\
 &= \frac{1}{N} N E[x_i] \\
 E[\bar{x}] &= E[x] = \langle x \rangle
 \end{aligned} \tag{2.18}$$

resulting in the expectation value of the mean being the mean itself. To obtain above, the features of the linearity of the operator are applied.

The variance of the mean is:

$$\begin{aligned}
 V[\bar{x}] &= V \left[ \frac{1}{N} \sum_{i=1}^N x_i \right] \\
 &= \frac{1}{N^2} V \left[ \sum_{i=1}^N x_i \right]
 \end{aligned}$$

$$\begin{aligned}
&= \frac{1}{N^2} \sum \sigma_i^2 \\
&= \frac{1}{N^2} N \sigma^2 \\
V[\bar{x}] &= \frac{1}{N} \sigma^2
\end{aligned} \tag{2.19}$$

or in the familiar form as the standard deviation of the mean:

$$\sigma_N = \frac{\sigma}{\sqrt{N}} \tag{2.20}$$

### 2.3 Random Numbers from arbitrary distributions

Given a sequence of random numbers uniformly distributed in  $[0, 1]$  the next step is to determine a sequence of random numbers  $x_1, x_2, \dots$  distributed according to a probability density function *p.d.f.*

The task is to find a suitable function  $x(r)$  which gives the same sequence of random numbers when evaluated with uniformly distributed values  $r$ . The probability to obtain a value  $r$  in the interval  $[r, r + dr]$  is  $u(r)dr$  and this should be equal to the probability to find  $x$  in  $[x, x + dx]$  which is  $f(x)dx$  (see fig 2.4):

$$\begin{aligned}
u(r')dr' &= f(x')dx' \\
\int_{-\infty}^r u(r')dr' &= \int_{-\infty}^x f(x')dx'
\end{aligned} \tag{2.21}$$

Using a random number  $R$  uniform in  $[0, 1]$  with  $R = \int_{-\infty}^r u(r')dr'$  we obtain:

$$R = \int_{-\infty}^x f(x')dx' = F(x)$$

with  $f(x) = \frac{dF(x)}{dx}$  being the probability density function *p.d.f.* (as defined before) with:

$$\begin{aligned}
\int_{-\infty}^{\infty} f(x)dx &= 1 \\
f(\infty) &= f(-\infty) = 0
\end{aligned}$$

Examples (assuming we have random numbers  $R_j$  uniformly distributed in  $[0, 1]$ ):

- **linear p.d.f:**  $f(x) = 2x$ .

The primitive function  $F(x)$  is:

$$\begin{aligned}
F(x) &= \int_0^x f(t)dt = \int_0^x 2tdt = x^2 \\
R &= F(x) = x^2 \\
x_j &= \sqrt{R_j}
\end{aligned}$$

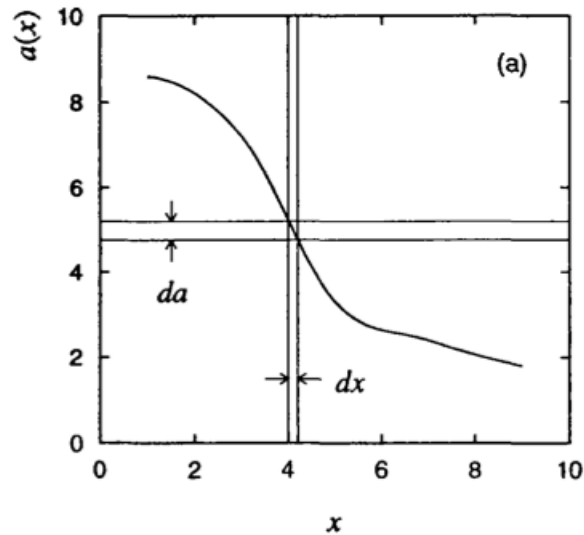


Figure 2.4: Illustration of  $a(r)dr = f(x)dx$ . Picture from [4] [p14]

For any uniformly distributed random numbers  $R_j$ , the  $x_j$  values are distributed according to the function  $f(x) = 2x$ , when calculated as  $x_j = \sqrt{R_j}$

- **exponential p.d.f:**  $f(x, \lambda) = \lambda \exp(-\lambda x)$ .  
The primitive function  $F(x)$  is:

$$\begin{aligned}
 F(x) &= \int_0^x f(t)dt = \int_0^x \lambda e^{(-\lambda t)}dt = \lambda \frac{-1}{\lambda} e^{(-\lambda t)} \Big|_0^x \\
 &= 1 - e^{-\lambda x} \\
 -R + 1 &= e^{-\lambda x} \\
 \log(1 - R) &= -\lambda x \\
 x_j &= \frac{-1}{\lambda} \log(R_j)
 \end{aligned}$$

The values  $x_j$  can be generated from a uniform distribution of random numbers  $R_j$  with  $x_j = \frac{-1}{\lambda} \log(1 - R_j) = \frac{-1}{\lambda} \log(R_j)$  since for a uniform distribution the probability of occurrence of  $1 - R_j$  is the same as for  $R_j$

- **p.d.f:**  $f'(x) = 1/x$  in the range  $[x_{min}, x_{max}]$   
The normalization integral is:

$$\int_{x_{min}}^{x_{max}} \frac{1}{t} dt = \log \frac{x_{max}}{x_{min}} \quad (2.22)$$

Since this function  $f'(x)$  is not normalized to unity, the normalization factor has to be included:

$$f(x) = \frac{f'(x)}{\log \frac{x_{max}}{x_{min}}} = \frac{1}{x} \frac{1}{\log \frac{x_{max}}{x_{min}}} \quad (2.23)$$

The primitive function  $F(x)$  is then:

$$\begin{aligned} F(x) &= \int_{x_{min}}^x f(t) dt \\ &= \frac{1}{\log \frac{x_{max}}{x_{min}}} \int_{x_{min}}^x \frac{1}{t} dt = \frac{1}{\log \frac{x_{max}}{x_{min}}} \log \frac{x}{x_{min}} \\ R &= \frac{\log \frac{x}{x_{min}}}{\log \frac{x_{max}}{x_{min}}} \\ \log \left( \frac{x_{max}}{x_{min}} \right)^R &= \log \left( \frac{x}{x_{min}} \right) \end{aligned} \quad (2.24)$$

The values  $x_j$  can be generated from a uniform distribution of random numbers  $R_j$  with  $x_j = x_{min} \left( \frac{x_{max}}{x_{min}} \right)^{R_j}$ .

- **brute force or hit and miss method:**

If there is no easy way to find an analytically integrable function, which can be inverted one can use the *hit-and-miss* method. Assume we want to generate random numbers according to a function  $f(x)$  in the interval  $[a, b]$ . The procedure is then the following: determine the maximum value, the function  $f(x)$  can reach in  $[a, b]$ , which is  $f_{max}$ . Then select  $x_i$  uniformly in the range  $[a, b]$  with  $x_i = a + (b - a)R_i$  with  $R_i$  in  $(0, 1)$ . Use another random variable  $R_j$  also in  $(0, 1)$ . Decide according to the following, if the pair  $R_i, R_j$  of random numbers is accepted or rejected.

$$\begin{aligned} \text{if } f(x_i) < R_j \cdot f_{max} &\rightsquigarrow \text{ reject} \\ \text{if } f(x_i) > R_j \cdot f_{max} &\rightsquigarrow \text{ accept} \end{aligned}$$

The accepted random numbers  $x_i$  follow then exactly the distribution of the function  $f(x)$ . The only disadvantage of this method is, that depending on the function  $f(x)$ , it can be rather inefficient.

- improvements of the *hit and miss method*.

Find a function  $g(x)$  which is similar to  $f(x)$  but which is integrable and invertible, i.e.  $G(x) = \int g(x)dx$  and  $G^{-1}(x)$  must exist. Then choose a constant such that always  $c \cdot g(x) > f(x)$  for all  $x$ . Generate  $x$  according to the function  $g(x)$  with the methods described above. Generate another random variable  $R_j$  and apply the *hit and miss method* as above:

$$\begin{aligned} \text{if } f(x_i) < R_j \cdot c \cdot g(x) &\rightsquigarrow \text{ reject} \\ \text{if } f(x_i) > R_j \cdot c \cdot g(x) &\rightsquigarrow \text{ accept} \end{aligned}$$

The accepted distribution of variables  $x_i$  will follow the original function  $f(x)$ .



## 2.4 Law of Large Numbers and Central Limit Theorem

The law of large numbers is fundamental for all the considerations above [4,10,11]. The law says, that for uniformly distributed random values  $u_i$  in the interval  $[a, b]$  the sum of the probability density functions converges to the true estimate of the mean of the function  $f(x)$ :

$$\frac{1}{N} \sum_{i=1}^N f(u_i) \rightsquigarrow \frac{1}{b-a} \int_a^b f(u) du \quad (2.25)$$

The law of large numbers has been applied in the sections before implicitly. The function  $f(x)$  must satisfy certain conditions: it must be integrable, and it must be finite in the whole range of  $[a, b]$ . The left hand side of eq.(2.25) is just a Monte Carlo estimate of the integral on the right hand side and the law of large numbers says that the Monte Carlo estimate of the integral is a consistent estimate of the true integral as the size of the random sample becomes large. At this stage, nothing is said, how large "large" has to be.

The law of large numbers tells that for infinitely large numbers the Monte Carlo estimate of the integral converges to the true estimate of the integral. The Central Limit Theorem tells us how the convergence goes for finite number of  $N$ . The Central Limit Theorem says that the sum of a large number of random variables follows a normal distribution (that is the sum of random variables is Gauss distributed) no matter according to which *p.d.f* the individual random variables were generated, only the number  $N$  must be large enough and the random variables must have finite expectation values and variances. An example of the application of the Central Limit Theorem is the construction of a Random Number generator for Gaussian distributed random numbers, which will be done in the exercises:

- take a sum of uniformly distributed random numbers  $R_i$ :

$$R_n = \sum_{i=1}^n R_i$$

The expectation value and the variance are calculated according to the rules in eq.(2.8,2.11):

$$\begin{aligned} E[R_1] &= \int u du = \frac{1}{2} \\ V[R_1] &= \int \left(u - \frac{1}{2}\right)^2 du = \frac{1}{12} \\ E[R_n] &= \frac{n}{2} \\ V[R_n] &= \frac{n}{12} \end{aligned}$$

According to the Central Limit Theorem the sum of random values is Gauss distributed. To obtain a distribution centered around 0 with  $\sigma = 1$  we take:

$$\frac{\sum_i x_i - \sum_i \mu_i}{\sqrt{\sum_i \sigma_i^2}} \rightarrow \mathcal{N}(0, 1)$$

For example we sum  $n = 12$  random numbers (many times  $N \rightarrow \infty$ ) and we obtain a "normal" (Gauss) distribution  $\mathcal{N}$  [11]:

$$\mathcal{N}(0, 1) \rightarrow \frac{R_n - n/2}{\sqrt{n/12}} = R_{12} - 6$$

## 2.5 Monte Carlo Integration

Already in the previous sections we had to deal with the problem to obtain a reliable estimate of the true value of an integral [9]:

$$I = \int_a^b f(x) dx$$

The integral  $I$  is directly connected to the expectation value of the function  $f(x)$  with the  $x$  values distributed according to a probability density function  $g(x)$ .

$$E[f] = \int_{-\infty}^{\infty} f(x)g(x)dx$$

where the *p.d.f.*  $g(x)$  must be defined such, that it vanishes outside the range of  $(a, b)$ . In the case of uniformly distributed  $x$  this reduces to  $g(x) = 1/(b - a)$  for  $a < x < b$  (and  $g(x) = 0$  otherwise) which gives:

$$E[f] = \int_{-\infty}^{\infty} f(x)g(x)dx = \frac{1}{b - a} \int_a^b f(x)dx$$

The Monte Carlo estimate of the integral is then:

$$I \approx I_{MC} = (b - a) \frac{1}{N} \sum_{i=1}^N f(x_i) \quad (2.26)$$

and the variance is:

$$V[I_{MC}] = \sigma_I^2 = V \left[ (b - a) \frac{1}{N} \sum_{i=1}^N f(x_i) \right] \quad (2.27)$$

$$= \frac{(b - a)^2}{N^2} V \left[ \sum_{i=1}^N f(x_i) \right] \quad (2.28)$$

$$= \frac{(b - a)^2}{N} V[f] \quad (2.29)$$

The variance depends on the number of times the integrand is evaluated, but also on the variance of  $f$ :  $V[f]$ .

Applying the definition of the variance eq.(2.11), the variance  $V[f]$  becomes (with  $\bar{f} = \int f dx = 1/N \sum f_i$  and assuming  $g(x)$  being uniform):

$$V[f] = \int (f - \bar{f})^2 g dx = \int (f^2 - 2f\bar{f} + \bar{f}^2) g dx \quad (2.30)$$

$$= \int f^2 g dx - \bar{f}^2 \quad (2.31)$$

$$= \sum \frac{f_i^2}{N} - \left( \frac{\sum f_i}{N} \right)^2 \quad (2.32)$$

$$(2.33)$$

Then the  $V[I]$  becomes:

$$V[I] = \frac{1}{N} (b-a)^2 \left( \frac{1}{N} \sum f_i^2 - \left( \frac{\sum f_i}{N} \right)^2 \right)$$

With this we can estimate the uncertainty of a Monte Carlo integration (use this in the exercises).

The Monte Carlo integration gives a probabilistic uncertainty band: we can only give a probability that the MC estimate lies within a certain range of the true values [3].

To further improve the accuracy of the Monte Carlo integration, several approaches exist:

- **importance sampling**

If an approximate function  $g(x)$  exists then the integral  $I$  can be estimated to:

$$\begin{aligned} I = \int_a^b f(x) dx &= \int_a^b \frac{f(x)}{g(x)} g(x) dx \\ &= \int h(x) g(x) dx \\ &= E \left[ \frac{f(x)}{g(x)} \right] \end{aligned}$$

provided  $g(x)$  is normalized and integrable in  $[a, b]$ . Thus the integration reduces to calculating the expectation value of  $E[f/g]$ , if the values of  $x$  are distributed according the *p.d.f*  $g(x)$ . The values of  $x$  can be generated according to the methods discussed in the previous sections and we obtain:

$$I = \frac{1}{N} \sum \frac{f(x_i)}{g(x_i)} \quad (2.34)$$

We assume that  $g(x)$  is a *p.d.f* normalized to 1 in the integration range. For example using  $g(x) = (1/x) 1/\log \left( \frac{x_{max}}{x_{min}} \right)$  (see eq.(2.23)) gives then:

$$I = \frac{\log \left( \frac{x_{max}}{x_{min}} \right)}{N} \sum \frac{f(x_i)}{\frac{1}{x_i}}. \quad (2.35)$$

The variance is then given by:

$$V \left[ \frac{f(x)}{g(x)} \right] = E \left[ \left( \frac{f(x)}{g(x)} - E \left[ \frac{f(x)}{g(x)} \right] \right)^2 \right] \quad (2.36)$$

A danger in this method is when  $g(x)$  becomes zero or approaches zero quickly [3].

- **subtraction method (control variates) [3]**

Find a function  $g(x)$  which is close to the true function  $f(x)$ :

$$\int_a^b f(x)dx = \int_a^b g(x)dx + \int_a^b (f(x) - g(x)) dx$$

This method also reduces the variances and is especially successful if the function  $f(x)$  has a divergent part. This method is often used in NLO QCD calculations.

- **stratified sampling**

divide the integration region into subintervals:

$$\int_a^b f(x)dx = \int_a^c f(x)dx + \int_c^b f(x)dx \quad (2.37)$$

Then the integral is:

$$I = \frac{c-a}{n/2} \sum_1 f_i + \frac{b-c}{n/2} \sum_2 f_i \quad (2.38)$$

with the variance (if we take  $c-a = b-c = (a-b)/2$ ):

$$\begin{aligned} V[I] &= V[I_1] + V[I_2] \\ &= \frac{(b-a)^2}{N} \left( \frac{\sum_1 f_i^2}{N} + \frac{\sum_2 f_i^2}{N} - 2 \left[ \left( \frac{\sum_1 f_i}{N} \right)^2 + \left( \frac{\sum_2 f_i}{N} \right)^2 \right] \right) \end{aligned}$$

We obtain a smaller variance, since the fluctuations in each interval are smaller.

- **brute force method**

The accept-reject method also works for MC integration. Defining  $I_0$  as the area in  $[a, b]$  and  $f_{max}$  as the maximum of the function  $f(x)$  in this range. With a random number  $R_i$  we generate  $x_i$  and another random number  $R_j$  is used to accept or reject the pair of random numbers  $i, j$  according to:

$$\begin{aligned} \text{if } f(x_i) < R_j \cdot f_{max} &\rightsquigarrow \text{ reject} \\ \text{if } f(x_i) > R_j \cdot f_{max} &\rightsquigarrow \text{ accept} \end{aligned}$$

We count the number of trails with  $N_0$  and the number of accepted events with  $N$ . Then we obtain:

$$\begin{aligned} I &= \int_a^b f(x) dx \\ &= I_0 \frac{N}{N_0} \end{aligned}$$

The variance  $V[r] = (\delta(N))^2 = \sigma^2$  is (using binomial statistics with  $E[r] = N_0 P$  and  $V[r] = N_0 P(1 - P)$  with  $P = N/N_0$ ):

$$V[r] = N(1 - P)$$

With this we can calculate the uncertainty of the integral estimate  $\delta(I)$  as:

$$\frac{\delta I}{I} = \frac{I_0 \sigma / N_0}{I_0 N / N_0} = \sqrt{\frac{N(1 - P)}{N^2}}$$



## Chapter 3

# Probing the Structure of Matter

The force that keeps matter together is the strong force which is described by the theory of Quantum Chromo Dynamics (QCD). Basically everything is included in the QCD Lagrangian, which describes the non-abelian nature of QCD.

Probing the structure of matter is in analogy to optics: to resolve objects the wavelength  $\lambda$  of the probe has to be smaller than the size  $d$  of the target:  $\lambda < d$ . In all calculations below we assume *natural units*:  $\hbar = c = 1$ .

For an introduction to the standard model see [12]. Calculations of QCD processes (including all the details for the calculation) are described nicely in [13]. A theoretical description and a discussion on parton showers and Monte Carlo generators is in the *Pink Book* [14]. A detailed discussion on parton evolution is given in [15].

### 3.1 Kinematics and Cross Section definition

#### 3.1.1 Four-Vector Kinematics

Four-vectors are used to characterize fully the state and the motion of a particle.

$$(E, \mathbf{p}) \stackrel{\text{def}}{=} (p^0, p^1, p^2, p^3) = p^\mu \stackrel{\text{def}}{=} p \quad (3.1)$$

A four-vector is defined in a specific frame. Boost (or Lorentz-) invariant quantities can be defined from four-vectors. The simplest example is the invariant mass of a particle defined as:

$$E^2 - \mathbf{p}^2 = m^2 \quad (3.2)$$

Products of four-vectors are Lorentz invariant. The four-vector product is defined as:

$$A.B \stackrel{\text{def}}{=} A^0 B^0 - \mathbf{A}\mathbf{B} \quad (3.3)$$

In the collision of two particles,  $p_1$  and  $p_2$  the invariant mass of the system is given by:

$$\begin{aligned} s &= (P_1 + P_2)^2 = P_1^2 + P_2^2 + 2P_1.P_2 \\ &= M_1^2 + M_2^2 + 2(E_1 E_2 - \vec{P}_1 \vec{P}_2) \end{aligned} \quad (3.4)$$

In the center-of-mass of the two colliding particles we have  $|\vec{P}_1| = |\vec{P}_2|$ . Assuming  $M_1 = M_2$  we get:

$$s = (P_1 + P_2)^2 = 2M^2 + 2(E^2 + P^2) \quad (3.5)$$

with  $M = M_1 = M_2$ ,  $E = E_1 = E_2$  and  $P = |\vec{p}_1| = |\vec{p}_2|$ . In the case of  $E \gg M$  we obtain:

$$s = (P_1 + P_2)^2 = 4E_b^2 = E_{cm}^2 \quad (3.6)$$

with  $E_b$  being the beam energy and  $E_{cm}$  being the center-of-mass energy.

At LHC the energy of the colliding protons was at start up  $E_b = 450$  GeV giving a center-of-mass energy of  $\sqrt{s} = 900$  GeV, at present the energy of each proton beam is  $E_b = 3500$  GeV giving a center-of-mas energy of  $\sqrt{s} = 7$  TeV, the highest energy achieved in a collider.

If one of the colliding particles is at rest ( $P_2 = (M, 0)$ ), in a so-called *fixed-target* experiment, the energy available in the collision is (assuming the mass of the other particle to be small  $M_1 = 0$ ):

$$s = (P_1 + P_2)^2 = M^2 + 2E \cdot M \quad (3.7)$$

In a *fixed-target* experiment with a muon beam of  $E = 280$  GeV colliding with protons at rest, the available center-of-mass energy squared was  $s = (P_1 + P_2)^2 \approx 560 \text{ GeV}^2$  which gives  $\sqrt{s} = 24$  GeV. At HERA, a electron-proton collider at DESY, electrons with an energy of  $E_e = 27$  GeV were collided with protons of energy of  $E_p = 920$  GeV yielding  $\sqrt{s} \approx 315$  GeV.

### 3.1.2 Light Cone Variables

Some calculations become easier and the results are easier understood when using so-called *light-cone* variables instead of the Cartesian variables (see for a description and discussion [16]). Any four-vector defined as:

$$V = (V^0, V^1, V^2, V^3) = (V^0, V_\perp, V^3)$$

with  $V_\perp$  being a two-component vector, can be changed to its lightcone representation:

$$V^+ = \frac{1}{\sqrt{2}} (V^0 + V^3) \quad (3.8)$$

$$V^- = \frac{1}{\sqrt{2}} (V^0 - V^3) \quad (3.9)$$

$$V_\perp = (V^1, V^2) \quad (3.10)$$

We also have:

$$V^0 = \frac{1}{\sqrt{2}} (V^+ + V^-) \quad (3.11)$$

$$V^3 = \frac{1}{\sqrt{2}} (V^+ - V^-) \quad (3.12)$$

$$(3.13)$$



From the definition of a four-vector product in eq.(3.3) we obtain for two four-vectors  $V$  and  $W$ :

$$V.W = V^+W^- + V^-W^+ - V_\perp W_\perp \quad (3.14)$$

$$V.V = 2V^+V^- - V_\perp^2 \quad (3.15)$$

The light-cone components transform simpler under boosts along the  $z$ -axis: only the  $V^\pm$  components are affected under the boost. When a vector is highly boosted, the light-cone variables show easily the large and small components.

Sometimes, the light-cone variables are used to define the *Sudakov* decomposition:  $p = p^+ + p^- + k_t$  where here  $p^\pm$  and  $k_t$  have four components. Let us consider the following example to calculate the invariant mass of two colliding particles with momenta  $p_1 = \mathbf{p}_1^+ + \mathbf{p}_1^- + k_{t1}$  and  $p_2 = \mathbf{p}_2^+ + \mathbf{p}_2^- + k_{t2}$  with

$$\mathbf{p}_1^+ = (p_1^+, 0^-, \vec{0})$$

$$\mathbf{p}_1^- = (0^+, p_1^-, \vec{0})$$

$$k_{t1} = (0^+, 0^-, \vec{k}_{t1})$$

and analogously for  $\mathbf{p}_2$ . The invariant mass  $s = (p_1 + p_2)^2$  is then :

$$\begin{aligned} s &= (\mathbf{p}_1^+ + \mathbf{p}_2^+ + \mathbf{p}_1^- + \mathbf{p}_2^- + k_{t1} + k_{t2})^2 \\ &= 2(\mathbf{p}_1^+ + \mathbf{p}_2^+)(\mathbf{p}_1^- + \mathbf{p}_2^-) + (k_{t1} + k_{t2})^2 \\ &= 2p_1^+ p_2^- \end{aligned}$$

where the last line was obtained since  $p_1^- = p_2^+ = 0$  and  $\vec{k}_{t1} = -\vec{k}_{t2}$ .

Lorentz boost appear very simple in terms of lightcone variables. The boosted vector  $V'^0$  and  $V'^3$  are defined as (with a boost along the  $z$  axis with velocity  $v$ ) :

$$V'^0 = \frac{V^0 + vV^3}{\sqrt{1-v^2}} \quad (3.16)$$

$$V'^3 = \frac{vV^0 + V^3}{\sqrt{1-v^2}} \quad (3.17)$$

$$V'^1 = V^1 \quad (3.18)$$

$$V'^2 = V^2 \quad (3.19)$$

Then we can calculate the boosted lightcone components:

$$V'^+ = \frac{1}{\sqrt{2}} \frac{V^0 + vV^3 + vV^0 + V^3}{\sqrt{1-v^2}} \quad (3.20)$$

$$= \frac{1}{\sqrt{2}} \frac{(V^0 + V^3)(1+v)}{\sqrt{1-v^2}} \quad (3.21)$$

$$= \frac{1}{\sqrt{2}} \sqrt{\frac{(1+v)(1+v)}{(1-v)(1+v)}} (V^0 + V^3) \quad (3.22)$$

$$= \frac{1}{\sqrt{2}} \sqrt{\frac{(1+v)}{(1-v)}} (V^0 + V^3) \quad (3.23)$$

and similarly for  $V'^{-}$  with

$$V'^{-} = \frac{1}{\sqrt{2}} \sqrt{\frac{(1-v)}{(1+v)}} (V^0 - V^3) \quad (3.24)$$

Defining

$$\psi = \frac{1}{2} \log \frac{1+v}{1-v}$$

one obtains

$$e^\psi = e^{\frac{1}{2} \log \frac{1+v}{1-v}} = \sqrt{\frac{1+v}{1-v}}$$

and thus

$$V'^{+} = V^{+} e^\psi \quad (3.25)$$

$$V'^{-} = V^{-} e^{-\psi} \quad (3.26)$$

Consider a particle at rest with

$$p^{rest} = \left( \frac{m}{\sqrt{2}}, \frac{m}{\sqrt{2}}, 0 \right)$$

which is obtained from  $p = (m, 0, 0)$  in Cartesian coordinates. In a moving frame the momentum becomes:

$$p' = (p'^{+}, p'^{-}, 0) = \left( \frac{m}{\sqrt{2}} e^\psi, \frac{m}{\sqrt{2}} e^{-\psi}, 0 \right)$$

with

$$\begin{aligned} \frac{p'^{+}}{p'^{-}} &= e^{2\psi} \\ \rightsquigarrow \log \frac{p'^{+}}{p'^{-}} &= 2\psi \end{aligned}$$

we obtain the expression for rapidity:

$$\psi = y = \frac{1}{2} \log \frac{p'^{+}}{p'^{-}} \quad (3.27)$$

### 3.1.3 Cross Section definition

In general the cross section of the scattering of two particles  $p_1$  and  $p_2$  with masses  $m_1$  and  $m_2$  into any number of final state particles  $p_i$  is defined as:

$$d\sigma = \frac{1}{flux} \cdot dLips \cdot |M|^2$$

where  $|M|^2$  is the squared matrix element, which contains the physics,  $flux$  is the flux of the incoming particles defined as:

$$flux = 4\sqrt{(p_1 p_2)^2 - m_1^2 m_2^2} \quad (3.28)$$

and  $dLips$  is the Lorentz-invariant-phase-space defined as

$$dLips = (2\pi)^4 \delta^4 \left( -p_1 - p_2 + \sum_i p_i \right) \prod_{i>2} \frac{d^4 p_i}{(2\pi)^3} \delta(p_i^2 - m_i^2) \quad (3.29)$$

$$= (2\pi)^4 \delta^4 \left( -p_1 - p_2 + \sum_i p_i \right) \prod_{i>2} \frac{d^3 p_i}{(2\pi)^3 2E_i} \quad (3.30)$$

$$= (2\pi)^4 \delta^4 \left( -p_1 - p_2 + \sum_i p_i \right) \prod_{i>2} \frac{1}{(2\pi)^3} \frac{dp_i^+}{p_i^+} d^2 p_{t i} \quad (3.31)$$

The cross section for a  $2 \rightarrow 2$  process of  $p_1 + p_2 \rightarrow p_3 + p_4$  can be then written as (for massless incoming particles) :

$$\frac{d\sigma}{dt} = \frac{1}{16\pi} \frac{1}{s^2} |M|^2 \quad (3.32)$$

If one particle has mass, like the virtual photon with virtual mass  $Q^2$ , then the formula is modified to (for  $p_1^2 = -Q^2$ ) :

$$\frac{d\sigma}{dt} = \frac{1}{16\pi} \frac{1}{s + Q^2} \frac{1}{s} |M|^2 \quad (3.33)$$

with  $s, t$  being the Mandelstam variables:

$$s = (p_1 + p_2)^2 = (p_3 + p_4)^2 \quad (3.34)$$

$$t = (p_1 - p_3)^2 = (p_2 - p_4)^2 \quad (3.35)$$

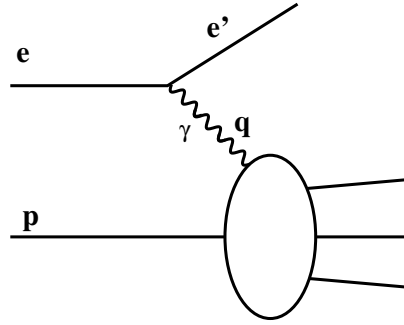
$$u = (p_1 - p_4)^2 = (p_2 - p_3)^2 \quad (3.36)$$

$$s + t + u = m_1^2 + m_2^2 + m_3^2 + m_4^2 \quad (3.37)$$

## 3.2 The Quark Parton Model

In analogy to optics, photons can be used to probe the structure of matter. In Quantum Theory every particle has a particular wave-length, so any particle with a small enough wave-length can be used as a probe to measure the structure of a target: photons from electron or muons,  $W/Z$  bosons and also jets produced in high energy collisions can be used to extract information on the colliding hadrons.

In the following the structure of the proton as tested in Deep Inelastic Scattering (DIS) of electrons (or muons) on a proton target (fig. 3.1) will be discussed. The following invariant quantities

Figure 3.1: General diagram for DIS scattering  $e + p \rightarrow e' + X$ 

can be defined (here the electron four-vector is denoted with  $e$ , the scattered electron with  $e'$  and the proton four vector with  $p$ ):

$$s = (e + p)^2 \quad (3.38)$$

$$q^2 = (e - e')^2 \stackrel{\text{def}}{=} -Q^2 \quad (3.39)$$

$$y = \frac{p \cdot q}{p \cdot e} \quad (3.40)$$

$$x_{Bj} = \frac{Q^2}{2p \cdot q} \quad (3.41)$$

If we neglect the electron and proton masses, then we obtain:

$$Q^2 = x \cdot y \cdot s \quad (3.42)$$

$$\begin{aligned} W^2 &= (q + p)^2 = -Q^2 + 2q \cdot p \\ &= -Q^2 + y s = -Q^2 + \frac{Q^2}{x} \end{aligned} \quad (3.43)$$

where the photon- $(\gamma)$  four-vector is  $q$ . The "invariant mass" (or virtuality) of the photon is given by  $Q^2 = -q^2$ , the "energy" of the photon is given by  $y$  which reduces to  $y = 1 - E'/E$  in the proton rest frame with  $E$  ( $E'$ ) being the energy of the electron (scattered electron) in the proton rest frame. The quantity  $x_{Bj}$  is called *x-Bjorken* after its inventor James Bjorken in 1969 [17]. Please note, that in the quark parton model (QPM)  $x_{Bj}$  can be associated with the momentum fraction the quark takes of the proton momentum (as we will discuss later). This interpretation is only true in the QPM in DIS, not if higher orders are included nor in hadron-hadron scattering.

Deep inelastic scattering is defined by:

$$\begin{aligned} Q^2 &\gg m_p^2 && \text{deep} \\ W^2 &\gg m_p^2 && \text{inelastic} \end{aligned}$$

where  $m_p$  is the proton mass.

The general form of the cross section in DIS is given by (see [12,14]):

$$d\sigma \sim L_e^\mu W_{\mu\nu} \quad (3.44)$$

with the leptonic  $L_e^{\mu\nu}$  and hadronic  $W^{\mu\nu}$  tensors given by:

$$L_e^{\mu\nu} = \frac{1}{2} \text{Tr}((\not{\epsilon}' + m)\gamma^\mu(\not{\epsilon} + m)\gamma^\nu) \quad (3.45)$$

$$W^{\mu\nu} = -W_1 g^{\mu\nu} + \frac{W_2}{M^2} p^\mu p^\nu + \frac{W_4}{M^2} q^\mu q^\nu + \frac{W_5}{M^2} (p^\mu q^\nu + q^\mu p^\nu) \quad (3.46)$$

where the structure functions  $W_i$  are introduced to parametrize the ignorance about the details of the structure of the proton. On very general grounds, assuming current conservation and symmetries only two out of the five structure functions  $W$  are independent (for unpolarized scattering). After a bit of algebra and rewriting using  $W_1 = F_1$  and  $\nu W_2 = F_2$  with  $\nu = \frac{Q^2 + W^2 - M^2}{2M}$ , we obtain the master formula for DIS scattering [14][p 89] :

$$\begin{aligned} \frac{d\sigma}{dx dQ^2} &= \frac{4\pi\alpha^2}{Q^4} \left[ (1 + (1-y)^2) F_1 + \frac{(1-y)}{x} (F_2 - 2xF_1) \right] \\ &= \frac{2\pi\alpha^2}{xQ^4} \left[ (1 + (1-y)^2) F_2 - \frac{y^2}{2} F_L \right] \end{aligned} \quad (3.47)$$

where in the second line the longitudinal structure function  $F_L = F_2 - 2xF_1$  is introduced. In case of purely transverse polarized photon interactions the *Callan-Cross* relation gives  $F_2 = 2xF_1$ . The *structure functions*  $F_1$ ,  $F_2$  and  $F_L$  are what can be measured in experiment and what will be the subject in the following sections.

The early measurements of Deep Inelastic Scattering lead to the interpretation of the structure function  $F_2$  in terms of the quark-parton model (QPM) where the proton is seen as composed of objects, the quarks and gluons (generically called partons). Inelastic scattering is interpreted as a incoherent superposition of scatterings on the individual partons. These partons (quarks) are supposed to be quasi-free such that any interaction between them can be neglected. A very nice and understandable discussion of this is in the original article by J. Bjorken and E. Paschos [17].

Whether the partons can be regarded as free during the interaction can be estimated by calculating the interaction and fluctuation time in DIS scattering (as done in the original paper [17]). If the interaction time  $\tau_i$  is small compared to the fluctuation time  $\tau_f$  in which a particle can fluctuate into partons, then the partons can be considered as free.

Assume scattering at large energies in the center-of-mass frame of the electron-proton system, where the electron mass can be neglected (see fig 3.2).

The proton splits into two partons  $q_1$  and  $q_2$  with momentum fractions  $x$  of the proton momentum  $P = (E_p, \vec{p})$ :

$$\begin{aligned} q_1 &= xP \\ q_2 &= (1-x)P \end{aligned}$$

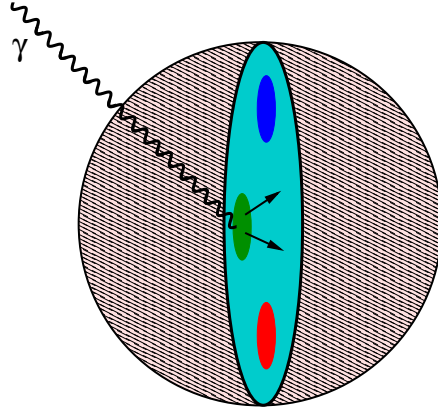


Figure 3.2: The proton in the high energy center-of-mass frame (or in the infinite momentum frame) looks like a pancake. The interaction time is small compared to the time where a parton can fluctuate into others ( $qq$ ).

The electron has four-momentum  $e = (E_p, \vec{p})$  and the photon has momentum  $q = e - e'$  with  $e'$  being the four momentum of the scattered electron. We now calculate the interaction time  $\tau_i = 1/\Delta E_{electron} = 1/E_{photon}$ . From energy momentum conservation we get  $e' = e - q$  and

$$e'^2 = (e - q)^2 = e^2 - 2e \cdot q + q^2$$

Since  $e^2 = e'^2 = m_e^2 \rightarrow 0$  we obtain with  $Q^2 = -q^2$

$$0 = -2e \cdot q - Q^2$$

and

$$Q^2 = -2e \cdot q = -2(E_\gamma E_p + \vec{p}_p \vec{q}) \quad (3.48)$$

where we have used the relations  $E_e = E_p$  (for  $m_p = m_0 = 0$ ) and  $\vec{p}_p = -\vec{p}_e$  valid in the center-of-mass frame. Using  $x = Q^2/(2p \cdot q)$  we obtain:

$$\begin{aligned} p \cdot q &= E_\gamma E_p - \vec{p}_p \vec{q} \\ \frac{Q^2}{2x} &= E_\gamma E_p - \vec{p}_p \vec{q} \\ \vec{p}_p \vec{q} &= -\frac{Q^2}{2x} + E_\gamma E_p \end{aligned}$$

Inserting this into eq.(3.48) we obtain:

$$Q^2 = -2E_\gamma E_p + \frac{2Q^2}{2x} - 2E_\gamma E_p \quad (3.49)$$

$$\rightsquigarrow Q^2 \left(1 - \frac{1}{x}\right) = -4E_\gamma E_p \quad (3.50)$$

$$\rightsquigarrow E_\gamma = -\frac{Q^2 \left(1 - \frac{1}{x}\right)}{4E_p} \quad (3.51)$$

The next step is to calculate the fluctuation time  $\Delta E_{qq}$  which is the energy of the  $qq$  pair.

$$\Delta E_{qq} = E_1 + E_2 - E_p$$

With  $q_1 = (E_1, \vec{k}_t, xP)$  and  $q_2 = (E_2, -\vec{k}_t, (1-x)P)$  using  $\sqrt{1+x} \approx 1 + (1/2)x + \dots$  we obtain:

$$\begin{aligned} E_1 &= \sqrt{(xP)^2 + k_t^2} = xP \sqrt{1 + \frac{k_t^2}{(xP)^2}} \\ &\approx xP \left( 1 + \frac{1}{2} \frac{k_t^2}{(xP)^2} + \dots \right) \\ E_2 &= \sqrt{((1-x)P)^2 + k_t^2} = (1-x)P \sqrt{1 + \frac{k_t^2}{((1-x)P)^2}} \\ &\approx (1-x)P \left( 1 + \frac{1}{2} \frac{k_t^2}{((1-x)P)^2} + \dots \right) \end{aligned}$$

Inserting the above into the expression for  $\Delta E_{qq}$

$$\begin{aligned} \Delta E_{qq} &= E_1 + E_2 - E_p \\ &= xP + \frac{1}{2} \frac{k_t^2}{xP} + (1-x)P + \frac{1}{2} \frac{k_t^2}{(1-x)P} - P \\ &= \frac{1}{2} \frac{(1-x)k_t^2 + xk_t^2}{x(1-x)P} \\ &= \frac{1}{2} \frac{k_t^2}{x(1-x)P} \end{aligned}$$

With

$$\tau_f = \frac{1}{\Delta E_{qq}} = \frac{2x(1-x)P}{k_t^2} \approx \frac{2xP}{k_t^2} \quad (3.52)$$

$$\tau_i = \frac{1}{\Delta E_{ee'}} = \frac{4P}{Q^2 \left(\frac{1-x}{x}\right)} \approx \frac{4xP}{Q^2} \quad (3.53)$$

where the last approximation is done for  $x \ll 1$ . We now have:

$$\frac{\tau_{interaction}}{\tau_{fluctuation}} \approx \frac{4xP}{Q^2} \frac{k_t^2}{2xP} = \frac{2k_t^2}{Q^2} \quad (3.54)$$

Thus for small  $k_t$  with  $k_t^2 \ll Q^2$  the interaction time is much smaller than the fluctuation time, and the partons can be considered as frozen and therefore behave as free partons.

### 3.3 Cross Section in DIS

In the previous section we have seen that the partons inside the proton can be considered free as long as transverse momentum squared  $k_t^2$  is small compared to  $Q^2$ .

In the following we calculate the cross section for  $eP \rightarrow e'X$  from the partonic cross section  $ep_q \rightarrow e'p'_q$  with  $p_q$  being the four-momentum of any type of quark with momentum fraction  $\xi$  such that  $p_q = \xi P$ . The Mandelstam variables are then:

$$\hat{s} = (e + p_q)^2 = 2e \cdot p_q \quad (3.55)$$

$$\hat{u} = (p_q - e')^2 = -2p_q \cdot e' \quad (3.56)$$

$$\hat{t} = (e - e')^2 = -Q^2 \quad (3.57)$$

$$(3.58)$$

The matrix element squared for  $ep_q \rightarrow e'p'_q$  is [12][p 124]:

$$|M|^2 = 2e_q^2(4\pi\alpha)^2 \frac{\hat{s}^2 + \hat{u}^2}{\hat{t}^2} \quad (3.59)$$

with  $e_q$  being the electric charge of the parton. Using the DIS variables (see eq.(3.38)) with  $q = e - e'$  gives:

$$y = \frac{q \cdot P}{e \cdot P} = \frac{q \cdot p_q}{e \cdot p_q} = 1 - \frac{e' \cdot p_q}{e \cdot p_q} = 1 + \frac{\hat{u}}{\hat{s}} \quad (3.60)$$

The matrix element can then be expressed as:

$$|M|^2 = 2e_q^2(4\pi\alpha)^2 \frac{1}{Q^4} (\hat{s}^2 + \hat{s}^2(y-1)^2) \quad (3.61)$$

$$= 2e_q^2(4\pi\alpha)^2 \frac{\hat{s}^2}{Q^4} (1 + (1-y)^2) \quad (3.62)$$

With this we obtain the cross section:

$$\frac{d\sigma}{d\hat{t}} = \frac{d\sigma}{dQ^2} = \frac{1}{16\pi\hat{s}^2} |M|^2 \quad (3.63)$$

$$= \frac{2e_q^2(4\pi\alpha)^2\hat{s}^2}{16\pi\hat{s}^2} \frac{1}{Q^4} (1 + (1-y)^2) \quad (3.64)$$

$$= (2\pi\alpha^2 e_q^2) \frac{1}{Q^4} (1 + (1-y)^2) \quad (3.65)$$

Before we compare this expression to the cross section for DIS in eq.(3.47) we investigate the meaning of  $\xi$ . Using the mass-shell condition (the quarks are assumed to be massless) we obtain:

$$p_q'^2 = (p_q + q)^2 = q^2 + 2p_q \cdot q + p_q^2 \quad (3.66)$$

$$= -Q^2 + 2p_q \cdot q = -Q^2 + 2\xi P \cdot q \quad (3.67)$$

$$= -2P \cdot q \cdot x + 2\xi P \cdot q \quad (3.68)$$

$$= -2P \cdot q(x - \xi) \quad (3.69)$$



thus we obtain for massless partons  $p_q^2 = p_q'^2 = 0$  that  $x = \xi$ . Using

$$\int dx \delta(x - \xi) = 1$$

we can rewrite eq.(3.65) as:

$$\frac{d\sigma^2}{dx dQ^2} = (4\pi\alpha^2) \frac{1}{Q^4} (1 + (1 - y)^2) e_q^2 \frac{1}{2} \delta(x - \xi) \quad (3.70)$$

Now we can compare eq.(3.70) with eq.(3.47) and find:

$$\hat{F}_1 = \frac{1}{2} e_q^2 \delta(x - \xi) \quad (3.71)$$

$$\hat{F}_2 = 2x \hat{F}_1 = x e_q^2 \delta(x - \xi) \quad (3.72)$$

Thus the structure function  $\hat{F}_2$  gives the probability to find a quark with momentum fraction  $x = \xi$ .

However, measurements have shown that the structure function  $F_2$  is not a delta function but rather a distribution, telling that the partons inside the proton carry a range of momentum fractions. Thus we are forced to introduce a distribution  $q(\xi) d\xi$  which represents the probability to find a quark that carried a momentum fraction  $\xi$  in the range  $\xi$  and  $\xi + d\xi$  within  $0 \leq \xi \leq 1$ .

The proton structure functions  $F_i$  are obtained by weighting the quark structure functions  $\hat{F}_i$  with the probability density functions  $q(\xi)$ :

$$F_2(x) = 2x F_1(x) = \sum_{q, \bar{q}} \int d\xi q(\xi) x \cdot e_q^2 \delta(x - \xi) \quad (3.73)$$

$$= \sum_{q, \bar{q}} e_q^2 x q(x) \quad (3.74)$$

Since there are different quark species in the proton, the electromagnetic structure function as obtained by scattering a charged lepton on a proton is:

$$F_2^{em}(x) = x \left[ \frac{4}{9} (u + \bar{u} + c + \bar{c}) + \frac{1}{9} (d + \bar{d} + s + \bar{s} + b + \bar{b}) \right] \quad (3.75)$$

with  $u, \bar{u}, \dots$  being the quark (antiquark) density functions.

Since the proton is build from two  $u_v$ -type and one  $d_v$ -type valence quarks, one can define the following sum rules:

$$\int_0^1 dx u_v(x) = 2 \quad (3.76)$$

$$\int_0^1 dx d_v(x) = 1 \quad (3.77)$$

## H1 and ZEUS

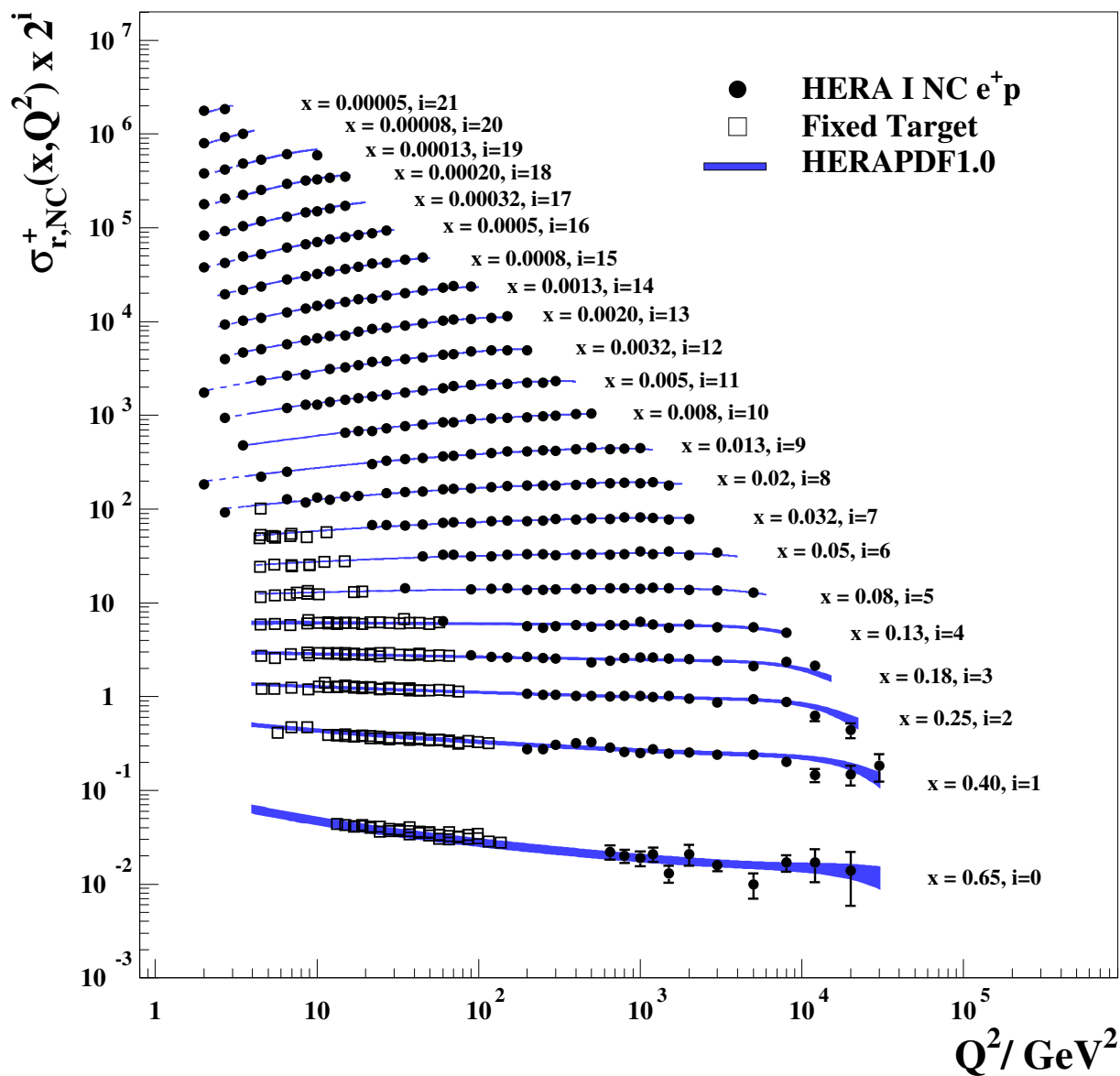


Figure 3.3: The structure function  $F_2(x, Q^2)$  as a function of  $Q^2$  as measured in DIS scattering  $e + p \rightarrow e' + X$  at HERA [18].

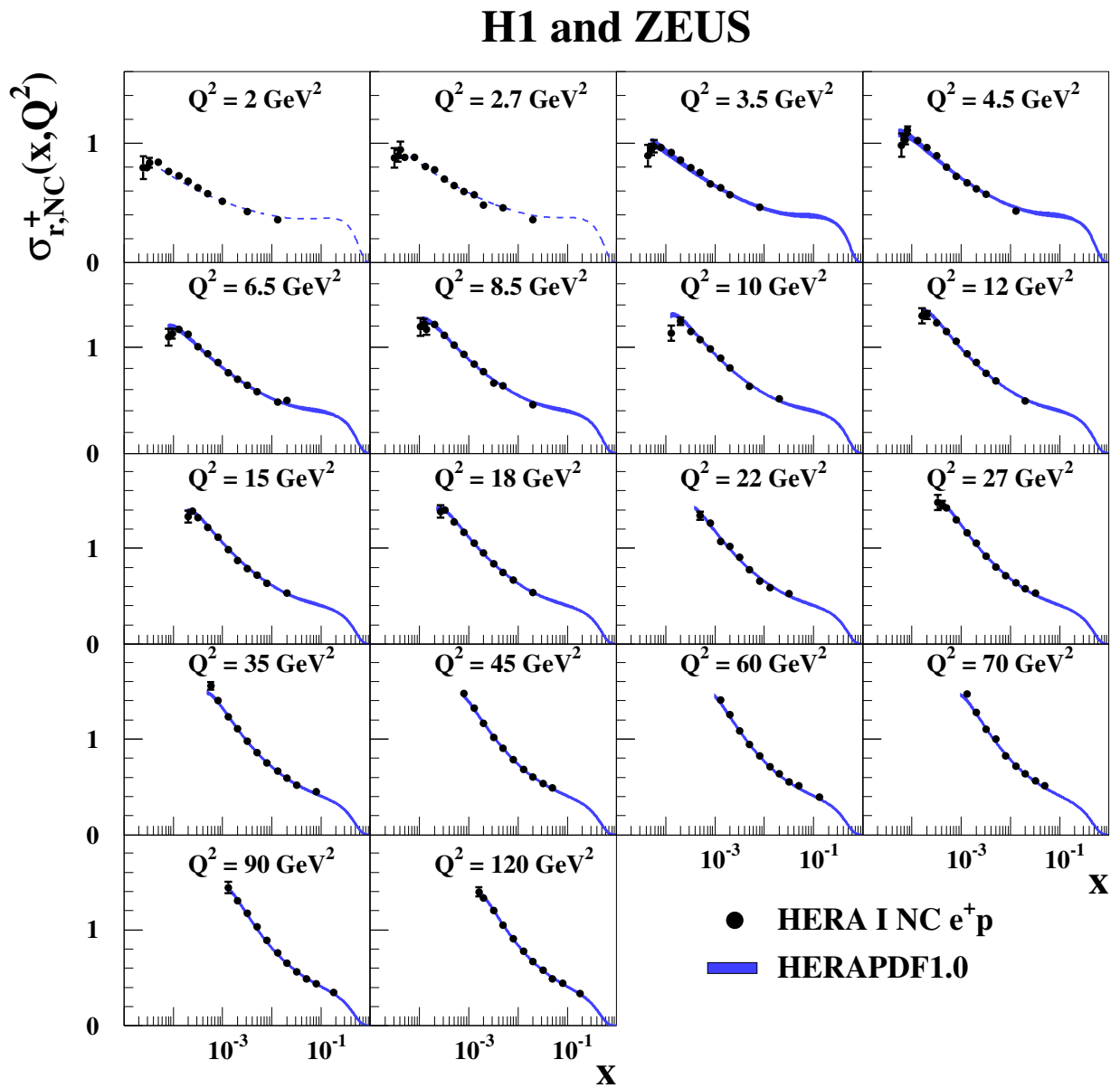


Figure 3.4: The structure function  $F_2(x, Q^2)$  as a function of  $x$  as measured in DIS scattering  $e+p \rightarrow e' + X$  at HERA [18].

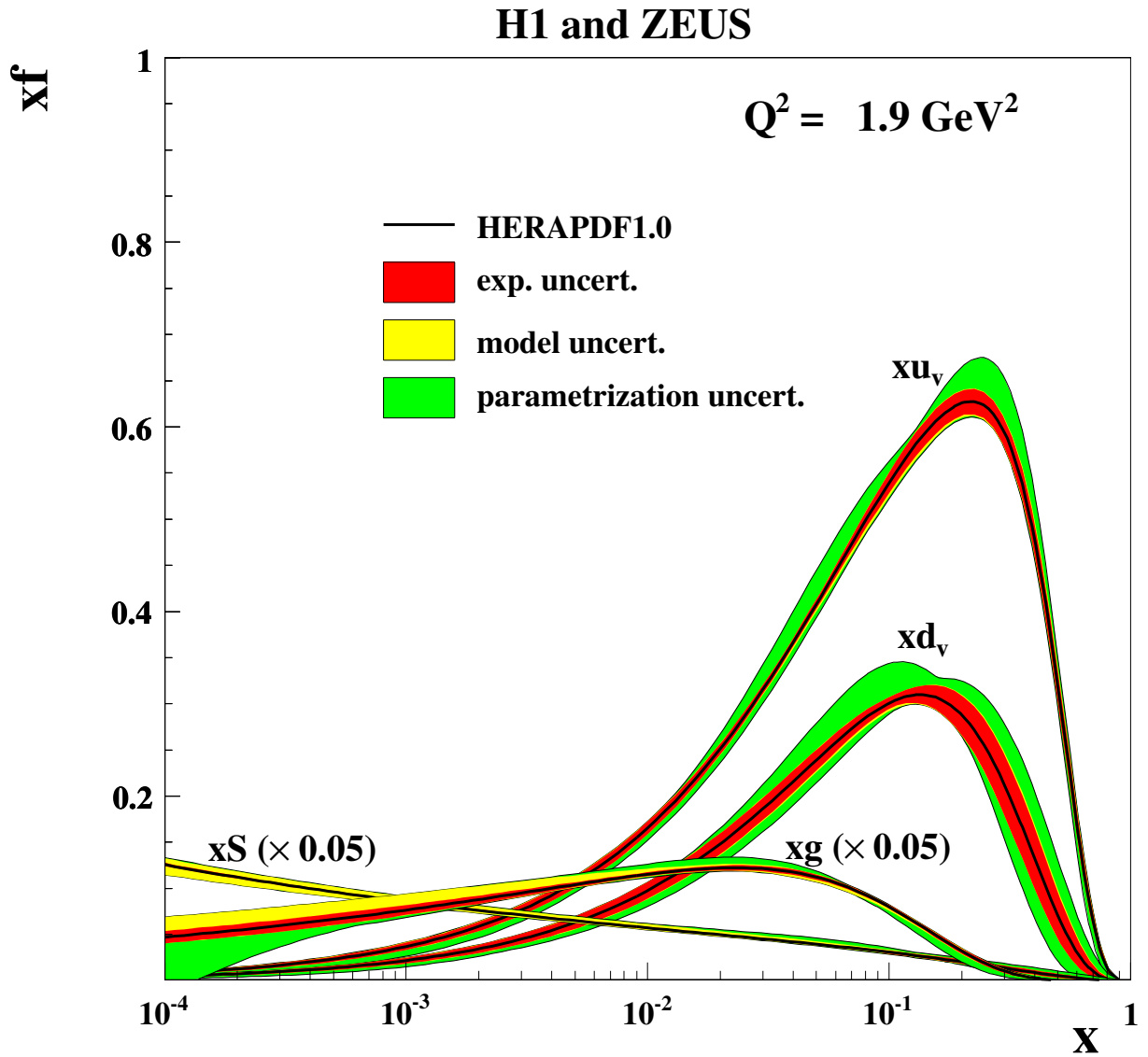


Figure 3.5: The parton density functions as a function of  $x$  extracted from DIS scattering  $e + p \rightarrow e' + X$  at HERA [18].

However it was found from experiment that the momentum sum over all quarks gives only about 50 % of the proton momentum:  $\int_0^1 dx x \sum_i q_i(x) \sim 0.5$  (note the relation to expectation values as discussed in the first chapter). If the QPM picture is correct, the remaining 50 % of the proton momentum is carried by partons other than the quarks, namely the gluons, such that

$$\int_0^1 dx x [\text{all pdfs}] = 1 \quad (3.78)$$

The momentum sum rules are subject of the exercises.

In fig. 4.1 the measurement of  $F_2(x, Q^2)$  as a function of  $Q^2$  obtained at HERA [18] is shown. In fig. 4.2  $F_2(x, Q^2)$  as a function of  $x$  is shown. In fig. 3.5 the parton density functions for quarks and gluons as obtained from the measurement of  $F_2(x, Q^2)$  is shown.

The measurements show, that the structure function  $F_2$  depends also on  $Q^2$ , which is not predicted in the simple QPM. These *scaling violations* are subject of the next sections.

### 3.4 The photon-proton cross section

The cross section for  $e + p_q \rightarrow e' + p'_q$  can be separated into two parts: the part at the lepton vertex and the part at the quark vertex. In the following we calculate the cross section for  $\gamma^* p_q \rightarrow p'_q$ . The matrix element for  $\gamma^* p_q \rightarrow p'_q$  can be found in [12][section 10.2]:

$$\begin{aligned} |M|^2 &= 2e_q^2 e^2 p_{q \cdot q} \\ &= 8\pi\alpha e_q^2 p_{q \cdot q} \end{aligned}$$

with  $\alpha = e^2/(4\pi)$ . We introduce

$$z = \frac{Q^2}{2q \cdot p_q} \quad (3.79)$$

The cross section is then:

$$\sigma = \int \frac{1}{flux} dLips |M|^2 \quad (3.80)$$

$$= 2\pi\alpha e_q^2 \cdot 2\pi\delta((p_q + q)^2) \quad (3.81)$$

$$= 2\pi\alpha e_q^2 \cdot 2\pi\delta(2p_q \cdot q(1 - z)) \quad (3.82)$$

$$= \frac{4\pi^2\alpha}{2p_q \cdot q} e_q^2 \delta(1 - z) \quad (3.83)$$

where we have used  $z = Q^2/(2q \cdot p_q)$  and for the *flux*:

$$flux = 4\sqrt{(p_q \cdot q)^2 - m_1^2 m_2^2} \quad (3.84)$$

$$= 4p_q \cdot q \quad (3.85)$$

and for  $dLips$  using  $(q + p_q)^2 = -Q^2 + Q^2/z$ :

$$\int dLips = (2\pi)^4 \int \delta^4(-p_q - q + p'_q) \frac{d^4 p'_q}{(2\pi)^3} \delta(p_q'^2 - m_q'^2) \quad (3.86)$$

$$= 2\pi \delta(p_q'^2) \quad (3.87)$$

$$= 2\pi \delta((p_q + q)^2) \quad (3.88)$$

We now compare full expression for  $e + p_q \rightarrow e' + p'_q$  as given in eq.(3.70) with the cross section for  $\gamma^* p_q \rightarrow p'_q$  of eq.(3.83):

$$\frac{d\sigma^2}{dx dQ^2} = (4\pi\alpha^2) \frac{1}{Q^4} (1 + (1-y)^2) e_q^2 \frac{1}{2} \delta(x - \xi) \quad (3.89)$$

$$= \frac{\alpha}{2\pi Q^2} (1 + (1-y)^2) \frac{4\pi^2 \alpha}{Q^2} e_q^2 \frac{1}{\xi} \delta\left(\frac{x}{\xi} - 1\right) \quad (3.90)$$

$$= \frac{\alpha}{2\pi Q^2} (1 + (1-y)^2) \frac{4\pi^2 \alpha}{Q^2} e_q^2 \frac{z}{x} \delta(z - 1) \quad (3.91)$$

$$= \frac{\alpha}{2\pi Q^2 x} (1 + (1-y)^2) \frac{4\pi^2 \alpha}{2p_{q \cdot q}} e_q^2 \delta(1 - z) \quad (3.92)$$

$$= \frac{\alpha}{2\pi Q^2 x} (1 + (1-y)^2) \sigma_0(z) e_q^2 \delta(1 - z) \quad (3.93)$$

where we have used  $z\xi = x$  with  $x = Q^2/(ys)$ . With the Jacobean  $\frac{\delta x}{\delta y} = \frac{x}{y}$  we obtain:

$$\frac{d\sigma^2}{dy dQ^2} = \frac{d\sigma^2}{dx dQ^2} \frac{\delta x}{\delta y} = \frac{\alpha}{2\pi Q^2 y} (1 + (1-y)^2) \sigma_0(z) e_q^2 \delta(1 - z) \quad (3.94)$$

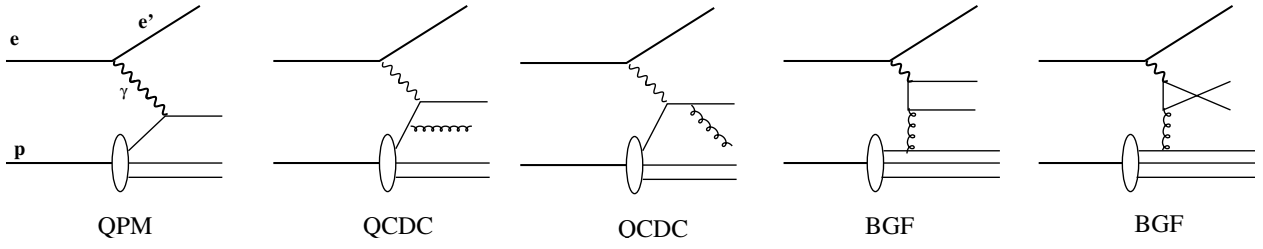
We have now separated the photon flux  $F_\gamma(y, Q^2)$  from the hadronic interaction. This is also called the *equivalent photon approximation*:

$$\begin{aligned} \frac{d\sigma^2}{dy dQ^2} &= F_\gamma(y, Q^2) \frac{4\pi^2 \alpha}{Q^2} e_q^2 F_2 \\ F_\gamma(y, Q^2) &= \frac{\alpha}{2\pi Q^2 y} (1 + (1-y)^2) \end{aligned}$$

### 3.5 $\mathcal{O}(\alpha_s)$ contribution to DIS

We can apply now this method to calculate the  $\mathcal{O}(\alpha_s)$  contributions to the total DIS cross section, which is the QCD Compton (QCDC)  $e + q \rightarrow e' + q' + g$  and the boson-gluon fusion (BGF)  $e + g \rightarrow e' + q + \bar{q}$  processes. By separating the lepton vertex from the hadron vertex, the calculations can be significantly simplified, since instead of a  $2 \rightarrow 3$  process we just need to calculate the  $2 \rightarrow 2$  subprocess (Fig. 3.6).

The matrix elements for both QCDC and BGF are singular in  $\hat{t}$ . Since we are interested in the dominant contribution to the cross section, we can take the limit of  $\hat{t} \rightarrow 0$ . We express  $\hat{t}$  with the

Figure 3.6: The  $\mathcal{O}(\alpha_s)$  contributions to  $e + p \rightarrow e' X$ .

transverse momentum  $k_t$ . After some algebra we obtain (the explicit calculation is shown in the appendix 8.1):

$$k_t^2 = \frac{\hat{t}\hat{u}\hat{s}}{(\hat{s} + Q^2)^2} \quad (3.95)$$

using  $z = Q^2/(2q \cdot p_2)$  where  $q$  ( $p_2$ ) are the photon (parton) four-momenta, we obtain in the limit of small  $\hat{t}$  (with  $\hat{u} = -Q^2 - \hat{s}$ ):

$$k_t^2 = -\hat{t}(1 - z) \quad (3.96)$$

The cross section is then obtained by:

$$\frac{d\sigma}{dk_t^2} = \frac{1}{16\pi} \frac{1}{\hat{s} + Q^2} \frac{1}{\hat{s}} \frac{1}{1 - z} |M|^2 \quad (3.97)$$

### 3.5.1 QCDC process

The matrix element for the QCD Compton process is given in [12][section 10.4]. Here we concentrate to isolate the dominant part of the matrix element (small  $t$  approximation):

$$|M|^2 = 32\pi^2 (e_q^2 \alpha_s) \frac{4}{3} \left[ \frac{-\hat{t}}{\hat{s}} - \frac{\hat{s}}{\hat{t}} + \frac{2\hat{u}Q^2}{\hat{s}\hat{t}} \right] \quad (3.98)$$

$$= 32\pi^2 (e_q^2 \alpha_s) \frac{4-1}{3} \frac{1}{\hat{t}} \left[ \hat{s} - \frac{2Q^2(-Q^2 - \hat{s})}{\hat{s}} - \frac{2Q^2(-\hat{t})}{\hat{s}} + \frac{\hat{t}^2}{\hat{s}} \right] \quad (3.99)$$

$$\rightsquigarrow \text{small } \hat{t} \text{ approximation} \quad (3.100)$$

$$\approx 32\pi^2 (e_q^2 \alpha_s) \frac{4-1}{3} \frac{1}{\hat{t}} \left[ \hat{s} + \frac{2Q^2(Q^2 + \hat{s})}{\hat{s}} + \dots \right] \quad (3.101)$$

$$= 32\pi^2 (e_q^2 \alpha_s) \frac{4-1}{3} \frac{1}{\hat{t}} \left[ \hat{s} + \frac{2Q^2}{1-z} + \dots \right] \quad (3.102)$$

$$= 32\pi^2 (e_q^2 \alpha_s) \frac{4-1}{3} \frac{1}{t} \left[ \frac{Q^2(1+z^2)}{z(1-z)} + \dots \right] \quad (3.103)$$

$$= 32\pi^2 (e_q^2 \alpha_s) \frac{(1-z)Q^2}{k_t^2} \frac{1}{z} P_{qq}(z) \quad (3.104)$$

where we have introduced the splitting function  $P_{qq}(z)$  with  $z = \frac{Q^2}{2q \cdot p_q}$ :

$$P_{qq} = \frac{4}{3} \frac{1+z^2}{1-z} \quad (3.105)$$

Inserting eq.(3.104) into eq.(3.97) we obtain:

$$\frac{d\sigma}{dk_t^2} = \frac{1}{16\pi} \frac{1}{\hat{s} + Q^2} \frac{1}{\hat{s}} \frac{1}{1-z} |M|^2 \quad (3.106)$$

$$= \frac{1}{16\pi} \frac{1}{\hat{s} + Q^2} \frac{1}{\hat{s}} \frac{1}{1-z} 32\pi^2 (e_q^2 \alpha_s) \frac{(1-z) Q^2}{k_t^2} P_{qq}(z) \quad (3.107)$$

$$= \frac{4\pi^2 \alpha}{\hat{s}} e_q^2 \frac{\alpha_s}{2\pi} \frac{1}{k_t^2} P_{qq}(z) \quad (3.108)$$

$$= \sigma_0 e_q^2 \frac{\alpha_s}{2\pi} \frac{1}{k_t^2} P_{qq}(z) \quad (3.109)$$

In order to obtain the contribution to the total cross section, we must integrate over  $k_t$ :

$$\sigma^{QCDC} = \int_{k_{tmin}}^{k_{tmax}} dk_t^2 \frac{d\sigma}{dk_t^2} \quad (3.110)$$

$$= \sigma_0 e_q^2 \frac{\alpha_s}{2\pi} P_{qq}(z) \log \frac{k_{tmax}^2}{k_{tmin}^2} \quad (3.111)$$

where  $k_{tmax}$  is the maximal  $p_t$  that can be reached:

$$k_{tmax}^2 = \frac{\hat{s}}{4} = \frac{Q^2(1-z)}{4z} \quad (3.112)$$

The integral in Eq.(3.111) is divergent for  $k_{tmin} \rightarrow 0$ , therefore we need to introduce a lower (artificial) cut,  $k_{tmin} = \kappa$ . We then obtain:

$$\begin{aligned} \sigma^{QCDC} &= \sigma_0 e_q^2 \frac{\alpha_s}{2\pi} P_{qq}(z) \log \frac{Q^2(1-z)}{4z\kappa^2} + \dots \\ &= \sigma_0 e_q^2 \frac{\alpha_s}{2\pi} P_{qq}(z) \left[ \log \frac{Q^2}{\kappa^2} + \log \frac{1-z}{4z} + \dots \right] \end{aligned}$$

In order to obtain a measurable cross section, we must include the parton density functions. We recall also the QPM result:

$$\sigma^{QPM} = \sigma_0 e_q^2 \int \delta(1-z) f_q(\xi) \delta(x - z\xi) dz d\xi \quad (3.113)$$

$$\sigma^{QPM} = \sigma_0 e_q^2 \int \frac{d\xi}{\xi} f_q(\xi) \delta\left(\frac{x}{\xi} - 1\right) \quad (3.114)$$

$$(3.115)$$



and for QCDC:

$$\sigma^{QCDC} = \sigma_0 e_q^2 \frac{\alpha_s}{2\pi} \int f_q(\xi) \delta(x - z\xi) dz d\xi P_{qq}(z) \left( \log \frac{Q^2}{\kappa^2} + \log \frac{1-z}{4z} + \dots \right) \quad (3.116)$$

$$\sigma^{QCDC} = \sigma_0 e_q^2 \frac{\alpha_s}{2\pi} \int \frac{d\xi}{\xi} f_q(\xi) P_{qq} \left( \frac{x}{\xi} \right) \left( \log \frac{Q^2}{\kappa^2} + \log \frac{1-z}{4z} + \dots \right) \quad (3.117)$$

We can connect this with the expression for the structure function  $F_2(x, Q^2)$  (see eq.(3.47):

$$\sigma^{\gamma p} = \frac{4\pi\alpha}{Q^2} F_2(x, Q^2) = \frac{F_2(x, Q^2)}{x} \sigma_0 \quad (3.118)$$

$$\frac{F_2}{x} = \frac{\sigma^{\gamma p}}{\sigma_0} = \sum e_q^2 \int \frac{d\xi}{\xi} f_q(\xi) \left[ \delta \left( 1 - \frac{x}{\xi} \right) + \right. \quad (3.119)$$

$$\left. \frac{\alpha_s}{2\pi} P_{qq} \left( \frac{x}{\xi} \right) \left[ \log \left( \frac{Q^2}{\kappa^2} \right) + \log \left( \frac{1-z}{4z} \right) + \dots \right] + C_q(z, \dots) \right] \quad (3.120)$$

### 3.5.2 BGF process

The matrix element for the boson gluon fusion process  $\gamma^* g \rightarrow q\bar{q}$  is given in :

$$|M|^2 = 32\pi^2 (e_q^2 \alpha \alpha_s) \frac{1}{2} \left[ \frac{\hat{u}}{\hat{t}} + \frac{\hat{t}}{\hat{u}} - \frac{2\hat{s}Q^2}{\hat{t}\hat{u}} \right] \quad (3.121)$$

$$\rightsquigarrow \text{small } \hat{t} \text{ approximation} \quad (3.122)$$

$$= 32\pi^2 (e_q^2 \alpha \alpha_s) \frac{1}{2} \frac{1}{\hat{t}} \left[ \hat{u} - \frac{2\hat{s}Q^2}{\hat{u}} \right] \quad (3.123)$$

$$= 32\pi^2 (e_q^2 \alpha \alpha_s) \frac{1}{2} \frac{1}{\hat{t}} \left[ -(Q^2 + \hat{s}) + \frac{2\hat{s}Q^2}{Q^2 + \hat{s}} \right] \quad (3.124)$$

$$= 32\pi^2 (e_q^2 \alpha \alpha_s) \frac{1}{2} \frac{1}{\hat{t}} \left[ \frac{(Q^2 + \hat{s})^2 - 2\hat{s}Q^2}{Q^2 + \hat{s}} \right] \quad (3.125)$$

$$= 32\pi^2 (e_q^2 \alpha \alpha_s) \frac{1}{2} \frac{1}{\hat{t}} \left[ \frac{Q^4 + \hat{s}^2}{Q^2 + \hat{s}} \right] \quad (3.126)$$

$$= 32\pi^2 (e_q^2 \alpha \alpha_s) \frac{1}{2} \frac{1}{\hat{t}} \frac{Q^2}{z} [z^2 + (1-z)^2] \quad (3.127)$$

Inserting eq.(3.127) into eq.(3.97) we obtain:

$$\frac{d\sigma}{dk_t^2} = \frac{1}{16\pi} \frac{1}{\hat{s} + Q^2} \frac{1}{\hat{s}} \frac{1}{1-z} |M|^2 \quad (3.128)$$

$$= \frac{1}{16\pi} \frac{1}{\hat{s} + Q^2} \frac{1}{\hat{s}} 32\pi^2 (e_q^2 \alpha \alpha_s) \frac{1}{2} \frac{Q^2}{z} \frac{1}{k_t^2} [z^2 + (1-z)^2] \quad (3.129)$$

$$= \pi\alpha\alpha_s e_q^2 \frac{1}{\hat{s}} \frac{1}{k_t^2} [z^2 + (1-z)^2] \quad (3.130)$$

$$= \sigma_0 e_q^2 \frac{\alpha_s}{2\pi} \frac{1}{k_t^2} \left[ \frac{1}{2} (z^2 + (1-z)^2) \right] \quad (3.131)$$

$$= \hat{\sigma}_0 e_q^2 \frac{\alpha_s}{2\pi} \frac{1}{k_{\perp}^2} [P_{qg}(z)] \quad (3.132)$$

where we have introduced the splitting function  $P_{qg}$ :

$$P_{qg} = \frac{1}{2} (z^2 + (1-z)^2) \quad (3.133)$$

Integrating the cross section eq(3.132) over  $k_t$  we obtain (in analogy to the QCDC process):

$$\sigma^{BGF} = \sigma_0 e_q^2 \frac{\alpha_s}{2\pi} P_{qg}(z) \log \frac{Q^2(1-z)}{4z\kappa^2} \quad (3.134)$$

$$= \sigma_0 e_q^2 \frac{\alpha_s}{2\pi} P_{qg}(z) \log \frac{Q^2}{\kappa^2} + \dots \quad (3.135)$$

In the BGF case the parton density is the gluon density (in contrast to the QCDC process). We rewrite the cross section in terms of  $F_2(x, Q^2)$  and obtain:

$$\sigma^{BGF} = \sigma_0 e_q^2 \frac{\alpha_s}{2\pi} \int g(\xi) \delta(x - z\xi) dz d\xi P_{qg}(z) \log \frac{Q^2}{\kappa^2} \quad (3.136)$$

$$\sigma^{BGF} = \sigma_0 e_q^2 \frac{\alpha_s}{2\pi} \int \frac{d\xi}{\xi} g(\xi) P_{qg} \left( \frac{x}{\xi} \right) \log \frac{Q^2}{\kappa^2} \quad (3.137)$$

Putting everything together we obtain for  $F_2/x$ :

$$\frac{F_2}{x} = \frac{\sigma^{\gamma P}}{\sigma_0} = \sum e_q^2 \int \frac{d\xi}{\xi} \left( f_q(\xi) \left[ \delta \left( 1 - \frac{x}{\xi} \right) + \frac{\alpha_s}{2\pi} P_{qg} \left( \frac{x}{\xi} \right) \log \left( \frac{Q^2}{\kappa^2} \right) \right] \right) \quad (3.138)$$

$$+ g(\xi) \left[ \frac{\alpha_s}{2\pi} P_{qg} \left( \frac{x}{\xi} \right) \log \left( \frac{Q^2}{\kappa^2} \right) \right] \quad (3.139)$$

We are still left with the arbitrary cutoff  $\kappa$ . Now we use a trick to remove it: we define scale dependent parton densities:

$$q_i(x, \mu^2) = q_i^0(x) + \frac{\alpha_s}{2\pi} \int_x^1 \frac{d\xi}{\xi} \left[ q_i^0(\xi) P_{qg} \left( \frac{x}{\xi} \right) \log \left( \frac{\mu^2}{\kappa^2} \right) + C_q \left( \frac{x}{\xi} \right) \right] + \dots$$

$$g(x, \mu^2) = g^0(x) + \frac{\alpha_s}{2\pi} \int_x^1 \frac{d\xi}{\xi} \left[ g^0(\xi) P_{qg} \left( \frac{x}{\xi} \right) \log \left( \frac{\mu^2}{\kappa^2} \right) + C_g \left( \frac{x}{\xi} \right) \right] + \dots \quad (3.140)$$

where we have now put the divergent part ( $\kappa \rightarrow 0$ ) into a redefinition of the parton density with the price that the parton density is now scale dependent with scale  $\mu^2$ . Inserting this into the

equation eq.(3.139), we obtain:

$$\begin{aligned} \frac{F_2}{x} = & \sum e_q^2 \int \frac{d\xi}{\xi} \left( q(\xi, \mu^2) \left[ \delta \left( 1 - \frac{x}{\xi} \right) + \frac{\alpha_s}{2\pi} P_{qq} \left( \frac{x}{\xi} \right) \log \left( \frac{Q^2}{\mu^2} \right) \right] \right. \\ & \left. + g(\xi, \mu^2) \left[ \frac{\alpha_s}{2\pi} P_{qg} \left( \frac{x}{\xi} \right) \log \left( \frac{Q^2}{\mu^2} \right) \right] \right) \end{aligned} \quad (3.141)$$



## Chapter 4

# Parton evolution equation

Here we will derive the evolution equation for the parton densities in the collinear (small  $t$ ) limit, the so called DGLAP evolution equations (named after the authors Dokshitzer, Gribov, Lipatov, Altarelli, Parisi [19–22]). The expression for the deep inelastic scattering cross section (or the structure function  $F_2$ ) including  $\mathcal{O}(\alpha_s)$  corrections is given by:

$$\begin{aligned} \frac{\sigma^{\gamma^*p}}{\sigma_0} = \frac{F_2}{x} &= \sum e_q^2 \int \frac{d\xi}{\xi} \left( q(\xi, \mu^2) \left[ \delta \left( 1 - \frac{x}{\xi} \right) + \frac{\alpha_s}{2\pi} P_{qq} \left( \frac{x}{\xi} \right) \log \left( \frac{Q^2}{\mu^2} \right) \right] \right. \\ &\quad \left. + g(\xi, \mu^2) \left[ \frac{\alpha_s}{2\pi} P_{qg} \left( \frac{x}{\xi} \right) \log \left( \frac{Q^2}{\mu^2} \right) \right] \right) \end{aligned} \quad (4.1)$$

The cross section for small transverse momenta (or at small  $t$ ) is divergent, and therefore gives a dominant contribution to the total cross section. For the price of a scale dependent parton density we have moved the divergent behavior into the bare (and not observable) parton densities, with the result that then the expression were finite (a procedure called renormalization). Since the  $\gamma p$  cross section  $\sigma^{\gamma^*p}$  (or equivalently the structure function  $F_2$ ) as an observable cannot depend on the arbitrary scale  $\mu^2$ , we must require, that it is  $\mu^2$ -scale independent. This is satisfied by the requirement

$$\frac{\partial F_2}{\partial \mu^2} = 0$$

Using eq.(4.1) (for simplicity we treat here only the quark part, the gluon part is treated similarly) we obtain:

$$\begin{aligned} \frac{\delta F_2}{\delta \mu^2} &= \int \frac{d\xi}{\xi} \left( \frac{\partial q(\xi, \mu^2)}{\partial \mu^2} \left[ \delta \left( 1 - \frac{x}{\xi} \right) + \frac{\alpha_s}{2\pi} P_{qq} \left( \frac{x}{\xi} \right) \log \left( \frac{Q^2}{\mu^2} \right) \right] \right. \\ &\quad \left. + q(\xi, \mu^2) \frac{\alpha_s}{2\pi} P_{qq} \left( \frac{x}{\xi} \right) \frac{\partial}{\partial \mu^2} [\log Q^2 - \log \mu^2] \right) \end{aligned} \quad (4.2)$$

$$\begin{aligned} &= \frac{\partial q(x, \mu^2)}{\partial \mu^2} + \int \frac{d\xi}{\xi} \frac{\alpha_s}{2\pi} P_{qq} \left( \frac{x}{\xi} \right) \log \frac{Q^2}{\mu^2} \frac{\partial q(\xi, \mu^2)}{\partial \mu^2} \\ &\quad + \int \frac{d\xi}{\xi} q(\xi, \mu^2) \frac{\alpha_s}{2\pi} P_{qq} \left( \frac{x}{\xi} \right) \left( -\frac{1}{\mu^2} \right) \end{aligned} \quad (4.3)$$

## H1 and ZEUS

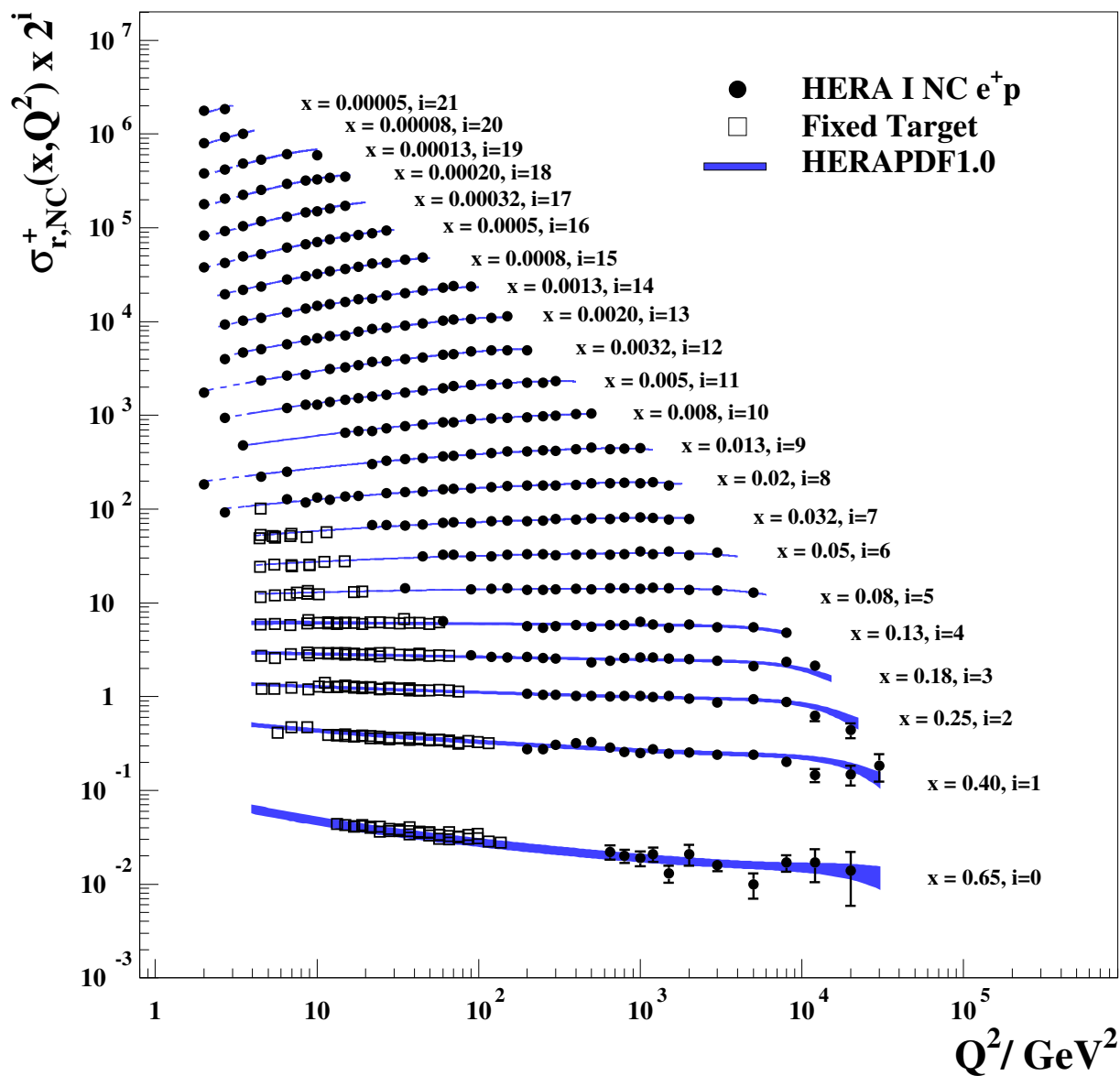


Figure 4.1: The structure function  $F_2(x, Q^2)$  as a function of  $Q^2$  as measured in DIS scattering  $e + p \rightarrow e' + X$  at HERA [18].

## H1 and ZEUS

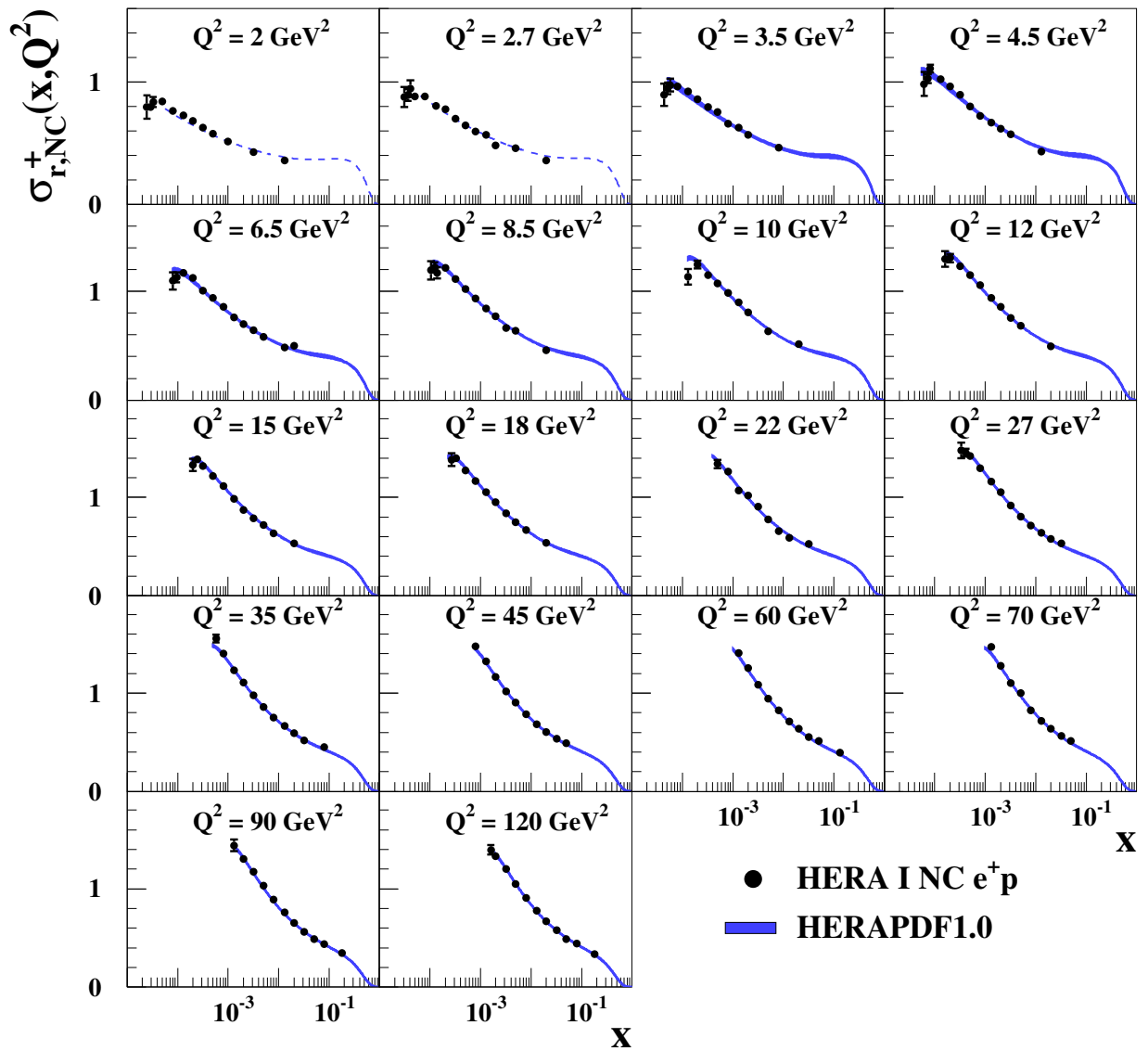


Figure 4.2: The structure function  $F_2(x, Q^2)$  as a function of  $x$  as measured in DIS scattering  $e+p \rightarrow e' + X$  at HERA [18].

Now we collect all terms of  $\mathcal{O}(\alpha_s)$  (note the second term in eq.(4.3) is of  $\mathcal{O}(\alpha_s^2)$  and therefore does not contribute) and obtain:

$$\frac{dq_i(x, \mu^2)}{d \log \mu^2} = \frac{\alpha_s}{2\pi} \int_x^1 \frac{d\xi}{\xi} \left[ q_i(\xi, \mu^2) P_{qq} \left( \frac{x}{\xi} \right) \right] \quad (4.4)$$

Including also the gluon part we obtain:

$$\frac{dq_i(x, \mu^2)}{d \log \mu^2} = \frac{\alpha_s}{2\pi} \int_x^1 \frac{d\xi}{\xi} \left[ q_i(\xi, \mu^2) P_{qq} \left( \frac{x}{\xi} \right) + g(\xi, \mu^2) P_{qg} \left( \frac{x}{\xi} \right) \right] \quad (4.5)$$

and similarly for the gluons

$$\frac{dg(x, \mu^2)}{d \log \mu^2} = \frac{\alpha_s}{2\pi} \int_x^1 \frac{d\xi}{\xi} \left[ \sum_i q_i(\xi, \mu^2) P_{gq} \left( \frac{x}{\xi} \right) + g(\xi, \mu^2) P_{gg} \left( \frac{x}{\xi} \right) \right] \quad (4.6)$$

The splitting functions are given by:

$$P_{qq} = \frac{4}{3} \left( \frac{1+z^2}{1-z} \right) \quad (4.7)$$

$$P_{gq} = \frac{4}{3} \left( \frac{1+(1-z)^2}{z} \right) \quad (4.8)$$

$$P_{qg} = \frac{1}{2} (z^2 + (1-z)^2) \quad (4.9)$$

$$P_{gg} = 6 \left( \frac{1-z}{z} + \frac{z}{1-z} + z(1-z) \right) \quad (4.10)$$

Eq.4.5 and 4.6 are the DGLAP evolution equations in leading order of  $\alpha_s$ . They describe the evolution of the parton density with the scale  $\mu^2$ . By knowing the parton density at any scale  $\mu^2$ , these equations predict the parton density at any other scale. Although we cannot calculate the parton densities from first principles, these equations allow us to predict the parton densities at any scale, once they are determined at another scale. In Fig. 4.1-4.2 is shown the comparison of the measurement of the structure function  $F_2(x, Q^2)$  with the prediction from a DGLAP evolution. The prediction agrees with the measurement remarkably well over several orders of magnitude in  $x$  and  $Q^2$ . This is a real triumph of the theory.

## 4.1 Conservation and Sum Rules

In the following we investigate further the evolution equations.

### 4.1.1 Flavor Conservation

The scale dependent quark density as a function of the bare parton density  $q_0$  and the scale dependent divergent part ( $\kappa \rightarrow 0$ ) can be written as:

$$q(x, \mu^2) = \int_x^1 \frac{d\xi}{\xi} q_0(\xi) \left[ \delta(1 - \frac{x}{\xi}) + \frac{\alpha_s}{2\pi} P_{qq} \left( \frac{x}{\xi} \right) \log \frac{\mu^2}{\kappa^2} + \dots \right] \quad (4.11)$$



$$= \int_x^1 \frac{d\xi}{\xi} q_0(\xi) \hat{q}(z, \mu^2) + \dots \quad (4.12)$$

$$= \int_x^1 d\xi \int_0^1 dz \delta(x - z\xi) q_0(\xi) \hat{q}(z, \mu^2) + \dots \quad (4.13)$$

with

$$\hat{q}(z, \mu^2) = \delta(1 - z) + \frac{\alpha_s}{2\pi} P_{qq}(z) \log \frac{\mu^2}{\kappa^2} \quad (4.14)$$

where we have used  $z = \frac{x}{\xi}$  and  $\delta(1 - z)dz = \delta(1 - \frac{x}{\xi})dz = \xi\delta(\xi - x)dz$ .

However, this is not the full expression in  $\mathcal{O}(\alpha_s)$ , since we have not yet included virtual gluon radiation, self-energy insertions on the quark leg and vertex corrections. One can calculate the virtual corrections explicitly, but here we use the argument of conservation of quark (and baryon) number: the integral over  $z$  of the quark distribution cannot vary with  $\mu^2$ :

$$\int_0^1 dz \hat{q}(z, \mu^2) = 1 \quad (4.15)$$

For this we redefine the splitting function as:

$$P_{qq}(z) = \hat{P}_{qq}(z) + k \cdot \delta(1 - z) \quad (4.16)$$

With this we get:

$$\int dz \left[ \delta(1 - z) + \frac{\alpha_s}{2\pi} \left( \hat{P}_{qq}(z) + k \cdot \delta(1 - z) \right) \log \frac{\mu^2}{\kappa^2} \right] = 1$$

With  $\log \frac{\mu^2}{\kappa^2} \neq 0$  we obtain

$$\int_0^1 dz \frac{\alpha_s}{2\pi} \left( \hat{P}(z) + k \cdot \delta(1 - z) \right) = 0$$

Some of the splitting functions are divergent for  $z \rightarrow 1$  and we cannot perform the integral easily. However we note, that  $z \rightarrow 1$  reduces to no-emission and this has a final state similar to a virtual contribution to the no-emission diagram. To treat this singularity formally we introduce a " + " distribution (similar to the  $\delta$  function which is only defined inside an integral):

$$\int_0^1 dx \frac{f(x)}{(1-x)_+} = \int_0^1 dx \frac{f(x) - f(1)}{(1-x)} \quad (4.17)$$

or in general [23]:

$$\int_0^1 dx f(x) [F(x)]_+ = \int_0^1 dx (f(x) - f(1)) F(x)$$

with  $\int_0^1 dx [F(x)]_+ = 0$

We now use the expression for the quark splitting  $\hat{P}_{qq}(z) = \frac{1+z^2}{(1-z)_+}$ :

$$\int_0^1 dz P_{qq}(z) = \int_0^1 dz \left[ \frac{1+z^2}{(1-z)_+} + k \cdot \delta(1-z) \right] \quad (4.18)$$

$$= \int_0^1 dz \frac{1+z^2-2}{1-z} + k \quad (4.19)$$

$$= k + \int_0^1 dz \frac{-(1-z^2)}{1-z} \quad (4.20)$$

$$= k - \int_0^1 dz \frac{(1+z)(1-z)}{1-z} \quad (4.21)$$

$$= k - \int_0^1 dz (1+z) = k - \frac{3}{2} \quad (4.22)$$

where in eq.(4.19) the expression  $f(z) - f(1) = (1-z)^2 - 2$  has been used. Thus we obtain:

$$P_{qq}(z) = \frac{1+z^2}{(1-z)_+} + \frac{3}{2}\delta(1-z) \quad (4.23)$$

With this expression for  $P_{qq}$  we ensure that soft singularities are properly cancelled. This expression is essential to ensure that the sum rules are fulfilled (here for the proton case) independent of  $\mu^2$ :

$$\int_0^1 dx u_v(x, \mu^2) = 2$$

$$\int_0^1 dx d_v(x, \mu^2) = 1$$

In Fig. 4.3 the different diagrams which contribute to  $F_2(x, Q^2)$  at  $\mathcal{O}(\alpha_s)$  are shown.

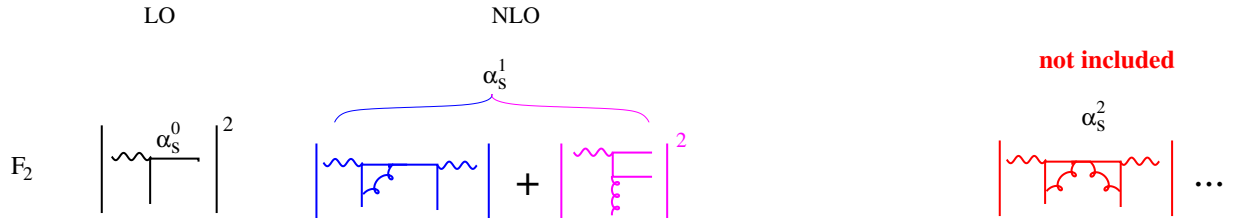


Figure 4.3: The different diagrams which contribute to  $F_2(x, Q^2)$  at  $\mathcal{O}(\alpha_s)$ . Note that at  $\mathcal{O}(\alpha_s)$  only the interference diagram of  $\mathcal{O}(\alpha_s^0)$  and the virtual contribution together with the real  $\mathcal{O}(\alpha_s)$  diagram contribute, while the virtual diagram squared would give  $\mathcal{O}(\alpha_s^2)$ .

### 4.1.2 Conservation Rules of Splitting Functions

In this section we will check explicitly the conservation of momentum fractions using the momentum sum rule:

$$\int_0^1 dx x \left( \sum_i q_i(x, Q^2) + g(x, Q^2) \right) = 1 \quad (4.24)$$

to obtain constraints on the splitting functions.

We apply the momentum sum rule and make use of the DGLAP evolution equation for the quark and gluons:

$$\begin{aligned} \frac{dq_i(x, \mu^2)}{d \log \mu^2} &= \frac{\alpha_s}{2\pi} \int_x^1 \frac{d\xi}{\xi} \left[ q_i(\xi, \mu^2) P_{qq} \left( \frac{x}{\xi} \right) + g(\xi, \mu^2) P_{qg} \left( \frac{x}{\xi} \right) \right] \\ \frac{dg(x, \mu^2)}{d \log \mu^2} &= \frac{\alpha_s}{2\pi} \int_x^1 \frac{d\xi}{\xi} \left[ \sum_i q_i(\xi, \mu^2) P_{gq} \left( \frac{x}{\xi} \right) + g(\xi, \mu^2) P_{gg} \left( \frac{x}{\xi} \right) \right] \end{aligned}$$

Summing over all quark flavors and integrating these equations over  $\log \mu^2$  gives:

$$\begin{aligned} \int_0^1 dx x \left( \sum_i q_i(x, Q^2) + g(x, Q^2) \right) &= \int d \log \mu^2 \int_0^1 dx \left[ \sum_i x q_i(x, \mu_0^2) \right. \\ &\quad \left. + \frac{\alpha_s}{2\pi} \int \frac{d\xi}{\xi} \left( \sum_i x q_i(\xi, \mu^2) P_{qq} + 2n_f x g(\xi, \mu^2) P_{qg} \right) \right. \\ &\quad \left. + x g(x, \mu_0^2) + \frac{\alpha_s}{2\pi} \int \frac{d\xi}{\xi} (x g(x, \mu^2) P_{gg} + x q(\xi, \mu^2) P_{gq}) \right] \end{aligned}$$

with  $n_f$  being the number of flavors. With a change of integration variables in the second integrals to  $z = x/\xi$  (and  $\xi dz = dx$ ) we obtain:

$$\begin{aligned} \int_0^1 dx x \left( \sum_i q_i(x, Q^2) + g(x, Q^2) \right) &= \int_0^1 dx \sum_i x q_i(x, \mu_0^2) + x g(x, \mu_0^2) \\ &\quad + \frac{\alpha_s}{2\pi} \int d \log \mu^2 \int_0^1 dz \int_x^1 d\xi \left[ \sum_i z \xi q_i(\xi, \mu^2) P_{qq} \right. \\ &\quad \left. + 2n_f z \xi g(\xi, \mu^2) P_{qg} + z \xi g(\xi, \mu^2) P_{gg} + z \xi q(\xi, \mu^2) P_{gq} \right] \\ &= \int_0^1 dx \sum_i x q_i(x, \mu_0^2) + x g(x, \mu_0^2) \\ &\quad + \frac{\alpha_s}{2\pi} \int d \log \mu^2 \int_0^1 dz \int_x^1 d\xi \left[ \sum_i \xi q_i(\xi, \mu^2) (z (P_{qq} + P_{gq})) \right. \\ &\quad \left. + \xi g(\xi, \mu^2) (z (P_{gg} + 2n_f P_{qg})) \right] \end{aligned}$$

Since the momentum sum rule is to be satisfied for all  $\mu^2$ , we obtain:

$$\int_0^1 dz z (P_{qq} + P_{gq}) = 0$$

$$\int_0^1 dz z (P_{gg} + 2n_f P_{qg}) = 0$$

## 4.2 Collinear factorization

A detailed discussion on factorization can be found in [24,25]. Collinear factorization means that the collinear singularities are factorized into process independent parton distributions leaving perturbatively calculable process dependent hard scattering cross sections (or coefficient functions) for a scattering process of vector boson  $V$  on a hadron  $h$ :

$$\sigma(V + h) = f_h(\mu_f) \otimes C_a^V(\mu_f, \mu_r) \quad (4.25)$$

Here  $f$  is the parton distribution function and  $C_a^V$  is the hard scattering cross section which is infrared safe and calculable in pQCD. The index  $a$  indicates, that this cross section depends on the type of the incoming partons. In addition  $C_a^V$  depends on the factorization ( $\mu_f$ ) and renormalization ( $\mu_r$ ) scales, but is independent from long distance effects, especially independent on the hadron  $h$ . For example, in deep inelastic scattering the  $C_a^V$  are the same for scattering on a pion, proton, neutron etc. The parton distribution function  $f$  contains all the infrared sensitivity and is specific for the hadron  $h$  and also depends on the factorization scale  $\mu_f$ . The parton distribution function  $f$  are universal and independent on the hard scattering.

Please note, that the factorization theorems are only proven for a few processes [25]:

- deep inelastic scattering (DIS)
- diffractive deep inelastic scattering
- Drell Yan (DY) production in hadron hadron collisions
- single particle inclusive spectra (fragmentation functions)

For all other processes, factorization is assumed (and it is shown by comparing predictions with measurements, that this assumption is rather successful).

### 4.2.1 Factorization Schemes

Different schemes for separating the long from short distance parts are available (factorization schemes). The difference between them is, which pieces of the cross section are factorized into the parton density functions. Common schemes are:

- DIS scheme

$$F_2(x, Q^2) = x \sum_i e_i^2 q_i(x, Q^2)$$

where the index  $i$  runs over all parton flavors and  $q(x, Q^2)$  is the quark (or antiquark) density. Gluons enter only via the evolution of the quark densities. This formula is required to hold at all orders in  $\alpha_s$ . The DIS scheme is obtained from  $\mu^2 = Q^2$ .

- $\overline{\text{MS}}$  scheme (modified minimal subtraction)  
Only the divergent pieces are absorbed into the quark and gluon densities. The structure function  $F_2(x, Q^2)$  is then:

$$F_2^{\overline{\text{MS}}}(x, Q^2) = x \sum e_q^2 \int \frac{dx_2}{x_2} \left[ q^{\overline{\text{MS}}}(x_2, Q^2) \left[ \delta \left( 1 - \frac{x}{x_2} \right) + \frac{\alpha_s}{2\pi} C_q^{\overline{\text{MS}}} \left( \frac{x}{x_2} \right) \right] + g^{\overline{\text{MS}}}(x_2, Q^2) \frac{\alpha_s}{2\pi} C_g^{\overline{\text{MS}}} \left( \frac{x}{x_2} \right) \right]$$

Once a specific scheme is chosen, it has to be used for both the parton density and the partonic cross section, otherwise inconsistent results are obtained.

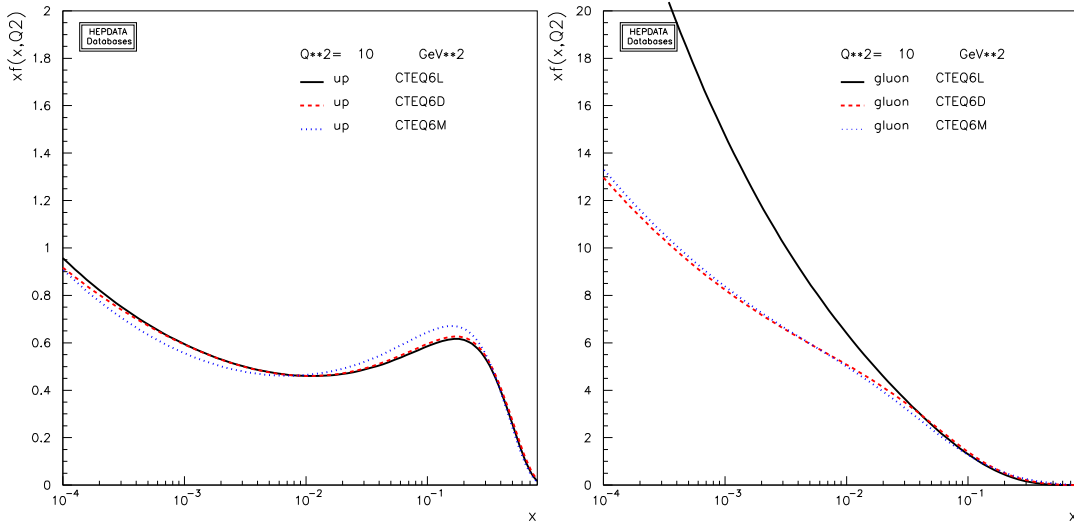


Figure 4.4: The up-quark (left) and gluon (right) densities as a function of  $x$  at  $\mu^2 = 10 \text{ GeV}^2$  obtained in [26] in LO (CTEQ6L) and in NLO in the DIS (CTEQ6D) and  $\overline{\text{MS}}$  (CTEQ6M) scheme [27].

### 4.3 Solution of DGLAP equations

Several methods exist to solve the DGLAP equations, here we only consider a numerical solution of the integro-differential equations. We first consider a solution of the evolution equation at small  $x$  and then discuss the more general case.

### 4.3.1 Double Leading Log approximation for small $x$

In this section we consider only the limit of small  $x$ . In this limit, only the gluon density contributes with the splitting function  $P_{gg}(x) \rightarrow 6/x$ . All other contributions are small and can be neglected. With this the evolution equation eq.(4.6) becomes:

$$\frac{dg(x, \mu^2)}{d \log \mu^2} = \frac{\alpha_s}{2\pi} \int_x^1 \frac{d\xi}{\xi} \left[ g(\xi, \mu^2) P_{gg} \left( \frac{x}{\xi} \right) \right] \quad (4.26)$$

This equation can be integrated to give:

$$xg(x, \mu^2) = xg(x, \mu_0^2) + \frac{\alpha_s}{2\pi} \int_{\mu_0^2}^{\mu^2} \frac{d\mu'^2}{\mu'^2} \int_x^1 \frac{d\xi}{\xi} xg(\xi, \mu'^2) P \left( \frac{x}{\xi} \right) \quad (4.27)$$

$$= xg(x, \mu_0^2) + \frac{3\alpha_s}{\pi} \int_{\mu_0^2}^{\mu^2} \frac{d\mu'^2}{\mu'^2} \int_x^1 \frac{d\xi}{\xi} \xi g(\xi, \mu'^2) \quad (4.28)$$

This equation is an integral equation of Fredholm type

$$\phi(x) = f(x) + \lambda \int_a^b K(x, y) \phi(y) dy$$

and can be solved by iteration (Neumann series):

$$\phi_0(x) = f(x)$$

$$\phi_1(x) = f(x) + \lambda \int_a^b K(x, y) f(y) dy$$

$$\phi_2(x) = f(x) + \lambda \int_a^b K(x, y_1) f(y_1) dy_1 + \lambda^2 \int_a^b \int_a^b K(x, y_1) K(y_1, y_2) f(y_2) dy_2 dy_1$$

This can be written in a compact form:

$$\phi_n(x) = \sum_{i=0}^n \lambda^i u_i(x) \quad (4.29)$$

with

$$u_0(x) = f(x)$$

$$u_1(x) = \int_a^b K(x, y) f(y) dy$$

$$u_n(x) = \int_a^b \cdots \int_a^b K(x, y_1) K(y_1, y_2) \cdots K(y_{n-1}, y_n) f(y_n) dy_1 \cdots dy_n$$

with the solution:

$$\phi(x) = \lim_{n \rightarrow \infty} q_n(x) = \lim_{n \rightarrow \infty} \sum_{i=0}^n \lambda^i u_i(x) \quad (4.30)$$

Applying this method to solve the evolution equation for the gluon density at small  $x$  eq.(4.28) with  $xg(x, \mu_0^2) = xg_0(x) = C$ , we obtain:

$$xg_1(x, t) = \frac{3\alpha_s}{\pi} C \int_{t_0}^t d \log t' \int_x^1 d \log \xi = \frac{3\alpha_s}{\pi} \log \frac{t}{t_0} \log \frac{1}{x} C \quad (4.31)$$

$$xg_2(x, t) = \frac{1}{2} \frac{1}{2} \left( \frac{3\alpha_s}{\pi} \log \frac{t}{t_0} \log \frac{1}{x} \right)^2 C \quad (4.32)$$

⋮

$$xg_n(x, t) = \frac{1}{n!} \frac{1}{n!} \left( \frac{3\alpha_s}{\pi} \log \frac{t}{t_0} \log \frac{1}{x} \right)^n C \quad (4.33)$$

$$xg(x, t) = \lim_{n \rightarrow \infty} \sum_n \frac{1}{n!} \frac{1}{n!} \left( \frac{3\alpha_s}{\pi} \log \frac{t}{t_0} \log \frac{1}{x} \right)^n C \quad (4.34)$$

Using the modified Bessel function:

$$I_0(z) = \sum_{k=0}^{\infty} \frac{(\frac{1}{4}z^2)^k}{(k!)^2} = \frac{e^z}{\sqrt{2\pi z}} \quad (4.35)$$

We identify

$$z = 2\sqrt{\frac{3\alpha_s}{\pi} \log \frac{t}{t_0} \log \frac{1}{x}}$$

to obtain:

$$xg(x, t) \sim C \exp \left( 2\sqrt{\frac{3\alpha_s}{\pi} \log \frac{t}{t_0} \log \frac{1}{x}} \right) \quad (4.36)$$

This result has been obtained by taking the limit of large double leading logarithms:

- small  $x$  limit in the splitting function which leads to  $\log 1/x$
- small  $t$  limit to obtain evolution equation, which leads to  $\log 1/t$ .

The DLL solution of the evolution equations results in a rapid rise of the gluon density at small  $x$ , however only so-called contributions from strongly ordered (decreasing) values of  $x$  and strongly ordered (increasing) values of  $t$  are considered. Note, that the unlimited rise at small  $x$  is of course unphysical, and for a realistic description a sort of taming (or saturation) of the distribution is required.

### 4.3.2 From evolution equation to parton branching

In the previous section we have seen how to solve the evolution equation iteratively. By performing the small  $x$  limit, we avoided the difficulties with the soft divergencies at large  $x$ ; we did not need to use the plus-prescription of the splitting function. Here we now discuss a different way

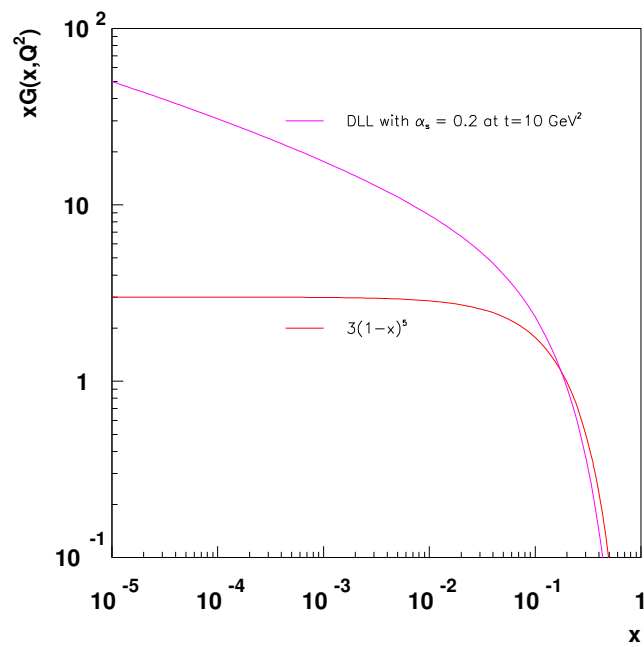


Figure 4.5: The gluon density from  $xG(x) = 3(1-x)^5$  and the DLL result with  $\alpha_s = 0.2$  and  $t = 10 \text{ GeV}^2$ .



to treat the soft limit. The divergency of a soft real emission is cancelled by virtual contributions, that is, we can define a "resolvable" branching, which is a splitting of one into two partons, where at least in principle we can resolve the splitting. The "non-resolvable" branching consist of a contribution without branching and the virtual contributions. A detailed discussion of the parton evolution can be found in [14].

We define a "Sudakov" form factor  $\Delta_s$ :

$$\Delta_s(t) = \exp\left(-\int_x^{z_{max}} dz \int_{t_0}^t \frac{\alpha_s}{2\pi} \frac{dt'}{t'} \tilde{P}(z)\right) \quad (4.37)$$

and use the evolution equation with the "+" prescription (using  $t = \mu^2$ ):

$$t \frac{\partial}{\partial t} f(x, t) = \int \frac{dz}{z} \frac{\alpha_s}{2\pi} P_+(z) f\left(\frac{x}{z}, t\right)$$

Inserting the explicit expression for  $P_+$  we obtain:

$$t \frac{\partial}{\partial t} f(x, t) = \int_0^1 \frac{dz}{z} \frac{\alpha_s}{2\pi} P(z) f\left(\frac{x}{z}, t\right) - \frac{\alpha_s}{2\pi} f(x, t) \int_0^1 dz P(z) \quad (4.38)$$

where we have used the definition in eq.(4.17):

$$\begin{aligned} \int_0^1 dz \frac{f(z)}{z} P_+(z) &= \int_0^1 dz \left( \frac{f\left(\frac{x}{z}\right)}{z} - f(x) \right) P(z) \\ &= \int_0^1 dz \frac{f\left(\frac{x}{z}\right)}{z} P(z) - f(x) \int_0^1 dz P(z) \end{aligned}$$

Using

$$\frac{\partial e^{-a(x)}}{\partial x} = -e^{-a(x)} \frac{\partial a(x)}{\partial x}$$

we obtain:

$$\frac{\partial \Delta_s}{\partial t} = -\Delta_s \left[ \frac{1}{t} \int dz \frac{\alpha_s}{2\pi} P(z) \right] \quad (4.39)$$

$$\rightsquigarrow \frac{t}{\Delta_s} \frac{\partial \Delta_s}{\partial t} = - \int dz \frac{\alpha_s}{2\pi} P(z) \quad (4.40)$$

Inserting this into eq.(4.38) we obtain:

$$t \frac{\partial}{\partial t} f(x, t) = \int \frac{dz}{z} \frac{\alpha_s}{2\pi} P(z) f\left(\frac{x}{z}, t\right) + f(x, t) \frac{t}{\Delta_s} \frac{\partial \Delta_s}{\partial t} \quad (4.41)$$

Multiplying eq.(4.41) with  $1/\Delta_s$  and using  $\frac{\partial}{\partial t} \frac{f}{\Delta_s} = \frac{1}{\Delta_s} \frac{\partial f}{\partial t} - \frac{f}{\Delta_s^2} \frac{\partial \Delta_s}{\partial t}$  we obtain:

$$\frac{t}{\Delta_s} \frac{\partial f(x, t)}{\partial t} - \frac{t}{\Delta_s^2} f(x, t) \frac{\partial \Delta_s}{\partial t} = \int \frac{dz}{z} \frac{1}{\Delta_s} \frac{\alpha_s}{2\pi} P(z) f\left(\frac{x}{z}, t\right) \quad (4.42)$$

$$t \frac{\partial}{\partial t} \frac{f(x, t)}{\Delta_s} = \int \frac{dz}{z} \frac{1}{\Delta_s} \frac{\alpha_s}{2\pi} P(z) f\left(\frac{x}{z}, t\right) \quad (4.43)$$

which is the DGLAP evolution equation in a form using the Sudakov form factor  $\Delta_s$  as defined in eq.(4.37).

We can now integrate eq.(4.43) to obtain:

$$f(x, t) = f(x, t_0)\Delta(t) + \int \frac{dt'}{t'} \frac{\Delta(t)}{\Delta(t')} \frac{\alpha_s(t')}{2\pi} \int \frac{dz}{z} P(z) f\left(\frac{x}{z}, t'\right) \quad (4.44)$$

where we have used

$$\int_{t_0}^t \frac{\partial}{\partial t'} \frac{f(x, t')}{\Delta_s} dt' = \int \frac{dt'}{t'} \frac{1}{\Delta_s} \frac{\alpha_s}{2\pi} \int \frac{dz}{z} P(z) f\left(\frac{x}{z}, t'\right) \quad (4.45)$$

From eq.(4.44) we can now interpret the Sudakov form factor as being the probability for evolution without any resolvable branching from  $t_0$  to  $t$ .

What did we gain ? We needed to treat the singularity at  $z \rightarrow 1$ . For this, we now introduce a upper cut-off  $z_{cut} = 1 - \epsilon(\mu)$ . Branchings with  $z > z_{cut}$  are now classified as unresolved: they involve the emission of undetectable partons [14]. The Sudakov form factor sums virtual and real corrections to all orders; the virtual corrections affect the non-branching probability are included via unitarity: the resolvable branching probability gives via unitarity the sum of virtual and unresolvable contributions.

Eq.(4.44) can now be solved by iteration, in the same way as before. The starting function  $f_0$  is just the first term in eq.(4.44). The first iteration  $f_1$  involves one branching:

$$\begin{aligned} f_0(x, t) &= f(x, t_0)\Delta(t) \\ f_1(x, t) &= f(x, t_0)\Delta(t) + \frac{\alpha_s}{2\pi} \int_{t_0}^t \frac{dt'}{t'} \frac{\Delta(t)}{\Delta(t')} \int_x^1 \frac{dz}{z} \tilde{P}(z) f(x/z, t_0)\Delta(t') \end{aligned} \quad (4.46)$$

The iteration is illustrated in fig.4.6 The term  $f_0$  in eq.(4.46) is illustrated in the left part of Fig. 4.6:

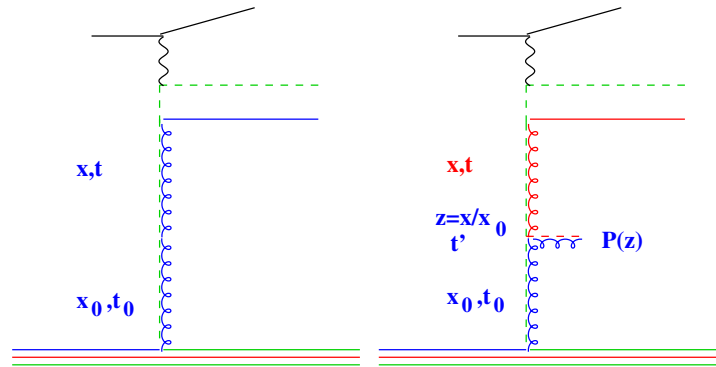


Figure 4.6: Schematic representation of the first branchings in an iterative procedure to solve the evolution equation

the evolution from  $t_0$  to  $t$  without any resolvable branching. The term  $f_1$  in eq.(4.46) is shown in

the right part of Fig. 4.6: there is evolution from  $t_0$  to  $t'$  without any resolvable branching, then at  $t'$  the branching happens, where the splitting is given by the splitting function  $P(z)$ ; then the evolution continues without any resolvable branching from  $t'$  to  $t$ .

The full solution of the integral equation by iteration is then:

$$\begin{aligned}
f_0(x, t) &= f(x, t_0)\Delta(t) \\
f_1(x, t) &= f(x, t_0)\Delta(t) + \frac{\alpha_s}{2\pi} \int_{t_0}^t \frac{dt'}{t'} \frac{\Delta(t)}{\Delta(t')} \int \frac{dz}{z} \tilde{P}(z) f(x/z, t_0)\Delta(t') \\
&= f(x, t_0)\Delta(t) + \log \frac{t}{t_0} A \otimes \Delta(t) f(x/z, t_0) \\
f_2(x, t) &= f(x, t_0)\Delta(t) + \log \frac{t}{t_0} A \otimes \Delta(t) f(x/z, t_0) + \\
&\quad \frac{1}{2} \log^2 \frac{t}{t_0} A \otimes A \otimes \Delta(t) f(x/z, t_0) \\
f(x, t) &= \lim_{n \rightarrow \infty} f_n(x, t) = \lim_{n \rightarrow \infty} \sum_n \frac{1}{n!} \log^n \left( \frac{t}{t_0} \right) A^n \otimes \Delta(t) f(x/z, t_0) \quad (4.47)
\end{aligned}$$

where  $A = \int \frac{dz}{z} \tilde{P}(z)$  is a symbolic representation of the integral over  $z$  and  $\otimes$  indicates that a convolution has to be performed. The eq.(4.47) shows the solution of the DGLAP evolution equation is a resummation to all orders in  $\alpha_s \log t$ .<sup>1</sup>

The Sudakov form factor can be interpreted in terms of a probability: it is a poisson distribution with zero mean  $P(0, p) = e^{-p}$ . If the poisson distribution gives the probability to observe  $n$  emissions, then  $P(0, p)$  gives the probability for no emission and is the so-called "non-branching probability". The one-branching probability is given in terms of Poisson statistics by:  $P(1, p) = pe^{-p}$ , which is exactly the first iteration of the evolution equation:

$$\begin{aligned}
f(x, t) &= f(x, t_0)\Delta_s(t) + \int dz \int dx' \int \frac{dt'}{t'} \cdot \frac{\Delta_s(t)}{\Delta_s(t')} \frac{\alpha_s}{2\pi} \tilde{P}(z) \times \\
&\quad \times f(x', t_0) \Delta_s(t') \delta(x - zx') \quad (4.48)
\end{aligned}$$

where delta function has been introduced to make the different integration steps visible.

We have introduced a cut to avoid the divergency when  $z \rightarrow 1$  via  $z_{cut} = 1 - \epsilon(\mu)$ , but we have not yet specified how this can be calculated. To some extent the value of  $z_{cut}$  is a matter of choice, here we give an argument based on the virtualities of the partons involved. We work in a frame, where all energies are much larger than the starting scale of the evolution  $Q_0$ . We use light-cone variables for the partons:  $p^+ = 1/\sqrt{2}(E + p_z)$  and we define

$$z = \frac{p_b^+}{p_a^+}$$

<sup>1</sup>It is interesting to note, that only the  $1/(1-z)$  part of the splitting functions is needed in the Sudakov form factor. This simplifies the solution process.

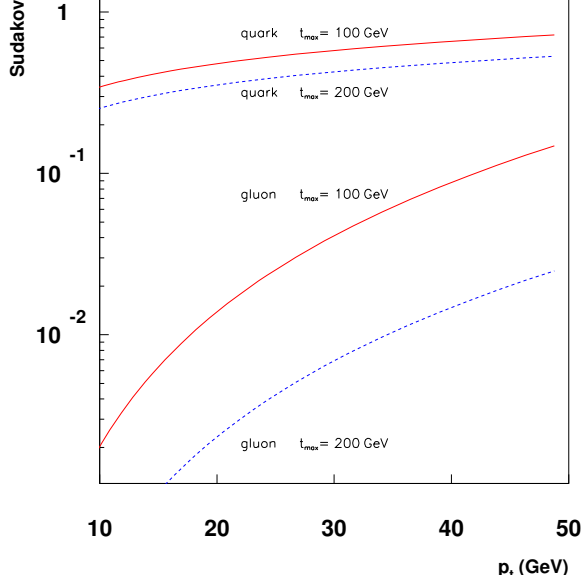


Figure 4.7: Sudakov form factor as a function of the lower scale  $p_t$  for gluon and quark splitting functions using  $\alpha_s = 0.2$ . The upper scale is set to  $t_{max} = 100(200)$  GeV.

being the splitting variable for a process  $a \rightarrow b+c$ . The light-cone vector satisfies:  $p_a^2 = 2p_a^+ p_a^- - k_{ta}^2$ . We work in a frame, where  $k_{ta} = 0$  and  $k_{tb} = -k_{tc} = k_t$ . Using conservation of the "+" and "-" components of the light-cone vectors we obtain:

$$\begin{aligned} p_a^- &= p_b^- + p_c^- \\ \frac{p_a^2}{2p_a^+} &= \frac{p_b^2 + k_{tb}^2}{2p_b^+} + \frac{p_c^2 + k_{tc}^2}{2p_c^+} \\ \rightsquigarrow p_a^2 &= \frac{p_b^2 + k_t^2}{z} + \frac{p_c^2 + k_t^2}{1-z} \end{aligned}$$

where for the last expression we have used  $p_b^+ = zp_a^+$  and  $p_c^+ = (1-z)p_a^+$ . This equation can be rewritten to give:

$$\begin{aligned} k_t^2 &= z(1-z)p_a^2 - (1-z)p_b^2 - zp_c^2 \\ \rightsquigarrow 0 &< (1-z)Q_b^2 - zQ_c^2 \end{aligned} \quad (4.49)$$

where we have defined  $Q_a^2 = -p_a^2$  and  $Q_b^2 = -p_b^2$  and  $Q_c^2 = p_c^2$  and  $Q_c^2 > Q_0^2$ , thus that parton  $a$  and  $b$  are spacelike partons while parton  $c$  is timelike. Note that  $k_t^2 > 0$  and  $z(1-z)p_a^2 < 0$  is

neglected. Using  $(1+x)^{-m} = 1 - mx + \dots$  we obtain from Eq.(4.49):

$$z < 1 - \frac{Q_0^2}{Q_b^2} + \dots \quad (4.50)$$

where we have used  $Q_c^2 > Q_0^2$ .

In Fig. 4.7 the sudakov form factor is shown for quark and gluon splittings for different scales  $t_{max}$  as a function of the lower scale  $p_t$ . The probability for quarks not to undergo any branching (the sudakov form factor gives the no-branching probability) is much higher than the corresponding one for gluons.

## 4.4 Solution of evolution equation with Monte Carlo method

AS described above, the evolution equations Eqs.(4.44) are integral equations of the Fredholm type

$$f(x) = f_0(x) + \lambda \int_a^b K(x, y) f(y) dy$$

and can be solved by iteration as a Neumann series

$$\begin{aligned} f_1(x) &= f_0(x) + \lambda \int_a^b K(x, y) f_0(y) dy \\ f_2(x) &= f_0(x) + \lambda \int_a^b K(x, y_1) f_0(y_1) dy_1 + \lambda^2 \int_a^b \int_a^b K(x, y_1) K(y_1, y_2) f_0(y_2) dy_2 dy_1 \\ &\dots \end{aligned} \quad (4.51)$$

using the kernel  $K(x, y)$ , with the solution

$$f(x) = \lim_{n \rightarrow \infty} \sum_{i=0}^n f_i(x). \quad (4.52)$$

In a Monte Carlo (MC) solution [28–30] we evolve from  $t_0$  to a value  $t'$  obtained from the Sudakov factor  $\Delta_s(t')$  (for a schematic visualisation of the evolution see fig. 4.8). Note that the Sudakov factor  $\Delta_s(t')$  gives the probability for evolving from  $t_0$  to  $t'$  without resolvable branching. The value  $t'$  is obtained from solving for  $t'$ :

$$R = \Delta_s(t'), \quad (4.53)$$

for a random number  $R$  in  $[0, 1]$ .

If  $t' > t$  then the scale  $t$  is reached and the evolution is stopped, and we are left with just the first term without any resolvable branching. If  $t' < t$  then we generate a branching at  $t'$  according to the splitting function  $\tilde{P}(z')$ , as described below, and continue the evolution using the Sudakov

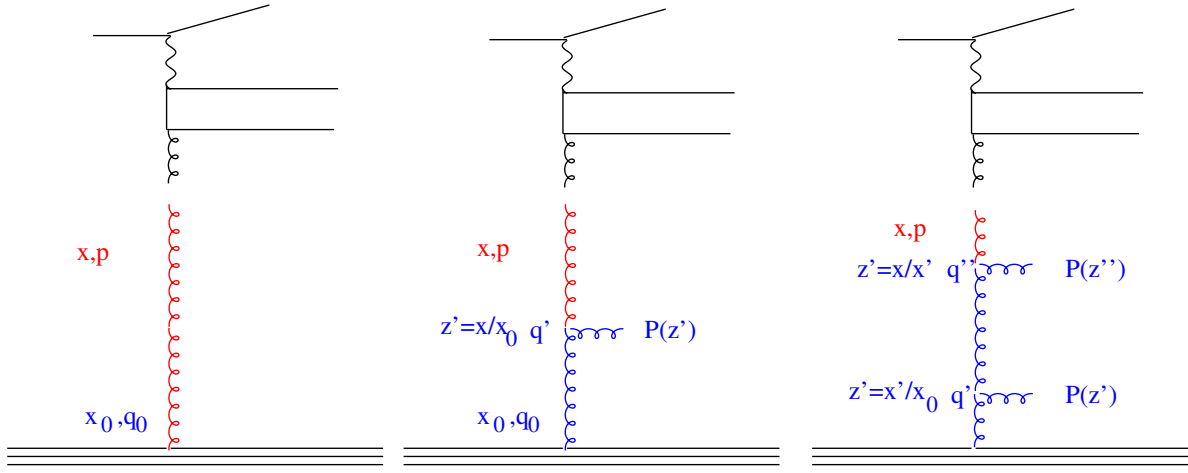


Figure 4.8: Evolution by iteration

factor  $\Delta_s(t'', t')$ . If  $t'' > t$  the evolution is stopped and we are left with just one resolvable branching at  $t'$ . If  $t'' < t$  we continue the evolution as described above. This procedure is repeated until we generate  $t$ 's which are larger than  $t$ . By this procedure we sum all kinematically allowed contributions in the series  $\sum f_i(x, p)$  and obtain an MC estimate of the parton distribution function.

With the Sudakov factor  $\Delta_s$  and using

$$\frac{\partial}{\partial t'} \Delta_s(t, t') = \frac{\partial}{\partial t'} \frac{\Delta_s(t)}{\Delta_s(t')} = \frac{\Delta_s(t)}{\Delta_s(t')} \left[ \frac{1}{t'} \right] \int^{z_{max}} dz \tilde{P}(z),$$

we can write the first iteration of the evolution equation as

$$f_1(x, t) = f_0(x, t) + \int_x^1 \frac{dz'}{z'} \int_{t_0}^t d\Delta_s(t, t') \tilde{P}(z') f_0(x/z', t') \left[ \int^{z_{max}} dz \tilde{P}(z) \right]^{-1}. \quad (4.54)$$

The integrals can be solved by a Monte Carlo method [11]:  $z$  is generated from

$$\int_{z_{min}}^z dz' \tilde{P}(z') = R_1 \int_{z_{min}}^{z_{max}} dz' \tilde{P}(z'), \quad (4.55)$$

with  $R_1$  being a random number in  $[0, 1]$ , and  $t'$  is generated from

$$\begin{aligned} R_2 &= \int_{-\infty}^x f(x') dx' = F(x) \\ &= \int_{t'}^t \frac{\partial}{\partial t''} \left( \frac{\Delta_s(t)}{\Delta_s(t'')} \right) dt'' \\ &= \Delta_s(t, t') \end{aligned} \quad (4.56)$$

solving for  $t'$ , using  $z$  from above and another random number  $R_2$  in  $[0,1]$ .

This completes the calculation on the first splitting. This procedure is repeated until  $t' > t$  and the evolution is stopped.

With  $z'$  and  $t'$  selected according to the above the first iteration of the evolution equation yields

$$\begin{aligned}
 x f_1(x, t) &= x f_0(x) \Delta_s(t) \\
 &+ \sum_i \tilde{P}(z'_i) x'_i f_0(x'_i, t'_i) \left[ \int^{z_{max}} dz \tilde{P}(z) \right]^{-1}, \quad (4.57)
 \end{aligned}$$

with  $x'_i = x/z_i$ .





## Chapter 5

# BFKL and CCFM evolution equations

In this chapter the small  $x$  evolution equations BFKL [31–33] (after the names of the authors Balitsky, Fadin, Kuraev and Lipatov) and the CCFM [34–37] (after Catani, Ciafaloni, Fiorani and Marchesini) will be introduced. Instead of a formal introduction we start arguing why the transverse momenta, even if they are small, play a role in the parton evolution. This leads us to introduce an extension of the evolution equation including a transverse momentum dependence. With this we then start to argue, which new effects could happen at small  $x$ , and in analogy to the Sudakov form factor (introduced to treat virtual and soft contributions at large  $x$ ) we introduce a “non-Sudakov” form factor to treat, in the same way, the virtual corrections at small  $x$ . With this analogy we are able to derive the BFKL evolution equation in integral form. By extension to include also the large  $z$  region we then arrive at the CCFM evolution equation and describe the features of angular ordering.

### 5.1 Why are transverse momenta important for the evolution ?

Consider the process  $q + p_1 \rightarrow p_2$  with  $q^2 = -Q^2$ ,  $p_1^2 = -k^2$  and  $p_2^2 = m^2$ . This is the basic process for DIS scattering, except that now we do not neglect masses and transverse momenta. We use the definition of  $x_{Bj} = \frac{Q^2}{2q \cdot P}$ . Using energy momentum conservation we obtain:

$$\begin{aligned}(q + p_1)^2 &= p_2^2 \\ -Q^2 + 2q \cdot p_1 - k^2 &= m^2\end{aligned}$$

Using the longitudinal momentum fraction  $\xi$  with  $p_1 = \xi P$ , with  $P$  being the proton momentum, we obtain:

$$\begin{aligned}\xi &= \frac{Q^2 + m^2 + k^2}{2q \cdot P} \\ \xi &\neq x_{Bj}\end{aligned}$$

Depending on the values of  $m^2$  and  $k^2$ ,  $\xi$  can be very different from  $x_{Bj}$ .

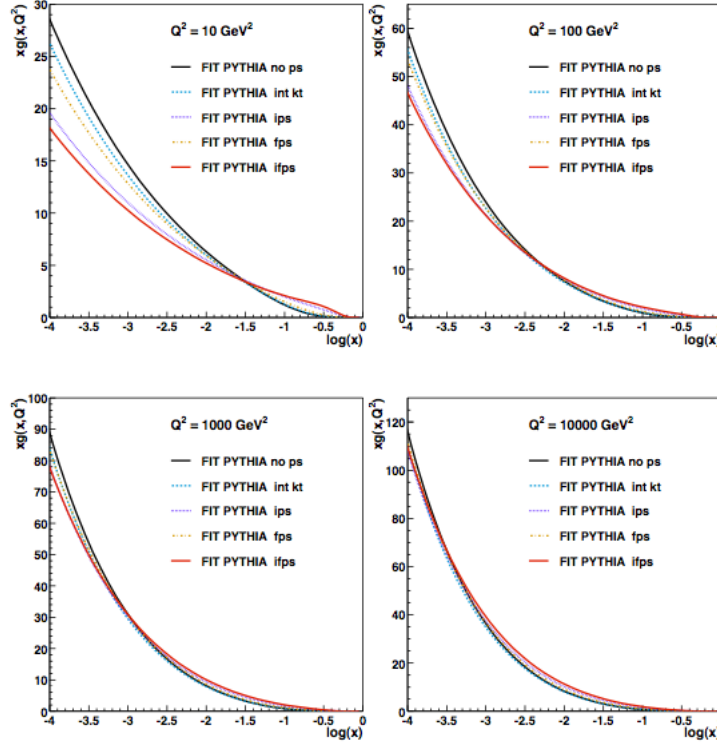


Figure 5.1: The gluon density as obtained from a DGLAP fit using the PYTHIA MC generator including parton showers.

Transverse momenta (or virtuality) in the initial state are coming from parton evolution: if a parton splits into two partons, the daughters must have transverse momenta. Therefore evolving a parton from a starting scale  $\mu_0^2$  up to a larger scale  $\mu^2$  involves automatically transverse momenta, up to the scale  $\mu^2$ . Such effects are visualized by using parton shower Monte Carlo event generators like PYTHIA [38, 39], HERWIG [40–42], or RAPGAP [43, 44]. The effect of transverse momenta to the parton evolution has been studied in [45]. A DGLAP fit to the structure function  $F_2(x, Q^2)$  has been performed using the PYTHIA MC event generator. Without intrinsic transverse momenta and without parton showers the fit to the structure function gave the same result as the CTEQ6 (LO) PDFs [26]. However when parton showers were turned on, the parameters for the PDFs were very different. An example of this is shown in Fig. 5.1

For the correct treatment of the kinematics in a process with multigluon radiation, not only the transverse momentum is important, but also the mass  $m_{rem}$  [46], as illustrated in Fig. 5.2.

In the following we calculate the relation between the transverse momentum  $k_t$  and the virtuality  $k^2$ . Consider a photon with light-cone vector  $q = (0, q^-, q_t)$ , a gluon with vector  $k = (xP^+, k^-, k_t)$  and the incoming proton with  $P = (P^+, 0, 0)$ . From this we obtain:

$$q^2 = -q_t^2$$

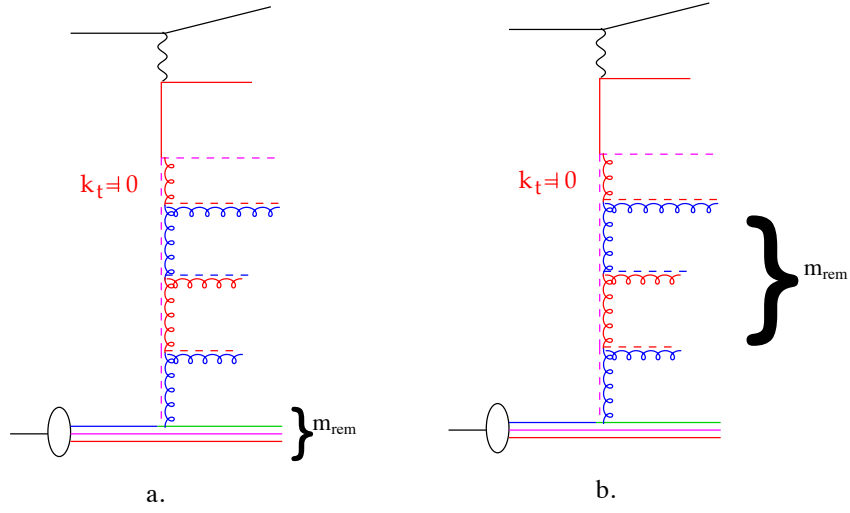


Figure 5.2: Illustration of the importance of the treatment of the mass  $m_{rem}$ : in the left only the proton remnants are included, in the right plot also the contribution of multiparton radiation is considered.

$$k^2 = 2xP^+k^- - k_t^2 \quad (5.1)$$

The mass of the remnant  $m_{rem}$  is (with  $P = k + r$  with  $r$  being the vector of the remnant system):

$$\begin{aligned}
 P &= k + r \rightsquigarrow r = P - k \\
 m_{rem}^2 &= (P - k)^2 = -2P^+k^- + k^2 = -2P^+k^- + 2xP^+k^- - k_t^2 \\
 &= -2P^+k^-(1-x) - k_t^2 \\
 \rightsquigarrow 2P^+k^- &= -\frac{k_t^2 + m_{rem}^2}{1-x} \\
 \rightsquigarrow k^2 &= -\frac{x(k_t^2 + m_{rem}^2) + k_t^2(1-x)}{1-x} \\
 &= -\frac{k_t^2 + xm_{rem}^2}{1-x}
 \end{aligned}$$

Thus we see clearly, that with increasing  $m_{rem}$  the virtuality is no longer dominated by  $k_t$ , and the full history of multiparton radiation must be included in the calculation.

## 5.2 $k_t$ -dependent Evolution Equation: BFKL Equation

We start from the integral form of the evolution equation, as given in Eq.(4.44):

$$f(x, t) = f(x, t_0)\Delta(t) + \int \frac{dt'}{t'} \frac{\Delta(t)}{\Delta(t')} \frac{\alpha_s(t')}{2\pi} \int \frac{dz}{z} P(z) f\left(\frac{x}{z}, t'\right)$$

using  $\Delta(t, t') = \frac{\Delta(t)}{\Delta(t')}$  we formally rewrite it for an unintegrated PDF (uPDF)  $\mathcal{A}(x, k_t, t)$  as a function of the scale  $q$ :

$$x\mathcal{A}(x, k_t, q) = x\mathcal{A}_0(x, k_t)\Delta_s(q) + \frac{\alpha_s}{2\pi} \int dz \int \frac{d^2q'}{\pi q'^2} \cdot \Delta_s(q, f(q')) \tilde{P}(z, q', k_t) \Theta(\mathcal{O}) \frac{x}{z} \mathcal{A}\left(\frac{x}{z}, k'_t, q'\right) \quad (5.2)$$

with

$$\frac{dt}{t} \rightarrow \frac{dq^2}{q^2} \rightarrow \frac{d^2q}{\pi q^2}$$

We have allowed for a more general form of the integration over  $q'$  by changing in the integration limit  $q' \rightarrow f(q')$ . We have also introduced a theta function  $\Theta(\mathcal{O})$  for the "ordering" condition in the evolution. Note that on the right side of the equation the argument in  $\mathcal{A}$  is  $k'_t$ , since it is determined by energy momentum conservation. The usual evolution equation is obtained back by:

$$xg(x, \mu^2) = \int \frac{d^2k_t}{\pi} x\mathcal{A}(x, k_t, q) \Theta(\mu - k_t)$$

As an example, the DLL approximation as discussed in a previous section is obtained by setting:  $P_{gg} = 6/z$ ,  $\Delta_s = 1$  and  $\Theta(\mathcal{O}) = \Theta(Q - q)$ .

With this equation we have the formal tool to study now the  $\frac{1}{z}$  singularity of the  $g \rightarrow gg$  splitting function. This splitting function becomes dominant at small  $z$  or at high energies.

We apply our knowledge from the  $\frac{1}{1-z}$  singularity: the singular behavior of the real emission was cancelled by the appropriate virtual correction, for the  $\frac{1}{1-z}$  singularity it was cancelled by the virtual vertex corrections why occurred for  $z \rightarrow 1$ . We suspect, that the  $\frac{1}{z}$  singularity is cancelled in a similar manner by virtual corrections, which can be treated by the concept of a form-factor (similar to the Sudakov form factor for the  $z \rightarrow 1$  case) which is called "non-Sudakov" form factor<sup>1</sup>  $\Delta_{ns}$  or "Regge" form factor. In Fig. 5.3 we show schematically the contributions which are divergent and which are cancelled by virtual corrections. The "non-DGLAP" limit would be obtained for  $k_t \sim k'_t$  and  $q_t \rightarrow 0$  (the DGLAP limit is  $k_t \gg k'_t$  which comes from taking  $k_t$  large). In this "non-DGLAP" limit we would have  $q^+$  large and  $q$  parallel to  $k'$  and  $k$ . In the following we show, how this can occur (for  $k_t \sim k'_t \rightsquigarrow q_t \rightarrow 0$ ) with  $x_1$  being the longitudinal momentum fraction:

$$\begin{aligned} k_t + q_t &= k'_t \\ k + q &= k' \\ k^+ + q^+ &= k'^+ \\ \rightsquigarrow x_1 p^+ + q^+ &= \frac{x_1}{z} p^+ \\ \rightsquigarrow x_1 p^+ \left(1 - \frac{1}{z}\right) &= -q^+ \end{aligned}$$

---

<sup>1</sup>"Non-Sudakov" form factor to distinguish from the Sudakov form factor.

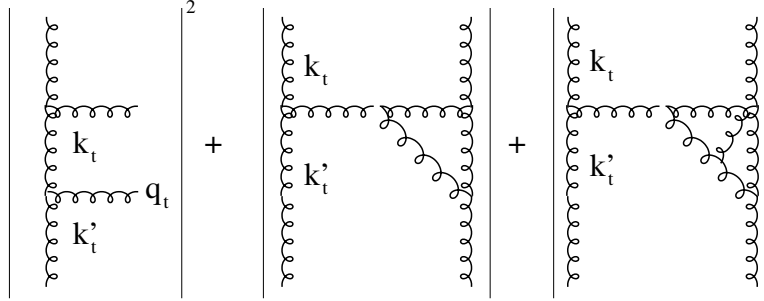


Figure 5.3: Schematic diagrams for the virtual corrections to cancel the divergent real emission.

$$\begin{aligned} \rightsquigarrow \frac{q^+}{p^+} &= \frac{x_1}{z}(1-z) \sim \frac{x_1}{z} = x_2 \\ \rightsquigarrow q^+ &\sim x_2 p^+ \sim k'^+ \end{aligned}$$

where the limit  $z \rightarrow 0$  has been taken and  $k^+ = x_1 p^+$ ,  $k'^+ = x_2 p^+$  and  $x_1 = z x_2$  has been used. Thus we see in the small  $z$  limit,  $q$  takes nearly all the energy of  $k'$ .

In order to obtain the BFKL evolution equation, we must now only relax the ordering condition from  $\Theta(\mathcal{O}) = \Theta(k_t^2 - k_t'^2)$  to  $\Theta(\mathcal{O}) = \Theta(k_t^2 - q_t^2)\Theta(q_t^2 - \mu^2)$ . Without the strong ordering in  $k_t$  a so-called random walk in  $k_t$  space can be performed, which means that all kinematically allowed values of  $k_t$  can appear. As a consequence of this, there is a diffusion into the soft region (the region where the scale  $\mu^2$  is small).

In analogy to the sudakov form factor which includes the  $\frac{1}{1-z}$  part of the splitting function to cancel the  $\frac{1}{1-z}$  singularity, we define the non-Sudakov form factor (including now only the  $\frac{1}{z}$  part of the splitting function as:

$$\Delta_{ns} = \exp\left(-\frac{3\alpha_s}{\pi} \int \frac{dq'^2}{q'^2} \int_z^1 \frac{dz'}{z'} \Theta(k_t^2 - q'^2)\Theta(q'^2 - \mu_0^2)\right) \quad (5.3)$$

$$= \exp\left(-\frac{3\alpha_s}{\pi} \log \frac{1}{z} \log \frac{k_t^2}{\mu_0^2}\right) \quad (5.4)$$

As the Sudakov form factor, the non-Sudakov form factor results in an all-order resummation of the virtual contributions. We can rewrite it as (using  $\bar{\alpha}_s = \frac{3\alpha_s}{\pi}$ ):

$$\begin{aligned} \Delta_{ns} &= \exp\left(\left(\log z\right)^{\bar{\alpha}_s \log \frac{k_t^2}{\mu_0^2}}\right) \\ &= z^\omega \text{ with } \omega = \bar{\alpha}_s \log \frac{k_t^2}{\mu_0^2} \end{aligned}$$

and we obtain the ( $k_t$ -dependent) BFKL splitting function as:

$$P_{BFKL} = \frac{6}{z} \Delta_{ns} = z^{-1+\omega}$$

With this we can now write the BFKL evolution equation in integral form [47, 48]:

$$\begin{aligned} x\mathcal{A}(x, k_t, q) &= x\mathcal{A}_0(x, k_t, q) + \frac{\alpha_s}{2\pi} \int dz \frac{6}{z} \Delta_{ns} \int \frac{dq'^2}{q'^2} \frac{x}{z} \mathcal{A}\left(\frac{x}{z}, k'_t, q'\right) \\ &= x\mathcal{A}_0(x, k_t, q) + \bar{\alpha}_s \int dz z^\omega \int \frac{dq'^2}{q'^2} \frac{x}{z} \mathcal{A}\left(\frac{x}{z}, k'_t, q'\right) \end{aligned}$$

where we just neglect the Sudakov form factor since we are working in the small  $x$  region.

### 5.3 $k_t$ -dependent Evolution Equation: CCFM Equation

In the following we describe the CCFM evolution equation [34–37] (after Catani, Ciafaloni, Fiorenza and Marchesini). This equation explicitly treats the emitted partons during the evolution by applying angular ordering. The equation was derived to be applicable both in the small and large  $x$  region. The angular ordering constraint ensures at large  $x$  an evolution similar to what is obtained by DGLAP while at small  $x$  it is equivalent to BFKL. Because the evolution explicitly treats the emitted partons, energy-momentum is conserved in each branching and therefore this equation is best suited for a simulation of the branching process with Monte Carlo event generators.

In the following we first describe angular ordering and then give the CCFM evolution equation.

#### 5.3.1 Angular Ordering

The ordering condition of successive parton emission determines how many partons can be radiated in a certain region of phase space. Subsequent emissions can be suppressed because of destructive interference effects. The angular ordering condition takes these interference effect approximately into account.

We first describe the angular ordering condition [14, 15] for the case of photon radiation from a  $e^+e^-$  pair, before we discuss the more complicated QCD case. We consider a process  $\gamma \rightarrow e^+e^- \gamma$  as shown in Fig. 5.4 and we calculate the lifetime of the  $e^+e^-$  pair:  $\Delta t = \frac{1}{\Delta E}$ . We use the following

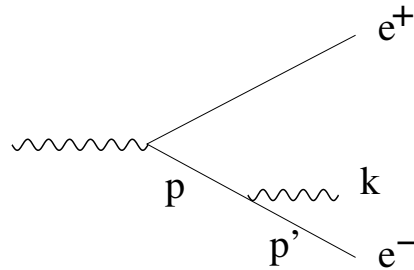


Figure 5.4: Schematic representation of the angular ordering constraint in  $e^+e^-$  scattering.

lightcone vectors (where we neglect the electron mass  $m_e$ ):

$$p = \frac{1}{\sqrt{2}}(p^+, p^-, 0) = \frac{1}{\sqrt{2}}(p^+, 0, 0)$$

$$\begin{aligned}
p' &= \frac{1}{\sqrt{2}} ((1-z)p^+, p^-, -k_t) = \frac{1}{\sqrt{2}} \left( (1-z)p^+, \frac{k_t^2}{(1-z)p^+}, -k_t \right) \\
k &= \frac{1}{\sqrt{2}} (zp^+, k^-, k_t) = \frac{1}{\sqrt{2}} \left( zp^+, \frac{k_t^2}{zp^+}, k_t \right)
\end{aligned}$$

where  $k$  is vector for the emitted photon,  $p'$  is the outgoing electron and  $p$  is the vector for the intermediate electron, before photon radiation. We calculate the energy imbalance  $\Delta E$  with:

$$\begin{aligned}
\Delta E &= p' + k - p \\
&= \frac{1}{2} ((p' + k)^+ + (p' + k)^-) - \frac{1}{2}(p^+ + p^-) \\
&= \frac{1}{2} \left( p^+ + \frac{k_t^2}{z(1-z)p^+} - p^+ \right) = \frac{1}{2} \frac{k_t^2}{z(1-z)p^+} \\
\rightsquigarrow \Delta E &= \frac{1}{2} \frac{k_t^2}{zp^+} \text{ for } z \rightarrow 0
\end{aligned}$$

using:

$$\begin{aligned}
p' + k &= \left( (1-z)p^+ + zp^+, \frac{k_t^2}{(1-z)p^+} + \frac{k_t^2}{zp^+}, 0 \right) \\
&= \left( p^+, \frac{zk_t^2 + (1-z)k_t^2}{z(1-z)p^+}, 0 \right) = \left( p^+, \frac{k_t^2}{z(1-z)p^+}, 0 \right)
\end{aligned}$$

For small angles we have  $k_t \sim zp^+ \Theta_{e\gamma}$

$$\Delta E \sim \frac{1}{2} \frac{z^2 p^{+2} \Theta_{e\gamma}^2}{zp^+} = \frac{1}{2} zp^+ \Theta_{e\gamma}^2 = \frac{1}{2} k \Theta_{e\gamma}^2$$

Introducing the transverse wavelength  $\lambda_\perp^{-1} = k_t = \Theta_{e\gamma} k$  we obtain for the lifetime  $\Delta t$ :

$$\Delta t = \frac{1}{\Delta E} = 2 \frac{\lambda_\perp}{\Theta_{e\gamma}} \quad (5.5)$$

During the time  $\Delta t$ , the  $e^+e^-$  pair travels a distance:

$$\rho_\perp^{e^+e^-} = \Delta x \Delta t \sim \Theta_{ee} \Delta t = \theta_{e^+e^-} \frac{\lambda_\perp}{\Theta_{e\gamma}}$$

For  $\Theta_{e\gamma} \gg \Theta_{e^+e^-}$  we obtain:

$$\rho_\perp < \lambda_\perp$$

which means that the radiated photon cannot resolve any structure of the  $e^+e^-$  pair, it probes only the total charge which is zero.

The  $e^-$  can emit photons if:

$$\begin{aligned} \rho_{\perp} &> \lambda_{\perp} \\ \rightsquigarrow \Theta_{e\gamma} &< \theta_{e^+e^-} \end{aligned}$$

which is the angular ordering condition for QED. Outside this region, the cross section for radiation is suppressed. The concept of angular ordering is known already from cosmic rays as the "Chudakov effect" (1955).

In QCD a similar picture emerges, but the radiation of soft gluons from a pair of quarks is no longer zero (since the color charge is non-zero, and gluons can radiate from gluons), but the radiation is, as if it were emitted from the parent gluon (see Fig. 5.5). In QCD gluon emission is

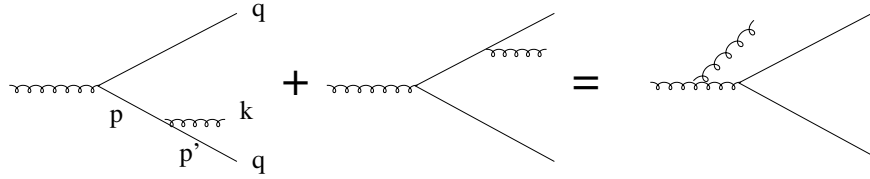


Figure 5.5: Schematic representation of radiation from a pair of quarks whose color charge is non-zero.

allowed:

$$\begin{aligned} \text{off } \bar{q} &\text{ for } \Theta_{k\bar{q}} < \Theta_{q\bar{q}} \\ \text{off } q &\text{ for } \Theta_{kq} < \Theta_{q\bar{q}} \\ \text{off parent } g &\text{ for } \Theta_{kg} > \Theta_{q\bar{q}} \end{aligned}$$

such that soft gluon emission at large angles is suppressed (an explicit calculation can be found in [14]).

In the following we describe how the angular ordering condition is applied to the parton evolution. The vector of the radiated parton is denoted with  $q$ , and the energy component of this

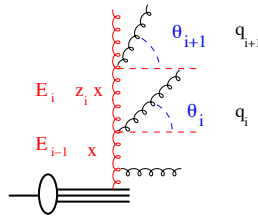


Figure 5.6: Schematic representation of radiation in an angular ordered region of phase space.

vector is given by  $q_0$ . The energy of the propagating parton is given by  $E$ . We define the transverse momenta as  $p_{ti} = |q_i^0| \sin \Theta_i$  (taking partons to be massless) where we define the splitting



variable  $z = \frac{E_i}{E_{i-1}}$  for the  $i$  and  $(i-1)$  parton. Defining  $q_i = \frac{p_{ti}}{1-z_i}$  and the angles

$$\begin{aligned}\Theta_i &= \frac{q_i}{E_{i-1}} \\ \Theta_{i+1} &= \frac{q_{i+1}}{E_i}\end{aligned}$$

we obtain:

$$\begin{aligned}\Theta_i &> \Theta_{i-1} \\ \rightsquigarrow \frac{q_i}{E_{i-1}} &> \frac{q_{i-1}}{E_{i-2}} \\ \rightsquigarrow q_i &> \frac{E_{i-1}}{E_{i-2}} q_{i-1} = z_{i-1} q_{i-1}\end{aligned}\tag{5.6}$$

We finally obtain for the angular ordering:

$$q_{max} > z_n q_n, q_n > z_{n-1} q_{n-1}, \dots, q_1 > Q_0\tag{5.7}$$

The angular ordering condition in Eq.(5.6) gives for  $z \rightarrow 0$  essentially no constraint on the values of  $q_i$  and therefore on  $p_t$ , allowing for a *random walk* in  $p_t$  space, as requested from the BFKL equation. On the other hand, at large  $z$  the angular ordering condition reduces to an ordering in  $q_i$ , as requested from the DGLAP evolution equations.

### 5.3.2 CCFM Equation

The CCFM [34–37] evolution equation is given by a straight forward application of the angular ordering constraint to the equation for unintegrated parton densities eq.(5.2) [37, 47, 49, 50]:

$$\begin{aligned}x\mathcal{A}(x, k_t, q) &= x\mathcal{A}_0(x, k_t)\Delta_s(q) + \int dz \int \frac{d^2q'}{\pi q'^2} \Theta(q - zq') \\ &\quad \cdot \Delta_s(q, zq') \tilde{P}(z, q', k_t) \frac{x}{z} \mathcal{A}\left(\frac{x}{z}, k'_t, q'\right)\end{aligned}\tag{5.8}$$

with  $\vec{k}'_t = \vec{k}_t + (1-z)\vec{q}$  and  $q$  being the upper scale for any emission:

$$q > z_n q_n, q_n > z_{n-1} q_{n-1}, \dots, q_1 > Q_0\tag{5.9}$$

The Sudakov form factor  $\Delta_s$  is given by:

$$\Delta_s(q, Q_0) = \exp\left(-\int_{Q_0^2}^{q^2} \frac{dq'^2}{q'^2} \int_0^{1-Q_0/q'} dz \frac{\bar{\alpha}_s(q'(1-z))}{1-z}\right)\tag{5.10}$$

with  $\bar{\alpha}_s = \frac{3\alpha_s}{\pi}$ . For inclusive quantities at leading-logarithmic order the Sudakov form factor cancels against the  $1/(1-z)$  collinear singularity of the splitting function.

The splitting function  $P_{gg}$  for branching  $i$  is given by:

$$P_{gg}(z_i, q_i, k_{ti}) = \frac{\bar{\alpha}_s(k_{ti})}{z_i} \Delta_{ns}(z_i, q_i, k_{ti}) + \frac{\bar{\alpha}_s(p_{ti})}{1 - z_i} \quad (5.11)$$

with  $p_{ti} = q_i(1 - z_i)$  and the non-Sudakov form factor  $\Delta_{ns}$  defined as:

$$\log \Delta_{ns}(z_i, q_i, k_{ti}) = -\bar{\alpha}_s \int_{z_i}^1 \frac{dz'}{z'} \int \frac{dq^2}{q^2} \Theta(k_{ti} - q) \Theta(q - z' q_i) \quad (5.12)$$

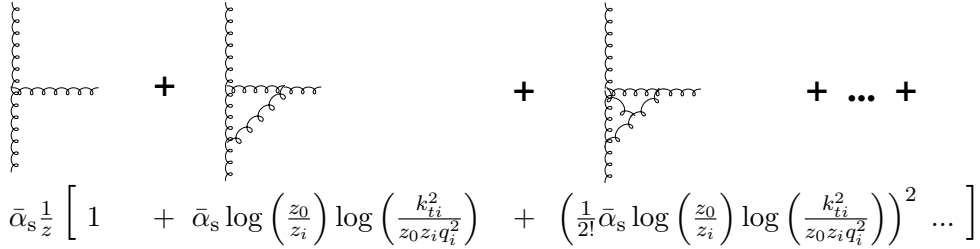
The upper limit of the  $z'$  integral is constrained by the  $\Theta$  functions in eq.(5.12) by:  $z_i \leq z' \leq \min(1, k_{ti}/q_i)$ , which results in the following form of the non-Sudakov form factor [47]:

$$\log \Delta_{ns} = -\bar{\alpha}_s(k_{ti}) \log \left( \frac{z_0}{z_i} \right) \log \left( \frac{k_{ti}^2}{z_0 z_i q_i^2} \right) \quad (5.13)$$

where

$$z_0 = \begin{cases} 1 & \text{if } k_{ti}/q_i > 1 \\ k_{ti}/p_{ti} & \text{if } z_i < k_{ti}/q_i \leq 1 \\ z_i & \text{if } k_{ti}/q_i \leq z_i \end{cases}$$

The non-Sudakov form factor can be written as:



$$\bar{\alpha}_s \frac{1}{z} \left[ 1 + \bar{\alpha}_s \log \left( \frac{z_0}{z_i} \right) \log \left( \frac{k_{ti}^2}{z_0 z_i q_i^2} \right) + \left( \frac{1}{2!} \bar{\alpha}_s \log \left( \frac{z_0}{z_i} \right) \log \left( \frac{k_{ti}^2}{z_0 z_i q_i^2} \right) \right)^2 \dots \right]$$

where the similarity with the Sudakov form factor becomes obvious. Note however, that the Sudakov form factor  $\Delta_s$  resums the large  $z$  contributions, whereas the non-Sudakov form factor  $\Delta_{ns}$  resums the small  $z$  ones.

## 5.4 High energy or $k_t$ -factorization

At large energies (small  $x$ ) the evolution of parton densities proceeds over a large region in rapidity  $\Delta y \sim \log(1/x)$  and effects of finite transverse momenta of the partons may become increasingly important. Cross sections can then be  $k_t$ -factorized [51–54] into an off-mass shell ( $k_t$  dependent) partonic cross section  $\hat{\sigma}(\frac{x}{z}, k_t)$  and an  $k_t$ -unintegrated parton density function  $\mathcal{F}(z, k_t)$ :

$$\sigma = \int \frac{dz}{z} d^2 k_t \hat{\sigma}\left(\frac{x}{z}, k_t\right) \mathcal{F}(z, k_t) \quad (5.14)$$

Carrying out the  $k_t$  integration in eq.(5.14) explicitly, a form fully consistent with collinear factorization can be obtained [55,56]: the coefficient functions and also the DGLAP splitting functions leading to  $f_a(z, \mu_f^2)$  are no longer evaluated in fixed order perturbation theory but supplemented with the all-order resummation of the  $\alpha_s \log 1/x$  contribution at small  $x$ .

It is also interesting to consider the limit  $k_t \rightarrow 0$  of the matrix elements [57]. To do that we define a reduced cross section  $\tilde{\sigma}$ :

$$\tilde{\sigma}(k_t) = \int d\text{Lips} |M|^2 \quad (5.15)$$

where we integrate over the Lorentz-invariant-phase-space (Lips) of the final state quarks. The matrix element  $|M|^2$  is taken from [53,54], where we have set  $16\pi^2\alpha_{em}\alpha_s e_q^2 \equiv 1$ . In Fig. 5.7 we

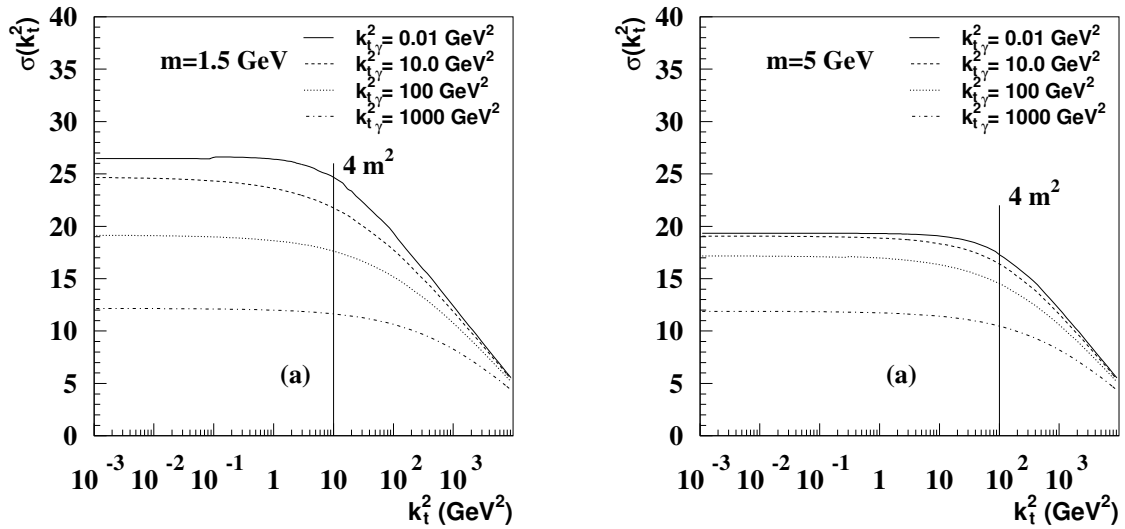


Figure 5.7: The reduced cross section  $\tilde{\sigma}(k_t)$  as a function of the transverse momentum  $k_t$  of the incoming gluon for different values of the transverse momentum of the incoming photon  $k_{t,\gamma}$  ( $m = 1.5$  GeV in (a),  $m = 5$  GeV in (b),  $\sqrt{s} = 30000$  GeV and a fixed  $x_\gamma = x_g = 0.01$ ). Figure from [57].

show  $\tilde{\sigma}(k_t)$  as a function of the transverse momentum of the incoming gluon  $k_t$  for quark masses of  $m = 1.5$  GeV in Fig. 5.7a and for  $m = 5$  GeV in Fig. 5.7b using  $\sqrt{s} = 30000$  GeV and a fixed  $x_\gamma = x_g = 0.01$ . In both cases a smooth behavior for  $k_t \rightarrow 0$  is observed. It is also interesting to note that in all cases the cross section starts to decrease at  $k_t^2 \gtrsim 4m^2$ . The region  $k_t^2 > 4m^2$  is still contributing to the total cross section significantly, indicating a difference to the usual collinear approximation, where this region is completely ignored.

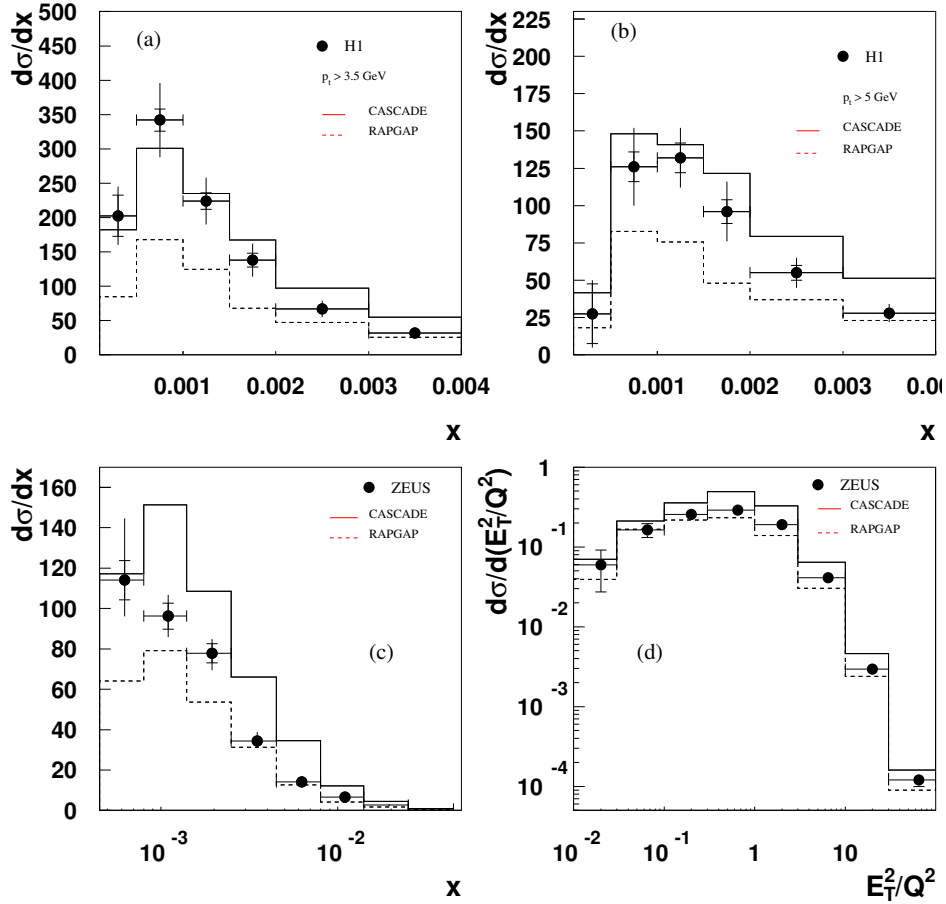


Figure 5.8: The cross section for forward-jet production obtained from the Monte Carlo CASCADE at hadron level (solid line); (a – c) The cross section for forward-jet production as a function of  $x$ , for different cuts in  $p_t$  compared to H1 data [58] (a – b) and compared to ZEUS data [59] (c); (d) The cross section for forward-jet production as a function of  $E_T^2/Q^2$  compared to [60].

## 5.5 Comparison with measurements in $ep$

In the following a few measurements performed at the  $ep$  collider HERA are compared with predictions obtained from a CCFM evolution convoluted with off-shell matrix elements as implemented in the Monte Carlo generator CASCADE [49, 61].

In [49] the production of “forward jets” is compared with measurements from [58–60] In Fig. 5.8 the cross section predicted for forward-jet production is shown and compared to measurements done at HERA. We observe a reasonable description of the data.

In [62] angular correlations for final states with two jets and three jets are calculated (see Fig. 5.9). The azimuthal distribution of di-jet and three-jet cross sections in the separation  $\Delta\phi$

between the leading jets is investigated. In Fig. 5.9 (from [62]) the distributions obtained by CASCADE and by HERWIG, compared with the measurement [63] are shown. Observe that the shape of the distribution is different for the two Monte Carlos.

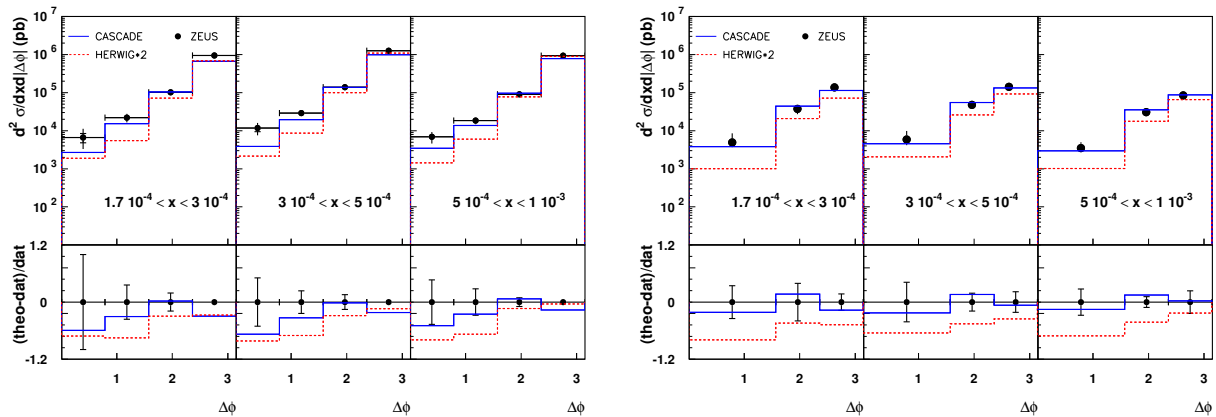


Figure 5.9: Angular jet correlations obtained by CASCADE and by HERWIG, compared with  $ep$  data [63]: (top) di-jet cross section; (bottom) three-jet cross section. The HERWIG results are multiplied by a factor of 2.



## Chapter 6

# Hadron-Hadron scattering

It is one of the striking features in particle physics that Feynman diagrams calculated for one process can be easily extended to other processes, where the incoming and final state particles are exchanged. This we can apply to use our knowledge obtained in  $ep$  scattering to the case of hadron hadron or  $pp$  or  $p\bar{p}$  scattering, as illustrated in Fig. 6.1

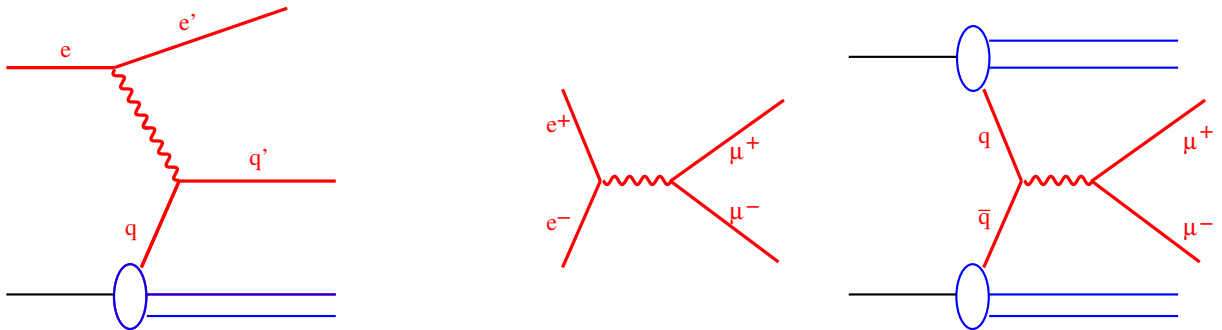


Figure 6.1: Schematic illustration of  $ep \rightarrow e'X$ ,  $e^+e^- \rightarrow \mu^+\mu^-$  and  $pp \rightarrow \mu^+\mu^-X$  diagrams

### 6.1 Drell-Yan production in $pp$

From the matrix element  $ep_q \rightarrow e'p_{q'}$  in eq.(3.59) we obtain the matrix element for  $e^+e^- \rightarrow \mu^+\mu^-$ :

$$|M|^2(e^+e^- \rightarrow \mu^+\mu^-) = 2(4\pi\alpha)^2 \frac{\hat{t}^2 + \hat{u}^2}{\hat{s}^2} \quad (6.1)$$

with

$$\begin{aligned} \hat{s} &= 4E_b^2 \\ \hat{t} &= -2E_b^2(1 - \cos\theta) \\ \hat{u} &= -2E_b^2(1 + \cos\theta) \end{aligned}$$

with  $\theta$  being the polar angle of the scattered  $\mu$  with respect to the incoming  $e^+$  and  $E_b$  being the energy of the incoming  $e^+$  in the center of mass frame of the  $e^+e^-$  pair.

The cross section is given by

$$\begin{aligned}\frac{d\sigma}{d\Omega} &= \frac{1}{64\pi^2\hat{s}}|M|^2 \\ &= \frac{1}{64\pi^2\hat{s}}(2\alpha^2(4\pi)^2)\frac{4E_b^4(1-\cos\theta)^2+4E_b^4(1+\cos\theta)^2}{16E_b^4} \\ &= \frac{\alpha^2}{4\hat{s}}(1+\cos^2\theta)\end{aligned}$$

This gives then the total cross section:

$$\sigma(e^+e^- \rightarrow \mu^+\mu^-) = \int_0^{2\pi} d\phi \int_{-1}^{+1} d\cos\theta \frac{\alpha^2}{4\hat{s}}(1+\cos^2\theta) = \frac{4\pi\alpha^2}{3\hat{s}}$$

If we calculate the cross section for the crossed diagram  $q\bar{q} \rightarrow e^+e^-$  we must take into account the fractional charge of the quarks  $e_q^2$ , giving:

$$\sigma(q + \bar{q} \rightarrow \mu^+\mu^-) = \frac{4\pi\alpha^2}{3\hat{s}}e_q^2$$

and since quarks are not free but confined in hadrons we obtain:

$$\frac{d\sigma}{dM^2} = \frac{1}{3} \frac{1}{3} 3 \sum_q \int dx_1 dx_2 f_q(x_1) f_{\bar{q}}(x_2) \frac{d\hat{\sigma}}{dM^2} \quad (6.2)$$

with  $f(x_1), f(x_2)$  being the parton distribution functions and  $x_1(x_2)$  being the fractional momenta of the protons carried by the partons and

$$\frac{d\hat{\sigma}}{dM^2} = \frac{4\pi\alpha^2}{3\hat{s}}e_q^2\delta(\hat{s}-M^2) \quad (6.3)$$

with  $\hat{s} = x_1x_2s$  (neglecting masses of the incoming particles and partons),  $M$  being the mass of the  $q\bar{q}$  system and  $s$  being the proton-proton center-of-mass energy. the factors  $\frac{1}{3}$  in eq.(6.2) come from averaging over the initial 3 color states of  $q$  and  $\bar{q}$  while the factor 3 comes from the sum over the final state color singlet combinations. The process  $pp \rightarrow \mu^+\mu^- + X$  is called Drell-Yan process (DY), after the authors who calculated first the cross section [64].

The rapidity  $y$  is related to the ratio of the momentum fractions  $\frac{x_1}{x_2}$  as shown in the following. Consider the process  $pp \rightarrow \mu^+\mu^- + X$  with the momenta of incoming partons

$$\begin{aligned}p_1 &= \frac{\sqrt{s}}{2}(x_1, 0, 0, x_1) \\ p_2 &= \frac{\sqrt{s}}{2}(x_2, 0, 0, -x_2)\end{aligned}$$



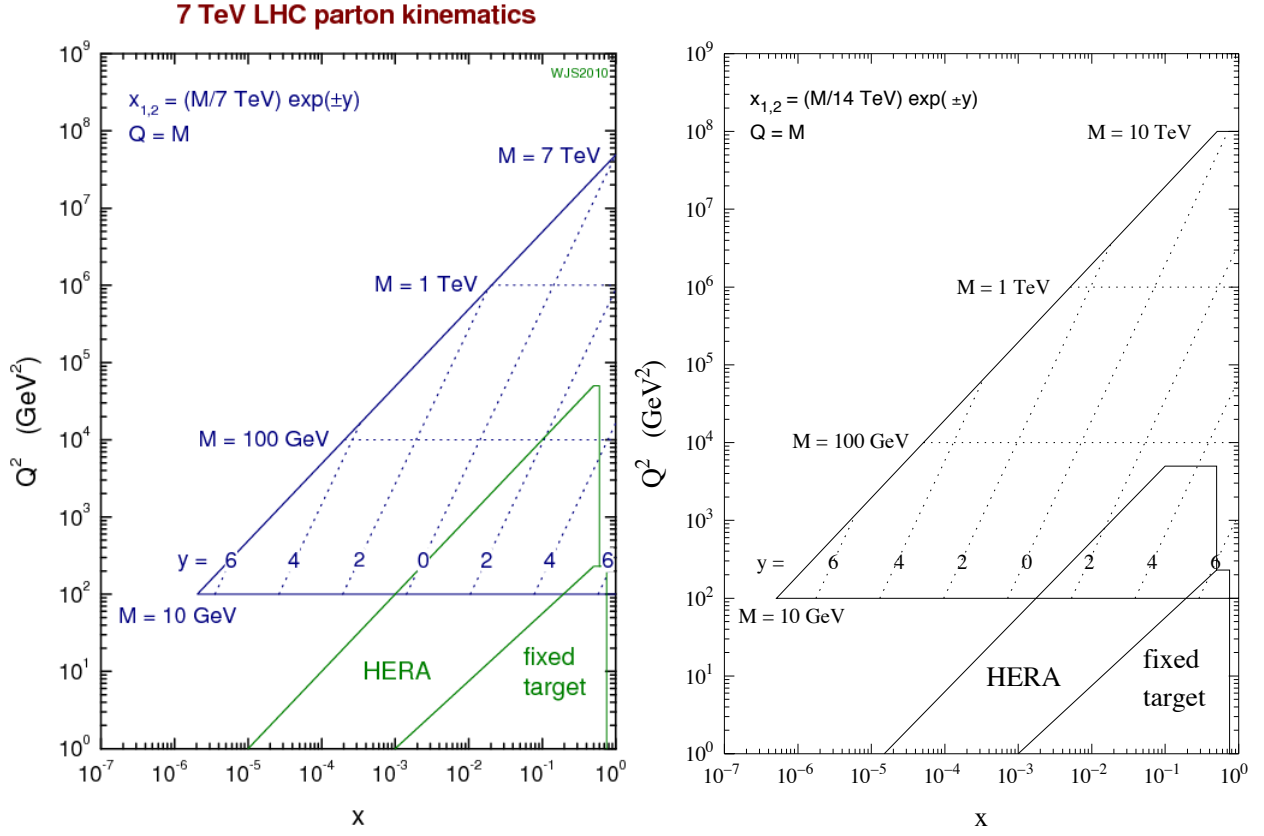


Figure 6.2: Kinematic relation of  $y$  with the momentum fraction  $x$  and the mass  $M$  for two different  $\sqrt{s}$  energies (taken from [65]).

then the rapidity  $y = \frac{1}{2} \log \frac{E+p_z}{E-p_z}$  of the  $\mu^+\mu^-$  is equal to the rapidity of the  $p_1p_2$  pair with

$$E = E_1 + E_2 = \frac{\sqrt{s}}{2}(x_1 + x_2)$$

$$p_z = p_{z1} + p_{z2} = \frac{\sqrt{s}}{2}(x_1 - x_2)$$

The rapidity  $y$  of the incoming parton pair is then:

$$y = \frac{1}{2} \log \frac{E + p_z}{E - p_z} = \frac{1}{2} \log \frac{x_1}{x_2}$$

Defining  $\tau = \frac{M^2}{s} = x_1x_2$  we obtain:

$$x_1 = \sqrt{\tau} \exp(y)$$

$$x_2 = \sqrt{\tau} \exp(-y)$$

In fig.6.2 from [65] the relation between rapidity and the momentum fraction  $x$  is shown for different  $M^2$ .

The lowest order Drell Yan cross section is then:

$$\frac{d\sigma}{dM^2} = \frac{4\pi\alpha^2}{9M^2} \sum_q \int dx_1 dx_2 f_q(x_1) f_{\bar{q}}(x_2) e_q^2 \delta(\hat{s} - M^2) \quad (6.4)$$

$$= \frac{4\pi\alpha^2}{9M^2} \frac{1}{s} \sum_q e_q^2 \int dx_1 dx_2 f_q(x_1) f_{\bar{q}}(x_2) \delta\left(x_1 x_2 - \frac{M^2}{s}\right) \quad (6.5)$$

$$= \frac{4\pi\alpha^2}{9M^2} \frac{1}{s} \sum_q e_q^2 \int dx_1 dx_2 f_q(x_1) f_{\bar{q}}(x_2) \frac{1}{x_1} \delta\left(x_2 - \frac{\tau}{x_1}\right) \quad (6.6)$$

$$= \frac{4\pi\alpha^2}{9M^2} \frac{1}{s} \sum_q e_q^2 \int \frac{dx_1}{x_1} f_q(x_1) f_{\bar{q}}\left(x_2 = \frac{\tau}{x_1}\right) \quad (6.7)$$

$$\left(\frac{d\sigma}{dM^2 dy}\right)_{Born} = \frac{4\pi\alpha^2}{9M^2} \frac{1}{s} \sum_q e_q^2 f_q(x_1) f_{\bar{q}}\left(x_2 = \frac{\tau}{x_1}\right) \quad (6.8)$$

with  $dy = \frac{dx_1}{x_1}$ , where the terminology *Born* means lowest order.

### 6.1.1 Factorization of production and decay in Drell Yan processes

Calculating  $\mathcal{O}(\alpha_s)$  correction to DY production involves  $2 \rightarrow 3$  processes. However, we can simplify the calculation if we apply the same methods as in DIS: we try to separate the production process from the decay, as illustrated in fig. 6.3. By doing so, we can reduce the problem to a

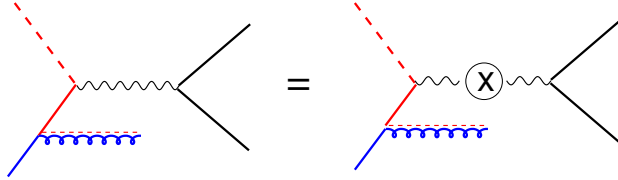


Figure 6.3: Schematic diagram to separate the production from the decay in a Drell Yan process.

simple calculation of a  $2 \rightarrow 2$  process. The cross section is then written in a factorized form:

$$d\sigma(q + \bar{q} \rightarrow l^+ + l^-) = d\sigma(q + \bar{q} \rightarrow \gamma^*) \otimes \frac{1}{Q^4} \otimes d\sigma(\gamma^* \rightarrow l^+ + l^-)$$

where the first term corresponds to the production, the second term is the photon propagator and the third term describes the decay.

The matrix element for  $\gamma^*(q) \rightarrow l^-(k_1) + l^+(k_2)$  is given by [12][see exercise 10.2]:

$$\begin{aligned} M(\gamma^* \rightarrow l^+ l^-) &= e \bar{u}(k_1) \gamma_\mu \nu(k_2) \\ |M(\gamma^* \rightarrow l^+ l^-)|^2 &= \frac{16\pi\alpha}{3} Q^2 \end{aligned}$$

with  $q^2 = Q^2$  being the timelike mass of  $\gamma^*$ .

The matrix element for  $q\bar{q} \rightarrow \gamma^*$  is given by:

$$|M(q\bar{q} \rightarrow \gamma^*)|^2 = \frac{4\pi\alpha}{3} M^2 e_q^2$$

with  $M^2 = Q^2$  being the mass of the  $q\bar{q}$  system (note: do not confuse this with the notation for the matrix element).

We write the cross section for  $q + \bar{q} \rightarrow l^+ + l^-$  as (where the particles are treated massless):

$$d\sigma(q + \bar{q} \rightarrow l^+ + l^-) = \frac{1}{M^2} |M(q\bar{q} \rightarrow l^+ l^-)|^2 \frac{d^4 k_1}{(2\pi)^3} \frac{d^4 k_2}{(2\pi)^3} (2\pi)^4 \delta^4(p_1 + p_2 - k_1 - k_2) \quad (6.9)$$

$$= \frac{1}{M^2} |M(q\bar{q} \rightarrow \gamma^*)|^2 d^4 q \delta^4(p_1 + p_2 - q) \frac{1}{Q^4} |M(\gamma^* \rightarrow l^+ l^-)|^2 \\ \times \frac{d^4 k_1}{(2\pi)^3} \frac{d^4 k_2}{(2\pi)^3} (2\pi)^4 \delta^4(q - k_1 - k_2)$$

$$= \frac{1}{2M^2} |M(q\bar{q} \rightarrow \gamma^*)|^2 d^4 q \delta^4(p_1 + p_2 - q) \frac{1}{Q^4} |M(\gamma^* \rightarrow l^+ l^-)|^2 \frac{d\Omega}{32\pi^2}$$

$$= \frac{1}{2M^2} \frac{4\pi\alpha}{3} M^2 e_q^2 d^4 q \delta^4(p_1 + p_2 - q) \frac{1}{Q^4} \frac{16\pi\alpha}{3} Q^2 \frac{d\Omega}{32\pi^2}$$

$$= \frac{1}{2M^2} \frac{4\pi\alpha}{3} M^2 e_q^2 d^4 q \delta^4(p_1 + p_2 - q) 2\pi \frac{\alpha}{3\pi M^2} \quad (6.10)$$

$$\frac{d\sigma}{dM^2} = \frac{4\pi^2 \alpha e_q^2}{3} \times \frac{\alpha}{3\pi M^2} \delta(Q^2 - M^2) \quad (6.11)$$

$$= \frac{4\pi^2 \alpha^2 e_q^2}{9M^2} \delta(Q^2 - M^2) \quad (6.12)$$

where we recovered in the last line again eq.(6.3). With this result we only need to calculate the cross sections for:

$$\begin{aligned} pp &\rightarrow Z_0 + X \\ pp &\rightarrow \gamma^* + X \\ pp &\rightarrow W^\pm + X \\ pp &\rightarrow H + X \text{ etc.} \end{aligned}$$

where  $H$  stands for the Higgs boson.

### 6.1.2 Factorization in Drell Yan processes

A crucial assumption of Bjorken scaling is, that the amplitude of a process is suppressed, when the virtuality of the partons become larger than a typical hadronic mass scale (see discussion in [14][p 304]). This assumption is equivalent to the requirement that the partons can have only limited transverse momenta with respect to the direction of the beam hadron. We can generalize

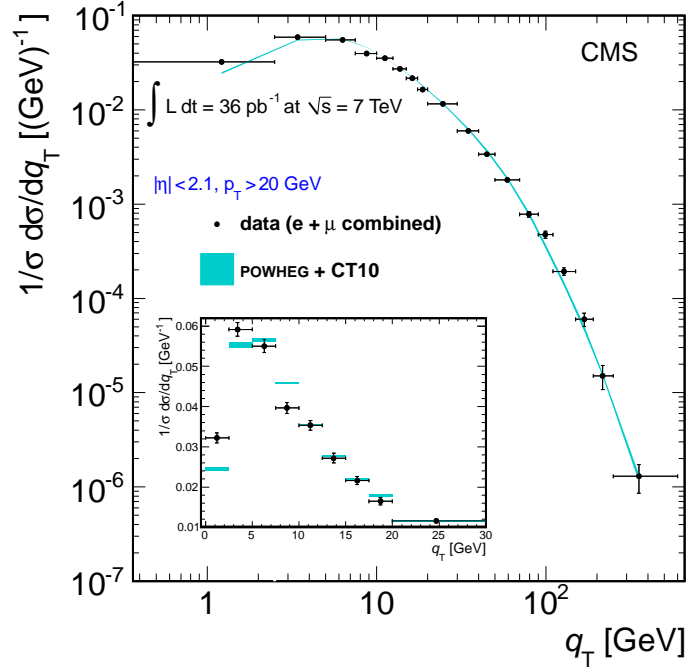


Figure 6.4: The transverse momentum of the  $Z_0$  boson as measured by [66].

the parton distribution function to take into account also transverse momenta (see discussion on unintegrated PDFs section 5.2)

$$d\xi f(\xi) \rightarrow d^2\vec{k}_t d\xi P(k_t, \xi) \text{ with } \int d^2\vec{k}_t P(\vec{k}_t, \xi) = f(\xi)$$

where  $\vec{k}_t$  is a 2-dimensional vector.

For a hard scattering scale in an inclusive process (where we do not investigate observables sensitive to  $k_t$ ) one can set

$$P(\vec{k}_t, \xi) = \delta(\vec{k}_t) f(\xi)$$

and neglect all transverse momenta (as was done in the discussion of the DGLAP PDFs). If the transverse momentum of the partons is zero, then also the DY pair has zero transverse momentum, which is in contrast to what is observed in measurements [66] (fig. 6.4).

Assuming a distribution function  $P(\vec{k}_t, \xi)$  with:

$$\begin{aligned} P(\vec{k}_t, \xi) &= h(\vec{k}_t) f(\xi) \\ h(\vec{k}_t) &= \frac{b}{\pi} \exp(-b\vec{k}_t^2) \end{aligned}$$

we obtain:

$$\frac{1}{\sigma} \frac{d\sigma}{dp_t} = \int d^2\vec{k}_{t1} d^2\vec{k}_{t2} \delta^{(2)}(\vec{k}_{t1} + \vec{k}_{t2} - \vec{p}_t) h(\vec{k}_{t1}) h(\vec{k}_{t2}) \quad (6.13)$$

$$= \int d^2 \vec{k}_{t1} h(\vec{k}_{t1}) h(\vec{p}_t - \vec{k}_{t1}) \quad (6.14)$$

Applying the substitution<sup>1</sup>  $\vec{k} = \frac{1}{2}\vec{p}_t - \vec{k}_{t1}$  we obtain (using  $d^2 \vec{k}_t = dk_t^2 \frac{d\phi}{2}$ ):

$$\frac{1}{\sigma} \frac{d\sigma}{dp_t} = \frac{b^2}{\pi^2} \int d^2 \vec{k} h\left(\frac{1}{2}\vec{p}_t - \vec{k}\right) h\left(\vec{k} + \frac{1}{2}\vec{p}_t\right) \quad (6.15)$$

$$= \frac{b^2}{\pi^2} \int d^2 \vec{k} \exp\left(-\frac{b}{2}p_t^2 - 2bk^2\right) \quad (6.16)$$

$$= \frac{b^2}{\pi} \exp\left(-\frac{b}{2}p_t^2\right) \int_0^\infty dk^2 \exp(-2bk^2) \quad (6.17)$$

$$= \frac{b}{2\pi} \exp\left(-\frac{b}{2}p_t^2\right) \quad (6.18)$$

Another way to solve the integral is shown in Appendix 8.2

At low  $p_t$  the measurements are well described by this expression, however a tail towards high  $p_t$  is observed (see fig. 6.4), which cannot be described by the (limited) intrinsic transverse momentum of partons inside the hadrons.

### 6.1.3 $\mathcal{O}(\alpha_s)$ contributions to Drell Yan production

From the early measurements of the transverse momentum spectrum of Drell Yan production (see fig. 6.4) it became clear, that the naive parton model is incomplete: the tail of large  $p_t$  could not be described assuming that the intrinsic  $p_t$  of the partons inside the hadrons is small. Already by comparing the measured cross section of Drell Yan production with the prediction based on the parton model, the so called  $K$ -factor defined as

$$K = \frac{\sigma^{\text{measured}}}{\sigma^{\text{calculated}}(\text{LO})}$$

was found to be large, of the order of 2 – 3, indicating that important contributions to the cross section were not included in the lowest order (LO) calculation.

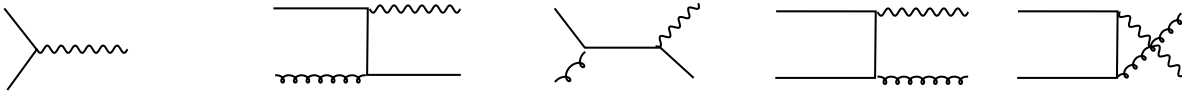


Figure 6.5: Diagrams contributing to Drell Yan production up to  $\mathcal{O}(\alpha_s)$ .

The  $\mathcal{O}(\alpha_s)$  contributions to Drell Yan production can be calculated using the same matrix elements, which have been used for the  $\mathcal{O}(\alpha_s)$  corrections to DIS (see section 3.5). The LO and  $\mathcal{O}(\alpha_s)$  diagrams are shown in Fig. 6.5, which are the diagrams from DIS with exchanged initial and final particles.

<sup>1</sup>Thanks to Radek Zlebcik for pointing out this elegant solution during the lecture at DESY 2013

The matrix element for  $q\bar{q} \rightarrow \gamma^* g$  is given by:

$$|M|^2 = 16\pi^2 \alpha_s \alpha \frac{8}{9} \left[ \frac{\hat{u}}{\hat{t}} + \frac{\hat{t}}{\hat{u}} + \frac{2(M^2 \hat{s})}{\hat{u}\hat{t}} \right] \quad (6.19)$$

$$= 16\pi^2 \alpha_s \alpha \frac{8}{9} \left[ \left( \frac{1+z^2}{1-z} \right) \left( \frac{-\hat{s}}{\hat{t}} + \frac{-\hat{s}}{\hat{u}} \right) - 2 \right] \quad (6.20)$$

$$= 16\pi^2 \alpha_s \alpha \frac{2}{3} \left[ P_{qq}(z) \left( \frac{-\hat{s}}{\hat{t}} + \frac{-\hat{s}}{\hat{u}} \right) - 2 \right] \quad (6.21)$$

where we have used  $z = \frac{M^2}{\hat{s}}$  and  $\hat{u} + \hat{t} = M^2 - \hat{s} = -\hat{s}(1-z)$ . We have also introduced the splitting function (known from DIS):

$$P_{qq} = \frac{4}{3} \frac{1+z^2}{1-z}$$

Similarly, we obtain for  $qg \rightarrow \gamma^* q$ :

$$|M|^2 = 16\pi^2 \alpha_s \alpha \frac{1}{3} \left[ -\frac{\hat{t}}{\hat{s}} - \frac{\hat{s}}{\hat{t}} - \frac{2(M^2 \hat{u})}{\hat{s}\hat{t}} \right] \quad (6.22)$$

$$= 16\pi^2 \alpha_s \alpha \frac{1}{3} [(z^2 + (1-z)^2) \times \dots] \quad (6.23)$$

$$= 16\pi^2 \alpha_s \alpha \frac{2}{3} [P_{qg}(z) \times \dots] \quad (6.24)$$

with the splitting function

$$P_{qg}(z) = \frac{1}{2}(z^2 + (1-z)^2)$$

We can now calculate the cross section for Drell Yan production up to  $\mathcal{O}(\alpha_s)$  using the relation for  $p_t$  as given in eq.(8.6) in section 8.1.2 with the Jacobean

$$dp_t^2 = d\hat{t} \frac{u-t}{s} = (1-z)d\hat{t}.$$

In order to simplify the calculation we consider again only the leading contribution at small transverse momenta (taking the small  $\hat{t}$  approximation, as done in the DIS case). We see, that we obtain a similar behavior of the cross section:

$$\begin{aligned} \frac{d\sigma}{dp_t^2} &= \frac{1}{1-z} \frac{d\sigma}{d\hat{t}} \\ &\propto \frac{1}{16\pi^2 \hat{s}} \frac{1}{1-z} P_{qq}(z) \hat{s} \left( \frac{-1}{t} + \dots \right) \\ &\propto \frac{1}{\hat{s}} P_{qq}(z) \frac{1}{p_t^2} \end{aligned}$$

We observe the same behavior as in DIS. The cross section is divergent if we perform the integral over  $p_t$  from zero, and we have to apply the same renormalization procedure as in the DIS case.

We also observe, that the renormalization is the same as in DIS, as we obtained the same splitting functions. This is one of the important results of the QCD improved parton model: the parton densities, including the renormalization of the bare parton densities, are the same in DIS lepton proton scattering as in  $pp$  or  $p\bar{p}$  scattering: this is a consequence of factorization.

#### 6.1.4 The $p_t$ spectrum of Drell Yan production

The complete calculation of the transverse momentum spectrum of Drell Yan production becomes complicated, because of the integration over the longitudinal and transverse components of the interaction partons. The original papers on this are very interesting [67,68]. Here we only consider the small  $p_t$  approximation and give the final result (without attempting to perform the calculation in detail, the full derivation can be found in [13]):

$$\frac{d\sigma}{dM^2 dy dp_t^2} = \frac{8}{27} \frac{\alpha^2 \alpha_s}{s M^2} \frac{1}{p_T^2} \int_{x_a^{min}}^1 dx_a H(x_a, x_b, M^2) \frac{x_a x_b}{x_a - x_1} \left( 1 + \frac{\tau^2}{(x_a x_b)^2} - \frac{x_T^2}{2x_a x_b} \right) \quad (6.25)$$

$$\sim \frac{8}{27} \frac{\alpha^2 \alpha_s}{s M^2} \frac{2}{p_T^2} H(x_a, x_b, M^2) \log \frac{s}{p_t^2} \quad (6.26)$$

$$= \left( \frac{d\sigma}{dM^2 dy} \right)_{Born} \times \left( \frac{4\alpha_s}{3\pi} \frac{1}{p_t^2} \log \frac{s}{p_t^2} \right)$$

with the product of the parton densities defined by:

$$H(x_a, x_b, Q^2) = \sum e_q^2 (q_i(x_a, Q^2) \bar{q}_i(x_b, Q^2) + \bar{q}_i(x_a, Q^2) q_i(x_b, Q^2))$$

and the lowest order ( $\mathcal{O}(\alpha_s^0)$ ) Born cross section given in eq.(6.8):

$$\left( \frac{d\sigma}{dM^2 dy} \right)_{Born} = \frac{4\pi\alpha^2}{9sM^2} H_q(x_a, x_b, M^2) \quad (6.27)$$

As we know already from the discussion of DIS, the divergent behavior is absorbed by virtual corrections, for example vertex corrections. As in the DIS case, we can calculate the virtual corrections explicitly, or argue on the basis of unitarity (and knowing that the final state of the virtual correction to the lowest order process is the same as the lowest order process). We use here a heuristic argument to obtain the behavior of the cross section at small  $p_t$ , by assuming that the virtual and the non-branching corrections will compensate the divergent behavior of the real emission cross section. We write:

$$\int_0^s \frac{d\sigma}{dM^2 dy dp_t^2} dp_t^2 = \left( \frac{d\sigma}{dM^2 dy} \right)_{Born} + \mathcal{O}(\alpha_s) \quad (6.28)$$

We rearrange the integral:

$$\int_0^s \frac{d\sigma}{dM^2 dy dp_t^2} dp_t^2 = \int_0^{p_t^2} \frac{d\sigma}{dM^2 dy dp_t'^2} dp_t'^2 + \int_{p_t^2}^s \frac{d\sigma}{dM^2 dy dp_t'^2} dp_t'^2 \quad (6.29)$$

giving:

$$\int_0^{p_t^2} \frac{d\sigma}{dM^2 dy dp_t'^2} dp_t'^2 = \int_0^s \frac{d\sigma}{dM^2 dy dp_t'^2} dp_t'^2 - \int_{p_t^2}^s \frac{d\sigma}{dM^2 dy dp_t'^2} dp_t'^2 \quad (6.30)$$

Assuming that the total cross section is the Born cross section multiplied with a  $k$ -factor  $k$  (which we will neglect) we can write:

$$\int_0^{p_t^2} \frac{d\sigma}{dM^2 dy dp_t'^2} dp_t'^2 = \left( \frac{d\sigma}{dM^2 dy} \right)_{Born} (1+k) - \int_{p_t^2}^s \frac{d\sigma}{dM^2 dy dp_t'^2} dp_t'^2 \quad (6.31)$$

$$= \left( \frac{d\sigma}{dM^2 dy} \right)_{Born} \left( 1 - \frac{4\alpha_s}{3\pi} \int_{p_t^2}^s \frac{\log \frac{s}{p_t'^2}}{p_t'^2} dp_t'^2 \right) \quad (6.32)$$

$$= \left( \frac{d\sigma}{dM^2 dy} \right)_{Born} \left( 1 - \frac{2\alpha_s}{3\pi} \left( \log \frac{s}{p_t^2} \right)^2 \right) \quad (6.33)$$

This form is suggestive to extend to higher orders in  $\alpha_s$ , and we assume that the corrections in the bracket will exponentiate:

$$1 + a + \frac{a^2}{2!} + \frac{a^3}{3!} + \dots = \exp a$$

and we write for the cross section:

$$\rightsquigarrow \int_0^{p_t^2} \frac{d\sigma}{dM^2 dy dp_t'^2} dp_t'^2 = \left( \frac{d\sigma}{dM^2 dy} \right)_{Born} \exp \left( -\frac{2\alpha_s}{3\pi} \log^2 \frac{s}{p_t^2} \right) \quad (6.34)$$

We have obtained a integrated cross section which with the assumption that the  $\alpha_s$  corrections exponentiate, is finite over the whole range in  $p_t$ . To obtain the the differential cross section as a function of  $p_t^2$ , we differentiate eq.(6.34) with respect to  $p_t^2$  and obtain:

$$\frac{d\sigma}{dM^2 dy dp_t^2} = \left( \frac{d\sigma}{dM^2 dy} \right)_{Born} \frac{4\alpha_s}{3\pi} \frac{1}{p_t^2} \log \frac{s}{p_t^2} \exp \left( -\frac{2\alpha_s}{3\pi} \log^2 \frac{s}{p_t^2} \right) \quad (6.35)$$

We see, that the cross section for  $p_t \rightarrow 0$  vanishes. This is the effect of the all order resummation of soft gluon emissions. A similar effect we have already observed in the discussion of the Sudakov form factor in section 4.3.2, where we found that the probability for no branching from one scale to another is very small: only if there is no resolvable branching, the  $p_t$  of the Drell Yan pair is zero (except if the emitted partons all compensate each other in transverse momentum).

In fig. 6.6 the measured cross section for  $W$ -boson production at LHC [66] is shown.

A more detailed discussion and calculation of the Drell Yan  $p_t$  spectrum can be found in [69].



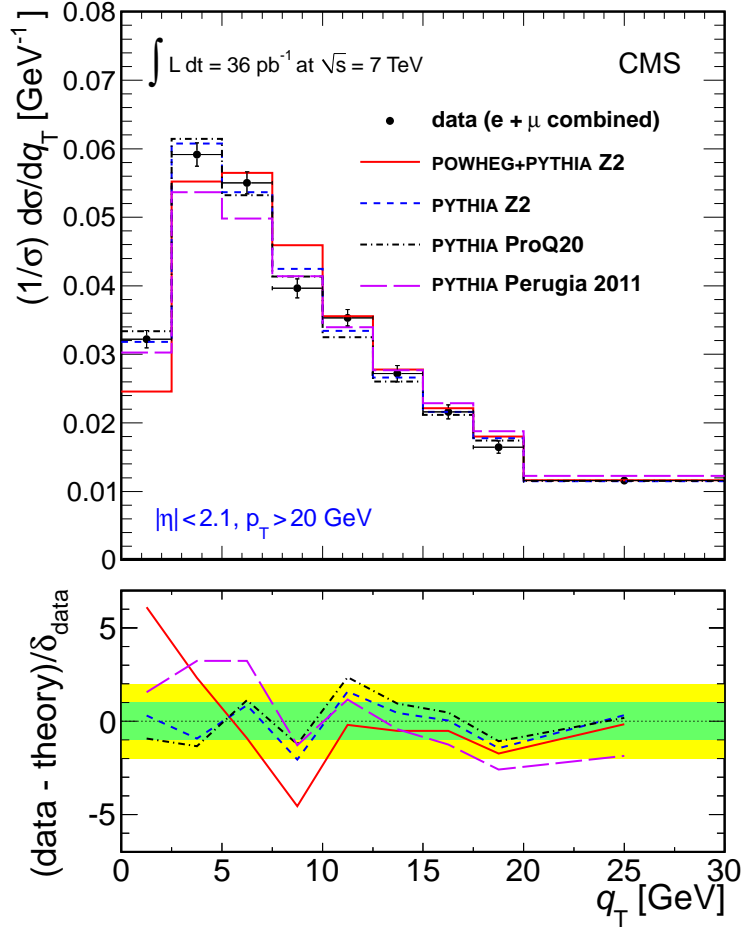


Figure 6.6: The transverse momentum of the  $W$  boson as measured by [66].

### 6.1.5 Measurement of the $W$ mass

The  $W$  boson can be detected via the decay products in a leptonic decay:

$$W \rightarrow l + \nu$$

where the  $\nu$  escapes detection.

In the rest frame of the  $W$ -boson the cross section for the leptonic decay is [14][p 320]:

$$\frac{1}{\sigma} \frac{d\sigma(W \rightarrow \nu l)}{d \cos \theta^*} = \frac{3}{8} (1 + \cos^2 \theta^*) \quad (6.36)$$

with the angular dependence similar to that of the process  $e^+e^- \rightarrow \mu^+\mu^-$ :

$$\frac{d\sigma}{d \cos \theta} \sim \frac{1}{s} (1 + \cos^2 \theta)$$

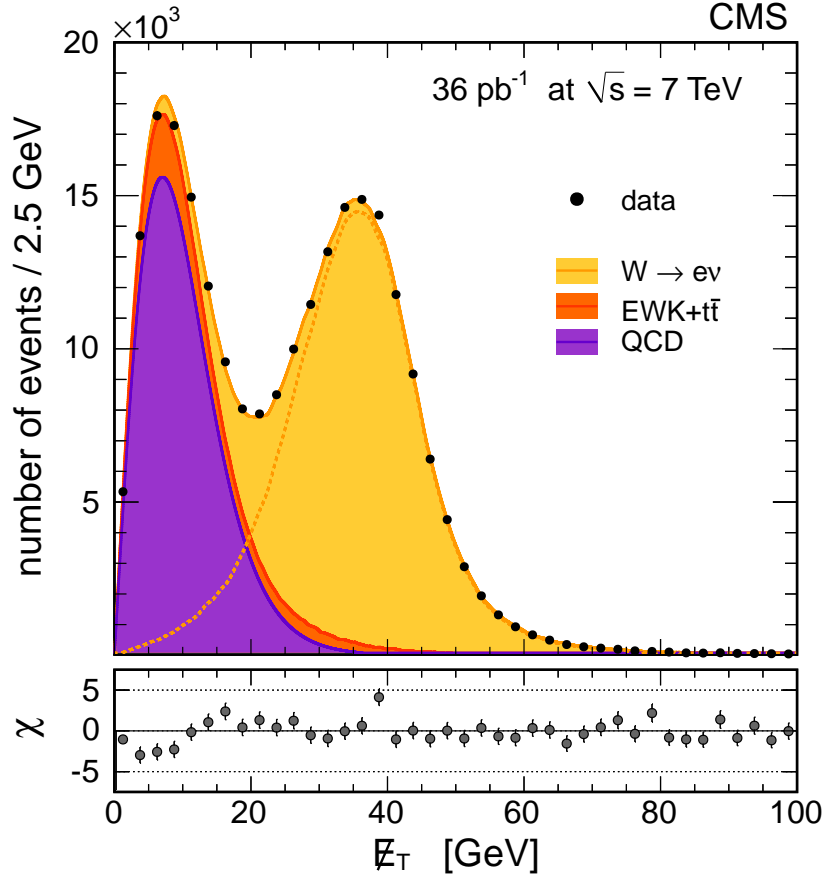


Figure 6.7: The transverse mass of the  $W$  boson as measured by [70].

where the difference in the pre-factors comes from the flux factor. In the  $W$  rest frame the transverse momentum of the lepton  $l$  and that of the neutrino are balanced. Changing the variables in eq.(6.36) from  $d \cos \theta$  to  $dp_t^2$  using  $p_t^2 = \frac{\hat{t}\hat{u}}{\hat{s}} = \frac{1}{4}\hat{s} \sin^2 \theta$  (see appendix 8.1.2) we obtain:

$$\begin{aligned} \frac{d \cos \theta}{dp_t^2} &= \frac{1}{2} \left(1 - \frac{4p_t^2}{\hat{s}}\right)^{-\frac{1}{2}} \frac{4}{\hat{s}} \\ &= \frac{2}{\hat{s}} \left(1 - \frac{4p_t^2}{\hat{s}}\right)^{-\frac{1}{2}} = \frac{2}{\hat{s} \cos \theta} \end{aligned} \quad (6.37)$$

With eq(6.37) we obtain for the cross section:

$$\frac{d\sigma}{dp_t^2} = \frac{d\sigma}{d \cos \theta} \frac{d \cos \theta}{dp_t^2} \quad (6.38)$$

$$\simeq \frac{1 + \cos^2 \theta}{\cos \theta} \quad (6.39)$$

$$\simeq \frac{2 \left(1 - \frac{2p_t^2}{\hat{s}}\right)}{\sqrt{1 - \frac{4p_t^2}{\hat{s}}}} \quad (6.40)$$

showing the Jacobean peak for  $p_t^2 = \frac{\hat{s}}{4} = \frac{M_W^2}{4}$ , which corresponds to  $\cos \theta = 0$  or  $\theta = \pi/2$ . Thus the cross section  $\frac{1}{\sigma} \frac{d\sigma}{dp_t^2}$  is strongly sensitive to  $M_W$  and can be used to measure the  $W$  mass.

The transverse mass  $M_\perp$  is defined as:

$$\begin{aligned} M_\perp^2 &= (|\vec{p}_\perp^e| + |\vec{p}_\perp^\nu|)^2 - (\vec{p}_\perp^e + \vec{p}_\perp^\nu)^2 \\ M^2 &= (|\vec{p}^e| + |\vec{p}^\nu|)^2 - (\vec{p}^e + \vec{p}^\nu)^2 \end{aligned}$$

Obviously, in the limit of vanishing longitudinal momentum  $M_\perp \rightarrow M$ . The transverse mass  $M_\perp$  can be calculated as:

$$\begin{aligned} M_\perp^2 &= (|\vec{p}_\perp^e| + |\vec{p}_\perp^\nu|)^2 - (\vec{p}_\perp^e + \vec{p}_\perp^\nu)^2 \\ &= 2|\vec{p}_\perp^e||\vec{p}_\perp^\nu|(1 - \cos \Delta\phi) \end{aligned}$$

with  $p_\perp^\nu$  being the neutrino transverse momentum (or identified as the missing transverse momentum as calculated from energy momentum conservation) and  $\Delta\phi$  being the angle between the observed electron and the missing transverse momentum vector.

The transverse mass has been obtained in early measurements at the LHC [70]. The measurement is shown in fig. 6.7.



## Chapter 7

# High Parton Densities and small $x$ effects

We have seen in the discussion of DIS and the parton densities that all evolution equations, DGLAP, BFKL and CCFM, predict a strong rise of the parton densities at high energies because of the dominance of the  $g \rightarrow gg$  splitting. However, the rise of the parton densities and the influence on observables of the hadronic final state will depend on the details of the parton evolution.

In this chapter we will discuss the high energy behavior of the  $\gamma^*p$  cross section, effects of small  $x$  evolution on the differential cross section of Drell Yan production at the high energies available at LHC, as well as effects on the final state coming from high parton densities which will result in contributions of multiple parton interaction (MPI).

### 7.1 The high energy behavior of the $\gamma^*p$ cross section

In Fig. 4.2 we have seen that the structure function  $F_2(x, Q^2)$  rises with decreasing  $x$ . The structure function  $F_2$  is connected directly with  $\sigma_{\gamma^*p}$ . The cross section for  $\gamma^*p$  as a function of  $W^2 = Q^2 \frac{1-x}{x}$  is shown in Fig. 7.1 (taken from [71]). The cross section increases with  $W^2$ , for small  $Q^2$  the increase is weak, whereas for large  $Q^2$  the increase is strong. At large values of  $W^2$  the partial cross section for large  $Q^2$  eventually becomes larger than the total  $\gamma p$  cross section, violating unitarity. At large  $W$  the rise of the cross section therefore has to become weaker, leading to so-called saturation effects: the parton density cannot increase forever, but saturates. The basic mechanism of saturation is gluon fusion  $g + g \rightarrow g$ . Where exactly this happens is unclear, it also depends on the spatial distribution of the partons inside the proton.

### 7.2 The $p_t$ spectrum of Drell Yan production at high energies

At high energies, when the transverse momenta can be of similar size as the longitudinal momenta of the interacting partons, the collinear approximation leading to the DGLAP evolution equation might be insufficient and the BFKL or CCFM evolution might be a better representation of parton evolution. Effects beyond DGLAP have been observed at HERA in energy flow

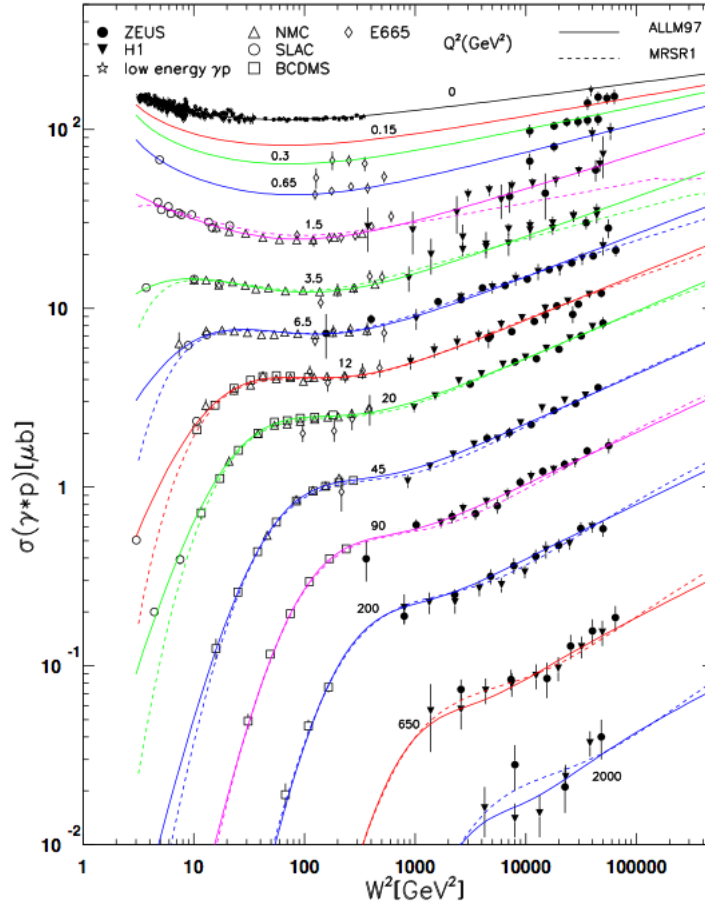


Figure 7.1:  $\gamma^*p$  cross section as a function of the  $W_{\gamma^*p}$  center of mass energy for different values of  $Q^2$  [71].

measurements [72],  $p_t$  spectra of charged particles [73] and the cross sections for forward jet production [58–60]. These measurements have been used in [74] to predict a significant broadening of the transverse momentum spectrum of Drell Yan pairs at LHC energies.

First measurements of forward Drell Yan production at LHCb [75] show a significant deviation of the measurement from the theoretical prediction as shown in Fig. 7.2

### 7.2.1 Multiparton interactions

When the parton densities are high, the probability to have more than one partonic interaction per hadron hadron collision increases [76–80]. For simplicity we illustrate the problem with (mini)-jet production at highest energies. The partonic cross section for (mini) - jet production diverges for

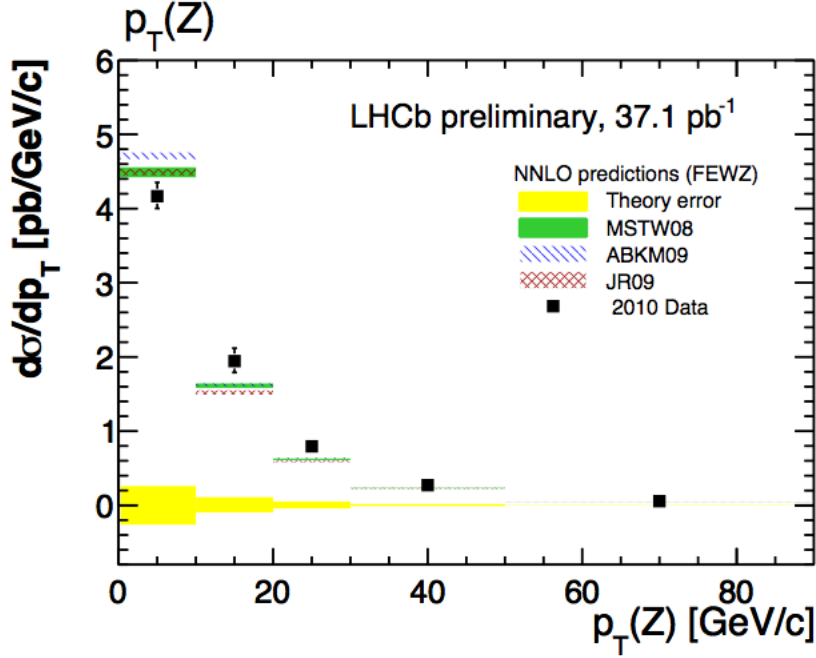


Figure 7.2: Cross section as a function of the transverse momentum  $p_t$  of the  $Z$  boson as measured by [75].

$p_{t \min} \rightarrow 0$ :

$$\sigma_{hard} = \int_{p_{t \min}^2} \frac{d\sigma_{hard}(p_t^2)}{dp_t^2} dp_t^2 \quad (7.1)$$

The partonic cross section as a function of  $p_{t \min}$  is shown in Fig. 7.3 (taken from [78]). One can see, that the cross section exceeds the inelastic (non-diffractive) cross section  $\sigma_{nd}$  at values of  $p_{t \min}$ , which are above a typical hadronic scale, at LHC for  $p_{t \min} \sim 5$  GeV. The solution out of this dilemma is to assume that there could be more than one partonic interaction per hadron - hadron collision, with the average number of interactions given by:

$$\langle n \rangle = \frac{\sigma_{hard}(p_{t \min})}{\sigma_{nd}} \quad (7.2)$$

Here,  $\sigma_{nd}$  is the non-diffractive inelastic  $pp$  cross section. However, this does not solve the problem of the divergency for  $p_t \rightarrow 0$ . To treat this we remember that the hadrons are color neutral and when  $p_t$  becomes small, the wavelength increases such that a gluon cannot resolve anymore any

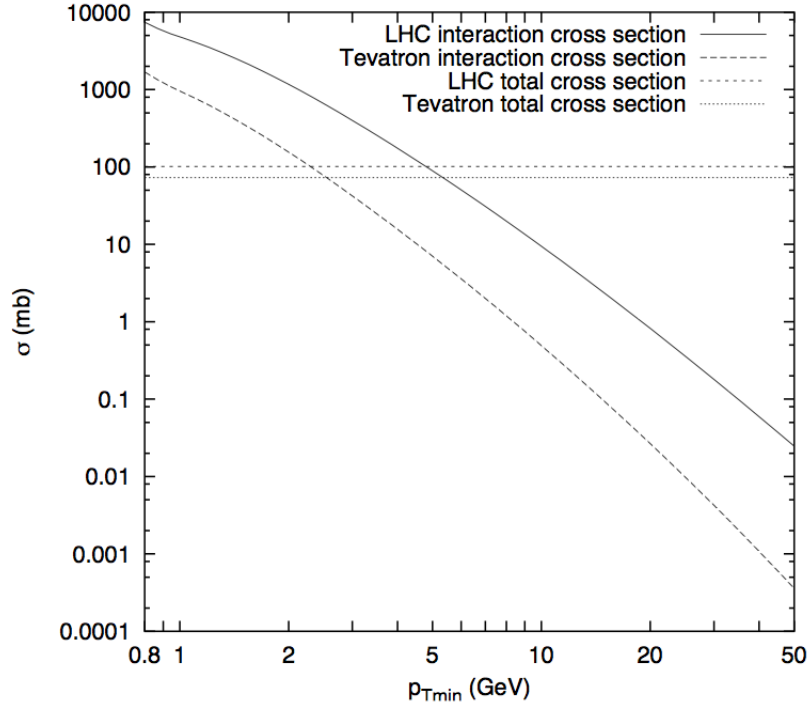


Figure 7.3: Mini jet cross section as a function of  $p_{t\min}$  for Tevatron and LHC energies (from [78]).

individual color charges (see discussion on angular ordering section 5.3.1), resulting in a reduction of the effective strong coupling.

Let us define (following the discussion in [77]):

$$p(x_t) = \frac{1}{\sigma_{nd}} \frac{d\sigma}{dx_t} \quad (7.3)$$

with  $x_t = \frac{2p_t}{\sqrt{s}}$ . To understand this argumentation, let us go back to the derivation of a Poisson distribution. If  $\lambda$  is the average rate for occurrence of specific events, then the probability that a single event happens at  $\delta t$  is:

$$\lambda \delta t$$

The probability that nothing happens is  $1 - \lambda \delta t$ . The probability that no event happens in  $[t, t + \delta t]$  under the condition that there was no event in  $[0, t]$  with  $P_0(t)$  is:

$$\begin{aligned} P_0(t + \delta t) &= P_0(t)(1 - \lambda \delta t) \\ \rightsquigarrow \frac{P_0(t + \delta t) - P_0(t)}{\delta t} &= -\lambda P_0(t) \\ \rightsquigarrow \frac{\partial P_0(t)}{\partial t} &= -\lambda P_0(t) \\ \rightsquigarrow P_0(t) &= \exp(-\lambda t) \end{aligned}$$



which is the Poisson distribution for the observation of  $r = 0$  events with a mean of the distribution of  $\mu = \lambda t$ .

To obtain the probability for the hardest scattering at  $x_{t1}$ :

$$P_1 = p(x_{t1}) \exp\left(-\int_{x_{t1}}^1 p(x')dx'\right) \quad (7.4)$$

The naive probability  $p(x_{t1})$  is multiplied by Sudakov type form factor to ensure, that there is no other scattering with  $x_t > x_{t1}$  in the event. Now we can calculate the probability to have the second hardest scattering at  $x_{t2}$ :

$$P_2 = \int_{x_{t2}}^1 dx_{t1} p(x_{t1}) \exp\left(-\int_{x_{t1}}^1 p(x')dx'\right) \exp\left(-\int_{x_{t2}}^{x_{t1}} p(x')dx'\right) p(x_{t2}) \quad (7.5)$$

$$= \int_{x_{t1}}^1 dx_{t1} p(x_{t1}) p(x_{t2}) \exp\left(-\int_{x_{t2}}^1 p(x')dx'\right) \quad (7.6)$$

This equation can be understood as follows: there is no scattering between  $x_{t1}$  and 1, we have a scattering at  $x_{t1}$  and there is no scattering between  $x_{t2}$  and  $x_{t1}$ . Finally we integrate over all possible values of  $x_{t1}$ . A similar argumentation was made for the parton evolution in terms of Sudakov form factors in section 4.3.2. The expression can be iterated to give:

$$P_n = p(x_t) \frac{1}{(n-1)!} \left[ \int_{x_t}^1 p(x')dx' \right]^{n-1} \exp\left(-\int_{x_t}^1 p(x')dx'\right) \quad (7.7)$$

which is a Poisson distribution with

$$\begin{aligned} \mu &= \int_{x_t}^1 p(x')dx' = \frac{1}{\sigma_{nd}} \int_{p_{tmin}^2} \frac{d\sigma_{hard}(p_t^2)}{dp_t^2} dp_t^2 \\ p_r &= \frac{\mu^r}{r!} \exp(-\mu) \end{aligned}$$

Summing up all  $p_r$  gives:

$$\sum_r p_r = \sum_r \frac{\mu^r}{r!} \exp(-\mu) = \exp(\mu) \exp(-\mu) = 1$$

which says, in the case of jet production, that the total rate of mini-jet production is not changed, the probability that a scattering occurs is 1, which is that the inclusive cross section is not changed by introducing the concept of multi-parton interactions.

The concept of multi-parton interaction has been successfully applied to describe event properties in soft collisions but also to describe details of the hadronic final state in perturbative processes.



# Chapter 8

## Appendix

### 8.1 Kinematics

In a  $2 \rightarrow 2$  process we can relate the Mandelstam variable  $\hat{t}$  to the transverse momentum of the  $\hat{t}$ -propagator.

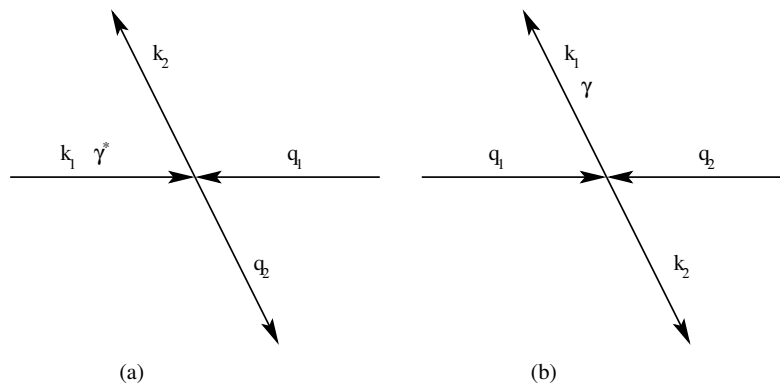


Figure 8.1: Schematic drawing of  $\gamma^* + g \rightarrow q\bar{q}$  (a) and  $g + g \rightarrow q\bar{q}$  (b) scattering..

#### 8.1.1 $ep$ - case

In the center of mass frame of the parton process  $\gamma^*(k_1)q(q_1) \rightarrow q(q_2)g(k_2)$  the four-vectors of the incoming and outgoing particles are (see Fig. 8.1(a)) :

$$\begin{aligned}
 k_1 &= (\sqrt{\vec{k}^2 - Q^2}, 0, 0, k) \\
 q_1 &= (k, 0, 0, -k) \\
 q_2 &= (q, -q \sin \theta, 0, -q \cos \theta) \\
 k_2 &= (q, q \sin \theta, 0, q \cos \theta)
 \end{aligned}$$

with  $k_1^2 = -Q^2$ . From this we obtain

$$\begin{aligned}\hat{s} &= (k_2 + q_2)^2 = 4q^2 \\ \hat{t} &= (k_1 - q_2)^2 = (q_1 - k_2)^2 = -2(kq + kq \cos \theta) = -2kq(1 + \cos \theta) \\ \hat{u} &= (q_1 - q_2)^2 = -2(kq - kq \cos \theta) = -2kq(1 - \cos \theta) \\ \hat{s}\hat{t}\hat{u} &= 4q^2 4(qk)^2 (1 + \cos \theta)(1 - \cos \theta) = (4kq)^2 q^2 \sin^2 \theta \\ \hat{t} + \hat{u} &= -\hat{s} - Q^2 = -2kq(1 + \cos \theta) - 2kq(1 - \cos \theta) = -4kq\end{aligned}$$

With this we obtain:

$$p_t^2 = q^2 \sin^2 \theta \quad (8.1)$$

$$= \frac{\hat{t}\hat{u}\hat{s}}{(\hat{s} + Q^2)^2} \quad (8.2)$$

In the small  $t$  limit we obtain from  $\hat{t} + \hat{u} + \hat{s} = -Q^2 \rightsquigarrow \hat{u} = -Q^2 - \hat{s}$ . Using  $z = \frac{Q^2}{2k_1 \cdot q_1}$  and  $\hat{s} = -Q^2 + Q^2/z$  we obtain:

$$p_t^2 = -\frac{\hat{t}\hat{s}}{\hat{s} + Q^2} \quad (8.3)$$

$$= -\hat{t}(1 - z) \quad (8.4)$$

### 8.1.2 $pp$ - case

Here we calculate the relation between the transverse momentum  $p_t$  of a final state parton in a  $2 \rightarrow 2$  process, like  $q(q_1)\bar{q}(q_2) \rightarrow \gamma^*(k_1)g(k_2)$  with the four-vectors indicated in the brackets. The four-vectors are given by (see Fig. 8.1(b)):

$$\begin{aligned}q_1 &= (q, 0, 0, q) \\ q_2 &= (q, 0, 0, -q) \\ k_1 &= (\sqrt{M^2 + \vec{k}^2}, -k \sin \theta, 0, -k \cos \theta) \\ k_2 &= (k, k \sin \theta, 0, k \cos \theta)\end{aligned}$$

with  $k_1^2 = M^2$ . From this we obtain

$$\begin{aligned}\hat{s} &= (q_1 + q_2)^2 = 4k_1 k_2 = 4q^2 \\ \hat{t} &= (q_1 - k_1)^2 = (q_2 - k_2)^2 = -2(qk + qk \cos \theta) = -2qk(1 + \cos \theta) \\ \hat{u} &= (q_1 - k_2)^2 = -2(qk - qk \cos \theta) = -2qk(1 - \cos \theta) \\ \hat{t}\hat{u} &= 4(qk)^2 (1 - \cos \theta)(1 + \cos \theta) = 4(qk)^2 \sin^2 \theta\end{aligned}$$

With this we obtain:

$$p_t^2 = k^2 \sin^2 \theta \quad (8.5)$$

$$= \frac{\hat{t}\hat{u}}{\hat{s}} \quad (8.6)$$

Please note that this is different compare to the DIS case (eq.(8.2), where we obtained:

$$p_t^2 = \frac{\hat{t}\hat{u}\hat{s}}{(\hat{s} + Q^2)^2}$$

However, performing the small  $t$  limit and using  $\hat{s} + \hat{t} + \hat{u} = M^2$  together with  $z = M^2/\hat{s}$  we obtain:

$$p_t^2 = \frac{\hat{t}\hat{u}}{\hat{s}} \quad (8.7)$$

$$\rightsquigarrow p_t^2 = \frac{\hat{t}(\hat{s} - M^2)}{\hat{s}} \quad (8.8)$$

$$= -\hat{t}(1 - z) \quad (8.9)$$

which agrees with what is obtained in the DIS case.

## 8.2 Calculation of transverse momentum of Drell Yan pair

Starting from eq.(6.14) we obtain:

$$\frac{1}{\sigma} \frac{d\sigma}{dp_t} = \int d^2\vec{k}_{t1} d^2\vec{k}_{t2} \delta^{(2)}(\vec{k}_{t1} + \vec{k}_{t2} - \vec{p}_t) h(\vec{k}_{t1}) h(\vec{k}_{t2}) \quad (8.10)$$

$$= \int d^2\vec{k}_{t1} h(\vec{k}_{t1}) h(\vec{p}_t - \vec{k}_{t1}) \quad (8.11)$$

$$= \frac{1}{2} \int_0^\infty dk_{t1}^2 \int d\phi \frac{b^2}{\pi^2} \exp(-2bk_{t1}^2) \exp(-bp_t^2) \exp(2bp_t k_{t1} \cos \phi) \quad (8.12)$$

$$= \frac{b^2}{2\pi^2} \exp(-bp_t^2) \int dk_{t1}^2 \exp(-2bk_{t1}^2) 2\pi I_0(2bp_t k_{t1}) \quad (8.13)$$

$$= \frac{b}{2\pi} \exp\left(-\frac{1}{2}bp_t^2\right) \quad (8.14)$$

where we have used the expression for the modified Bessel function:

$$\int_0^{2\pi} d\phi \exp(z \cos \phi) = 2\pi I_0(z)$$

with:

$$I_0(z) = \sum_n \frac{\left(\frac{1}{4}z^2\right)^n}{(n!)^2} \quad (8.15)$$

and have integrated this expression term by term<sup>1</sup>. Using eq.(8.13):

$$\begin{aligned}\frac{1}{\sigma} \frac{d\sigma}{dp_t} &= \int d^2\vec{k}_{t1} d^2\vec{k}_{t2} \delta^{(2)}(\vec{k}_{t1} + \vec{k}_{t2} - \vec{p}_t) h(\vec{k}_{t1}) h(\vec{k}_{t2}) \\ &= \frac{b^2}{2\pi^2} \exp(-bp_t^2) \int dk_{t1}^2 \exp(-2bk_{t1}^2) 2\pi I_0(2bp_t k_{t1})\end{aligned}$$

together with eq.(8.15):

$$I_0(z) = \sum_n \frac{\left(\frac{1}{4}z^2\right)^n}{(n!)^2}$$

gives:

$$\frac{1}{\sigma} \frac{d\sigma}{dp_t} = \frac{b^2}{2\pi^2} \exp(-bp_t^2) \int dk_{t1}^2 \exp(-2bk_{t1}^2) 2\pi \sum_{n=0}^{n=\infty} \frac{\left(\frac{1}{4}(2bp_t k_{t1})^2\right)^n}{(n!)^2}$$

and we can perform the integration term by term giving:

$$\begin{aligned}S &= \frac{1}{\sigma} \frac{d\sigma}{dp_t} \\ &= \sum_{n=0}^{n=\infty} S_n\end{aligned}$$

with:

$$\begin{aligned}S_0 &= \frac{b^2}{2\pi^2} \exp(-bp_t^2) \int dk_{t1}^2 2\pi \exp(-2bk_{t1}^2) \\ &= \frac{b^2}{\pi} \exp(-bp_t^2) \frac{1}{2b} \\ &= \frac{b}{2\pi} \exp(-bp_t^2) \\ S_1 &= \frac{b^2}{2\pi^2} \exp(-bp_t^2) \int dk_{t1}^2 2\pi \exp(-2bk_{t1}^2) \frac{1}{4} (2bp_t k_{t1})^2 \\ &= \frac{b^2}{\pi} \exp(-bp_t^2) \frac{1}{4} 4b^2 p_t^2 \int dk_{t1}^2 \pi \exp(-2bk_{t1}^2) k_{t1}^2 \\ &= \frac{b}{2\pi} \exp(-bp_t^2) \frac{b}{2} p_t^2 \\ S_2 &= \frac{b^2}{2\pi^2} \exp(-bp_t^2) \int dk_{t1}^2 2\pi \exp(-2bk_{t1}^2) \frac{1}{4} (4b^2 k_{t1}^2 p_t^2)^2 \\ &= \frac{b^2}{2\pi} \exp(-bp_t^2) \frac{1}{2} b^4 p_t^4 \int dk_{t1}^2 \pi \exp(-2bk_{t1}^2) k_{t1}^4\end{aligned}$$

---

<sup>1</sup>Courtesy of K. Kutak, who showed how to perform the integral

$$= \frac{b}{2\pi} \exp(-bp_t^2) \frac{b^2}{8} p_t^4$$

$$\vdots$$

Summing up all terms gives:

$$\begin{aligned} S &= S_0 + S_1 + S_2 + \dots \\ &= \frac{b}{2\pi} \exp(-bp_t^2) \left( 1 + \frac{b}{2} p_t^2 + \frac{1}{8} b^2 p_t^4 + \dots \right) \\ &= \frac{b}{2\pi} \exp(-bp_t^2) \left( 1 + \frac{1}{1!} \frac{bp_t^2}{2} + \frac{1}{2!} \left( \frac{bp_t^2}{2} \right)^2 + \dots \right) \\ &= \frac{b}{2\pi} \exp\left(-\frac{1}{2} bp_t^2\right) \end{aligned}$$





# Acknowledgments

I am grateful to the participants of the course *QCD and Monte Carlos* which I held in the winter term 2011-2014 in Antwerp where these lecture notes were written. I am particularly grateful to Christophe De Beule, Roeland Juchtmans, Alexis Kalogeropoulos, Alexandre Leonard, Thomas Reis, Florian Zenoni for careful reading the manuscript and identifying many inconsistencies and typos. Many thanks go also to Zlatka Staykova, Samantha Dooling and Paolo Gunnellini for assisting me during the exercises. I am grateful to Radek Zlebcik for his careful reading of the manuscript during the lecture course 2013 at DESY. I am also grateful to Laura Raes for pointing to misprints and unclear formulations during the winter course 2013.



# Bibliography

- [1] Random.Org, True Random Number Service, <http://www.random.org/>.
- [2] ID QUANTIQUÉ SA, Quantique random number generator, <http://www.idquantique.com/true-random-number-generator/products-overview.html>.
- [3] S. Weinzierl, (2000), arXiv:hep-ph/0006269.
- [4] G. Cowan, *Statistical data analysis*, Oxford, UK: Clarendon (1998) 197 p.
- [5] D. E. Knuth, *The Art of Computer Programming Volumes 1-3 Boxed Set* (Addison-Wesley Longman Publishing Co., Inc., Boston, MA, USA, 1998).
- [6] F. James, *Comput.Phys.Comm.* **79**, 111 (1994).
- [7] M. Luscher, *Comput. Phys. Commun.* **79**, 100 (1994), arXiv:hep-lat/9309020.
- [8] M. Luscher, A Portable high quality random number generator for lattice field theory simulations, <http://luscher.web.cern.ch/luscher/ranlux/index.html> C++ code.
- [9] V. Blobel and E. Lohrmann *Statistische und numerische Methoden der Datenanalyse* Vol. 54 (Teubner, 1998).
- [10] G. Bohm and G. Zech, *Introduction to statistics and measurement analysis for physicists*, Hamburg, Germany: DESY (2005) 331 p.
- [11] F. James, *Rept.Prog.Phys.* **43**, 1145 (1980).
- [12] F. Halzen and A. D. Martin, *Quarks and Leptons: An introductory course in modern particle physics*, New York, USA: Wiley (1984) 396p.
- [13] R. D. Field, *Applications of Perturbative QCD* (Addison-Wesley Longman Publishing Co., Inc., 1989).
- [14] R. K. Ellis, W. J. Stirling, and B. R. Webber, *QCD and collider physics* (Camb.Monogr.Part.Phys.Nucl.Phys.Cosmol., 1996).

- [15] Y. L. Dokshitzer, V. A. Khoze, A. H. Mueller, and S. I. Troian, *Basics of perturbative QCD*, Gif-sur-Yvette, France: Ed. Frontieres (1991) 274 p.
- [16] J. C. Collins, (1997), arXiv:hep-ph/9705393.
- [17] J. Bjorken and E. A. Paschos, *Phys.Rev.* **185**, 1975 (1969).
- [18] H1 and ZEUS Collaboration, F. Aaron *et al.*, *JHEP* **1001**, 109 (2010), arXiv:0911.0884, 61 pages, 21 figures.
- [19] V. N. Gribov and L. N. Lipatov, *Sov. J. Nucl. Phys.* **15**, 438 (1972).
- [20] L. N. Lipatov, *Sov. J. Nucl. Phys.* **20**, 94 (1975).
- [21] G. Altarelli and G. Parisi, *Nucl. Phys.* **B126**, 298 (1977).
- [22] Y. L. Dokshitzer, *Sov. Phys. JETP* **46**, 641 (1977).
- [23] G. Altarelli, *Phys. Rept.* **81**, 1 (1982).
- [24] CTEQ, R. Brock *et al.*, *Rev.Mod.Phys.* **67**, 157 (1995).
- [25] J. C. Collins, D. E. Soper, and G. F. Sterman, *Adv.Ser.Direct.High Energy Phys.* **5**, 1 (1988), arXiv:hep-ph/0409313, To be publ. in 'Perturbative QCD' (A.H. Mueller, ed.) (World Scientific Publ., 1989).
- [26] J. Pumplin *et al.*, *JHEP* **0207**, 012 (2002), arXiv:hep-ph/0201195.
- [27] M. Whalley, The durham hepdata project, <http://hepdata.cedar.ac.uk/pdf/pdf3.html>.
- [28] G. Marchesini and B. R. Webber, *Nucl. Phys.* **B349**, 617 (1991).
- [29] G. Marchesini and B. R. Webber, *Nucl. Phys.* **B386**, 215 (1992).
- [30] F. Hautmann, H. Jung, and S. T. Monfared, (2014), arXiv:1407.5935.
- [31] E. A. Kuraev, L. N. Lipatov, and V. S. Fadin, *Sov. Phys. JETP* **44**, 443 (1976).
- [32] E. A. Kuraev, L. N. Lipatov, and V. S. Fadin, *Sov. Phys. JETP* **45**, 199 (1977).
- [33] I. I. Balitsky and L. N. Lipatov, *Sov. J. Nucl. Phys.* **28**, 822 (1978).
- [34] M. Ciafaloni, *Nucl. Phys.* **B296**, 49 (1988).
- [35] S. Catani, F. Fiorani, and G. Marchesini, *Phys. Lett.* **B234**, 339 (1990).
- [36] S. Catani, F. Fiorani, and G. Marchesini, *Nucl. Phys.* **B336**, 18 (1990).
- [37] G. Marchesini, *Nucl. Phys.* **B445**, 49 (1995), arXiv:hep-ph/9412327.

- [38] T. Sjöstrand, S. Mrenna, and P. Skands, JHEP **05**, 026 (2006), arXiv:hep-ph/0603175.
- [39] T. Sjöstrand, S. Mrenna, and P. Z. Skands, Comput. Phys. Commun. **178**, 852 (2008), arXiv:0710.3820.
- [40] G. Marchesini *et al.*, Comput. Phys. Commun. **67**, 465 (1992).
- [41] G. Corcella *et al.*, (2002), arXiv:hep-ph/0210213.
- [42] M. Bahr *et al.*, Eur.Phys.J. **C58**, 639 (2008), arXiv:0803.0883.
- [43] H. Jung, Comp. Phys. Commun. **86**, 147 (1995).
- [44] H. Jung, The RAPGAP Monte Carlo version 3.2, <http://projects.hepforge.org/rapgap/>, 2011.
- [45] F. Von Samson-Himmelstjerna, Determination of parton density functions using monte carlo event generators, Master's thesis, [/afs/desy.de/group/h1/psfiles/theses/h1th-516.pdf](http://afs.desy.de/group/h1/psfiles/theses/h1th-516.pdf), 2009.
- [46] J. Collins and H. Jung, (2005), arXiv:hep-ph/0508280.
- [47] J. Kwiecinski, A. D. Martin, and P. J. Sutton, Phys. Rev. **D52**, 1445 (1995), arXiv:hep-ph/9503266.
- [48] J. Kwiecinski, A. D. Martin, and P. Sutton, Z.Phys. **C71**, 585 (1996), arXiv:hep-ph/9602320.
- [49] H. Jung and G. P. Salam, Eur. Phys. J. **C19**, 351 (2001), arXiv:hep-ph/0012143.
- [50] G. Bottazzi, G. Marchesini, G. Salam, and M. Scorletti, JHEP **9812**, 011 (1998), arXiv:hep-ph/9810546.
- [51] L. Gribov, E. Levin, and M. Ryskin, Phys.Rept. **100**, 1 (1983).
- [52] E. M. Levin, M. G. Ryskin, Y. M. Shabelski, and A. G. Shuvaev, Sov. J. Nucl. Phys. **53**, 657 (1991).
- [53] S. Catani, M. Ciafaloni, and F. Hautmann, Nucl. Phys. **B366**, 135 (1991).
- [54] J. C. Collins and R. K. Ellis, Nucl. Phys. Proc. Suppl. **18C**, 80 (1991).
- [55] S. Catani, (2000), arXiv:hep-ph/0005233.
- [56] S. Catani, (1996), arXiv:hep-ph/9608310.
- [57] S. P. Baranov, H. Jung, L. Jonsson, S. Padhi, and N. P. Zotov, Eur. Phys. J. **C24**, 425 (2002), arXiv:hep-ph/0203025.
- [58] H1, C. Adloff *et al.*, Nucl.Phys. **B538**, 3 (1999), arXiv:hep-ex/9809028.

- [59] ZEUS, J. Breitweg *et al.*, Eur.Phys.J. **C6**, 239 (1999), arXiv:hep-ex/9805016.
- [60] ZEUS, J. Breitweg *et al.*, Phys.Lett. **B474**, 223 (2000), arXiv:hep-ex/9910043.
- [61] H. Jung *et al.*, Eur.Phys.J. **C70**, 1237 (2010), arXiv:1008.0152.
- [62] F. Hautmann and H. Jung, JHEP **10**, 113 (2008), arXiv:0805.1049.
- [63] ZEUS, S. Chekanov *et al.*, Nucl.Phys. **B786**, 152 (2007), arXiv:0705.1931.
- [64] S. Drell and T.-M. Yan, Phys.Rev.Lett. **25**, 316 (1970).
- [65] J. M. Campbell, J. W. Huston, and W. J. Stirling, Rept. Prog. Phys. **70**, 89 (2007), arXiv:hep-ph/0611148.
- [66] CMS Collaboration, S. Chatrchyan *et al.*, Phys.Rev. **D85**, 032002 (2012), arXiv:1110.4973.
- [67] Y. L. Dokshitzer, D. Diakonov, and S. I. Troian, Phys. Lett. **B79**, 269 (1978).
- [68] G. Parisi and R. Petronzio, Nucl. Phys. **B154**, 427 (1979).
- [69] S. D. Ellis, N. Fleishon, and W. J. Stirling, Phys. Rev. **D24**, 1386 (1981).
- [70] CMS Collaboration, S. Chatrchyan *et al.*, JHEP **1110**, 007 (2011), arXiv:1108.0566, \*  
Temporary entry \*.
- [71] H. Abramowicz and A. Levy, (1997), arXiv:hep-ph/9712415.
- [72] H1, C. Adloff *et al.*, Eur. Phys. J. **C12**, 595 (2000), arXiv:hep-ex/9907027.
- [73] H1, C. Adloff *et al.*, Nucl. Phys. **B485**, 3 (1997), arXiv:hep-ex/9610006.
- [74] S. Berge, P. M. Nadolsky, F. Olness, and C.-P. Yuan, Phys.Rev. **D72**, 033015 (2005), arXiv:hep-ph/0410375.
- [75] LHCb-CONF-2011-039, Updated measurements of  $w$  and  $z$  production at  $\sqrt{s} = 7$  tev with the lhcb experiment, <http://cdsweb.cern.ch/record/1367851?ln=en>, 2011.
- [76] T. Sjostrand and M. van Zijl, Phys. Lett. **B188**, 149 (1987).
- [77] T. Sjöstrand and M. van Zijl, Phys. Rev. **D36**, 2019 (1987).
- [78] T. Sjöstrand and P. Skands, JHEP **03**, 053 (2004), arXiv:hep-ph/0402078.
- [79] T. Sjöstrand and P. Skands, (2004), arXiv:hep-ph/0401060.
- [80] P. Skands and T. Sjöstrand, Eur. Phys. J. **C33**, s548 (2004), arXiv:hep-ph/0310315.